Applications of jump processes to neuroscience

Romain Veltz

▶ **To cite this version:**

Romain Veltz. Applications of jump processes to neuroscience. Mathematics [math]. Université Côte d'Azur, 2024. tel-04892967

HAL Id: tel-04892967
https://inria.hal.science/tel-04892967v1

Submitted on 17 Jan 2025

HAL is a multi-disciplinary open access archive for the deposit and dissemination of scientific research documents, whether they are published or not. The documents may come from teaching and research institutions in France or abroad, or from public or private research centers.

L'archive ouverte pluridisciplinaire **HAL**, est destinée au dépôt et à la diffusion de documents scientifiques de niveau recherche, publiés ou non, émanant des établissements d'enseignement et de recherche français ou étrangers, des laboratoires publics ou privés.

Distributed under a Creative Commons Attribution 4.0 International License

MÉMOIRE D'HABILITATION À DIRIGER DES RECHERCHES

Réalisé au Centre Inria d'Université Côte d'Azur, Sophia Antipolis, équipe CRONOS

Spécialité: **Mathématiques appliquées et applications des mathématiques**

par

Romain Veltz

Applications of jump processes to neuroscience

Soutenue le 1er Octobre 2024 devant le jury composé de :

Rapporteurs:

José A. Carrillo	(Professeur, Université d'Oxford)
Eva Löcherbach	(Professeure, Université Paris 1 Panthéon-Sorbonne, France)

Examinateurs:

Jean-Baptiste Caillau	(Professeur, Laboratoire Jean Alexandre Dieudonné)
Alain Destexhe	(Directeur de recherche, Université Paris-Saclay)
Jack Mellor	(Professeur, Université Walk Bristol)
Patricia Reynaud-Bouret	(Directrice de recherche, Laboratoire Jean Alexandre Dieudonné)

après les rapports de José A. Carrillo, Wulfram Gerstner & Eva Löcherbach.

Contents

Contents i

1 Introduction 3
- 1.1 Biological concepts . . . 3
- 1.2 Supervision and teaching . . . 4
- 1.3 Context and research activity . . . 5
- 1.4 Plan of the memoir . . . 6
- 1.5 Topics not presented in this memoir . . . 6

2 Mean-field of networks of generalized integrate-and-fire neurons 9
- 2.1 Description of the model . . . 10
  - 2.1.1 Description of the finite network . . . 10
  - 2.1.2 The McKean-Vlasov SDE in the mean-field limit . . . 11
  - 2.1.3 The nonlinear Fokker-Planck equation . . . 11
- 2.2 Selection of earlier works . . . 12
  - 2.2.1 Remarks on the choice of the network elements . . . 12
  - 2.2.2 Related studies based on jump processes . . . 13
- 2.3 PDE based approach . . . 14
  - 2.3.1 Notations . . . 14
  - 2.3.2 Main result . . . 14
  - 2.3.3 Interpretation using dynamical system theory . . . 15
  - 2.3.4 Difficulties and strategy of proof . . . 16
  - 2.3.5 Idea of proof . . . 16
  - 2.3.6 Numerical evidences for Hopf bifurcation . . . 18
- 2.4 Approach based on integral equation, PhD of Q. Cormier . . . 18
  - 2.4.1 General strategy . . . 19
  - 2.4.2 First main result: local stability of invariant distributions . . . 21
  - 2.4.3 Idea of proof . . . 23
  - 2.4.4 Second main result: around the Hopf bifurcation . . . 23
  - 2.4.5 Idea of proof . . . 25
- 2.5 Perspectives . . . 26

3 Networks of neurons interacting through their dendrites **29**
3.1 Description of the network . . . 30
3.1.1 Dendritic compartment . . . 31
3.1.2 Somatic compartment . . . 31
3.2 Heuristic scales and relevant quantities . . . 32
3.3 Formulation of the nonlinear problem . . . 32
3.4 Notations and main results . . . 33
3.4.1 Partial order and associated longest chains . . . 33
3.4.2 The functional Γ . . . 35
3.4.3 The spiking model . . . 35
3.4.4 Main results . . . 36
3.5 On the stationary solutions of the limit model . . . 38
3.6 Ideas of proofs and related hypothesis . . . 40
3.6.1 Idea of proof of proposition 3.6 . . . 42
3.6.2 Idea of proof of proposition 3.14 . . . 44
3.7 Bibliographical comments on the longest increasing sequences . . . 46
3.8 Perspectives . . . 46

4 Modelling the excitatory synapse **49**
4.1 Introduction . . . 50
4.2 Description of one particular experimental protocol . . . 52
4.3 Brief description of the model without the readout . . . 52
4.3.1 Description of the readout and of one experimental result . . . 55
4.4 Perspectives . . . 56

5 Conclusion **57**

6 List of publications **59**

Acknowledgments

First of all, I would like to warmly thank the members of the jury. It is an honor to present my work to you, to which each of you has contributed through your support, your results, and the enriching discussions we have shared. It is clear that you have been a source of inspiration, and I hope this memoir reflects that. I would also like to sincerely thank the reviewers who, despite the summer break, took the time to read this memoir, write reports, and provide valuable suggestions.

Next, I wish to express my deep gratitude to Étienne Tanré. We now know more about our respective grandmothers, and thanks in large part to our daily discussions, my (our?) binocular vision has greatly expanded. Private jokes aside, I am grateful for his insights, both on a scientific and personal level, and for helping me deepen my understanding of the probabilistic world, often challenged by my analytical approach.

I am particularly fortunate that Eva Löcherbach agreed to be part of the jury and attend my defense at Inria. It is no exaggeration to say that half of this memoir is built upon her work. I still remember the day I read her article with Nicolas Fournier and had the audacity to think I could improve a minor proposition in it.

I would like to thank Patricia Reynaud-Bouret for agreeing to be the "garante" of my HDR and a member of the jury. Her impressive scientific drive is highly beneficial to the local environment. I look forward to future collaborations.

My gratitude also goes to Nicolas Fournier for joining the dendritic action potentials project. Without his expertise, this project would not have reached such a scale.

Cian O'Donnell played a crucial role in fostering my interest in synaptic plasticity and shaping my research direction. I feel lucky to have met such a talented neuroscientist and, even more so, to call him a friend.

I thank Hélène Marie and Emmanuel Deval for agreeing to collaborate with me. Without them, my contributions to computational neuroscience would have been much more modest. I also thank Stéphane Barland for initiating a collaboration and reconnecting me with my first love: physics.

I would also like to express my gratitude to the students who agreed to embark on an adventure under my supervision. Some experienced the challenges of my early attempts at supervision, but I am glad that we shared many "eureka" moments together.

I would also like to warmly thank my thesis advisor, Olivier Faugeras, who had a decisive influence on my scientific career. His curiosity and enthusiasm for science have always been a source of inspiration, and I hope I have inherited at least a small part of these qualities.

I warmly thank my colleagues at Inria, NeuroMod and LJAD for creating such friendly and stimulating environments.

Finally, my last thanks go to my friends and most importantly to my family.

To Guilhem, Alice, Sylvain and Magali.

Index

$C_b^1(\mathbb{R}_+)$, the set of C^1-functions ϕ on $[0,\infty)$ such that ϕ and ϕ' are bounded , 15
$\mathcal{P}(\mathcal{X})$, the set of probability measures on $\mathcal{X}$, i.e. positive measures with mass 1., 11
$\mathbb{1}_A$, the indicator function of the set A, 10
$\mathcal{B}(\mathcal{X})$, the Borel sets of a topological space $\mathcal{X}$, 21
$\mathcal{L}(X)$, distibution of the random variable X, 11
N, Poisson measure on $\mathbb{R}_+ \times \mathbb{R}_+$ with Lebesgue intensity measure, 10

Action potential (AP), also called spike, 4
AMPA receptor, α-amino-3-hydroxy-5-methyl-4-isoxazolepropionic, 52
axon, 3

bAP, back propagating action potential, 4

Ca, Calcium, 53
CaM, calmodulin protein, 52
CaMKII, Calcium/Calmodulin-dependent protein kinase II, 49
CaN, Calcinerin, 53

dAP, dendritic action potential, 4
dendrite, 3

GIF, generalized integrate-and-fire model, 12
Glu, Glutamate, neurotransmitter, 52

i.i.d, independent and identically distributed, 11
IF, integrate-and-fire model, 5

LTP, long term depression : decrease of synaptic weight, 50
LTP, long term potentiation : increase of synaptic weight, 50

NMDA receptor, N-methyl-D-aspartate receptors, 52
non-plastic networks, networks for which synaptic plasticity is neglected, 5

ODE, ordinary differential equation, 6

PDE, partial differential equation, 7
PDMP, piecewise deterministic Markov process, 5
propagation of chaos, 11, 32

SDE, stochastic differential equation, 9
SK, Small Potassium ion channel, 52
soma, 3
spike, synonym of action potential (AP), 4
STDP, spike-timing-dependent plasticity, 50
synapse, 3
synaptic plasticity, 4
synaptic weight, 4

VGCC, 53
VGCC, voltage-gated calcium channel. Has different subtypes named L, N, P/Q, R and T, 52

Chapter 1

Introduction

1.1 Biological concepts

To enhance the readability of this memoir, we start with a brief overview of some fundamental concepts related to the biology of neurons. These concepts are idealized for simplicity, the rigor would entail a much longer introduction. Neurons, specialized cells within the central nervous system, consist of distinct subcellular domains [Kan13], each serving specific functions: the dendrite, the cell body (soma), and the axon (see figure 1.1 for a simplified representation). Synapses connect neurons to each other and are situated at the interface between axons and dendrites.

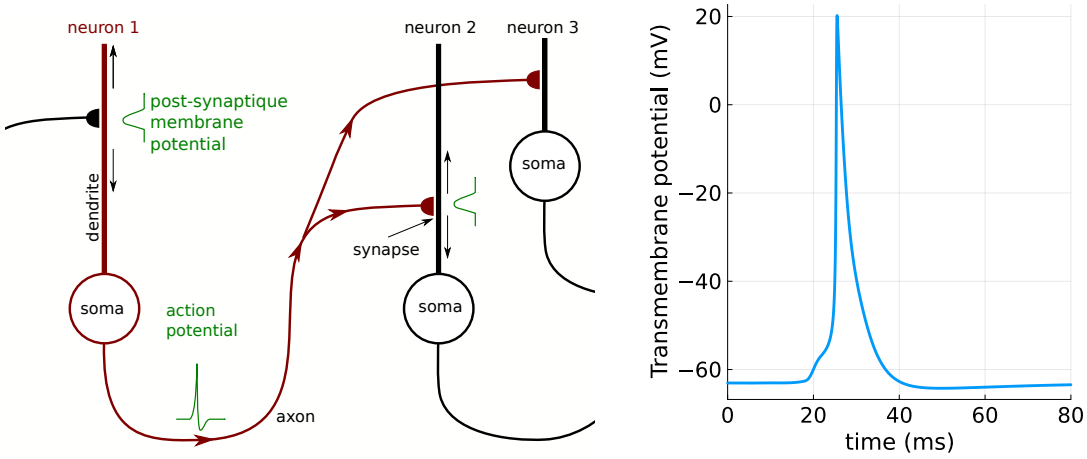

Figure 1.1: Left: Plots of the main neural components used in this memoir. Right: Simulation of action potential using the Hodgkin-Huxley model.

In figure 1.1 left, the axon of neuron 1 is connected, by synapses[1], to the dendrites of neurons 2 and 3. Neurons transmit information using electrical impulses called *action potentials* (AP) or *spikes*, see figure 1.1 right. When the electrical potential difference across the soma membrane reaches a sufficient level, a series of spikes occurs near the soma-axon interface, and the transmembrane electrical potential at the soma returns to an equilibrium value. This spike sequence is then transmitted, without alteration (shape or amplitude), to the axon terminals where the (excitatory / inhibitory) synapses are located.

When a spike reaches a synapse, it induces a localized change in the membrane potential difference of the dendrite, in the post-synaptic neuron. We define the *synaptic weight* as the amplitude of this local variation. Synaptic weights therefore measure the transmission of signals.

This local dendritic electrical perturbation then propagates along the dendrite, in a first approximation, in a diffusive way [Koc04] in both directions: *i.e.* towards the soma and towards the other end of the dendrite, interacting with the other electrical activities of the dendrite. The dendritic current reaching the soma affects the electric potential of the latter and can cause action potentials. Very simplified networks of such neurons are studied in chapter 2.

Some dendrites exhibit nonlinear behavior [MRH+17; LWD+22] and produce dendritic action potentials (dAP); an idealization of this case is studied mathematically in chapter 3.

Additionally, the spikes generated in the soma can back propagate along the dendrite in some cases ; they are called back propagating action potentials (bAP). They are important for coincidence detection and are considered in chapter 4 where a model of synapse is exposed. See [PWI+23] for a recent experimental imaging of dAPs and bAPs.

The synaptic weight is a characteristic of the synapse, essentially related to its number of AMPA receptors in the case of excitatory synapses. The fact that this synaptic weight can vary over time is called *synaptic plasticity* [Kan13]. Some of the changes of synaptic weight can persist over the long term, which naturally places synaptic plasticity as a building block of learning, memory, and adaptation in the brain. The synapse has mainly access to the pre-synaptic action potentials arriving via the axon, and to the bAPs coming from the soma. The conditions on the arrival times, the frequency, the number of these AP/bAP which give rise to an increase/decrease in the synaptic weight are commonly called *plasticity rules*, see [GKN+14]. A model of synaptic plasticity in an excitatory synapse in the rat hippocampus is presented in chapter 4.

1.2 Supervision and teaching

In the past years, I have co-supervised three PhD students (P. Helson, Q. Cormier and Y. Rodrigues) and three post-docs (A. Drogoul, B. Aymard and N. Vattuone). I have also mentored a dozen master students.

I have taught every year since 2013, with Etienne Tanré (Inria), a mathematical neuroscience course within the Master 2 Research "Mathematics, Vision and Learning"(ENS Cachan). The course is essentially an introduction to dynamical systems/stochastic processes applied to neu-

[1] We only plot one synapse per dendrite but axons typically contact the same neuron with many synapses.

roscience. I take care of the part of the course and tutorials on deterministic dynamics. See course webpage.

1.3 Context and research activity

During my postdoc at the Salk Institute, I became passionate about synaptic plasticity and how the connections between neurons evolve together with neuronal activity. This resulted in a collaboration with C. O'Donnell (University of Ulster), then a postdoc at the same institute.

"How the dynamics of neurons influence their connections which themselves shape this neuronal dynamics" is the common thread of my research. This lead to two non-independent lines of research:

1. Mathematical study of the dynamics of networks of spiking neurons.
2. Study / model synaptic plasticity.

The (stochastic) dynamics of synapses is generally modeled with plasticity rules [GKN+14] which are expressed as functions of the action potentials emission times from the connected neurons. Consequently, to mathematically study how synaptic plasticity impacts the dynamics of a network, one needs a simple and mathematically tractable model of a spiking neural network. It is essential, *at the very least*, to be able to study the network when synaptic plasticity is disregarded. We shall call them *non-plastic networks*.

In practice, I studied a *mean-field limit* approximation of these non-plastic networks in which the number of neurons is infinite.

It is natural to resort to jump processes [Dav93] to account for the phenomena described in the previous section. The jumps can be used to model the emission times of the action potentials and also the increments (decrements) of the value of the synaptic weights. However, the usual models of plasticity [GKN+14] must be adapted to follow the formalism of jump processes (see Pascal Helson's PhD thesis [Hel21] and also [RV21]).

In 2015, the authors of [DGL+15] introduced a model of stochastic spiking and a non-plastic neural network for which the dynamics of the neurons is described by a piecewise deterministic Markov process (PDMP) [Dav93]. N. Fournier and E. Löcherbach further studied this model in [FL16]. The advantage of this model compared to the classical model of network of *integrate-and-fire* (IF) neurons is that it is well-posed when the number of neurons tends to infinity [DIR+15]. It is also a natural stochastic generalization [GKN+14] of the IF model and has been my subject of study with two postdocs (Audric Drogoul, Benjamin Aymard) and a doctoral student (Quentin Cormier). Some results are presented in chapter 2.

Still as part of the research on non-plastic networks of spiking neurons, I also tried to take into account the fact that neurons have a dendrite which is, in particular, the receptacle of synaptic inputs from other neurons. This dendrite propagates electrical potentials generated by the synaptic inputs and its membrane potential is generally described with a linear model [Koc04; IT15]. When nonlinearities are taken into account, the dendrite can generate dendritic action potentials (dAP) that propagate along the dendrite [MRH+17; GVG+18]. Very nice mathematical questions arise when describing the dynamics of non-plastic networks of neurons with a

dendrite endowed with nonlinear dynamics; this was the subject of our work [FTV20] with N. Fournier (Sorbonne University) and E. Tanré (Inria). This is presented in chapter 3.

Finally, my collaboration with Cian O'Donnell led to the development of a stochastic model of excitatory synapse which accounts for a large number of biological phenomena related to synaptic plasticity. This model is based on a PDMP and was formulated during Yuri Rodrigues' thesis [Rod21] co-supervised with H. Marie (IPMC). The parameters of this model were adjusted by analyzing the stochastic dynamics of the proteins activation in a phase plane. This work is presented in chapter 4.

Thus, my research on synaptic plasticity led me to study and develop models of networks of neurons and of synapses described by PDMPs. I used methods from dynamical systems or probability theory to study the law of these processes.

1.4 Plan of the memoir

In connection with the description of the research program presented above, I have chosen to present the following work from my research.

- Study of the dynamics of a generalization of the non plastic network model from [DGL+15], see chapter 2.
- Study of a model of network of neurons interacting through their dendrites, see chapter 3.
- Modeling the CA3-CA1 excitatory synapse in the rat hippocampus, see chapter 4.

This choice is motivated by the desire to emphasize my ability to conduct research and to supervise students on mathematical subjects (cf. chapters 2, 3) or on modeling subjects, in collaboration with biologists (cf. chapter 4).

1.5 Topics not presented in this memoir

In addition to the studies detailed in this memoir, I worked on the following topics which I shall not develop here.

- *Modeling the visual cortex with spatially distributed models* [VCF15; SFV19; FSV22]. The tools are mainly based on equivariant bifurcation theory to study visual hallucinations using neural field models[2] [WC72] by taking advantage of the idealized symmetries of the visual cortex anatomy. This is a theme of my PhD thesis that I pursued with O. Faugeras (Inria) so I decided to not present it.
- *Study of delayed systems.* Application to spatially distributed models of cortex [Vel13] where the propagation delays between the neural populations are taken into account. The tools are based on bifurcation theory [HI11] and semigroup theory [EN00] to study the dynamics of delayed systems as function of parameters. This is another theme of my PhD thesis which I shall not present.

[2] These are ODEs in Banach spaces.

- *Study of slow-fast systems.* These systems display a difference of time scales which allows a specific analysis of their dynamics. We proved the local existence of a slow (invariant) manifold for infinite-dimensional dynamical systems in [ADV+20] such as PDEs, spatially distributed neural networks, etc. The goal of this project was to extend the *geometric singular perturbation theory* [Fen79] pioneered by Fenichel in the 1970s and developed for ODEs. It is too removed from the subject of this memoir to be developed here.

- In [CDI+23], we studied the processing of pain information by the spinal cord in collaboration with E. Deval (IPMC). Interestingly, we modeled specific ion channels that are activated by the acidity in the synaptic cleft unlike "classical" ion channels. This is an interesting collaboration with biologists but it does not relate well to the topic of this memoir, so I decided to leave this work aside.

- I will not present, for lack of space, the work [Hel21] of the PhD student Pascal Helson concerning the mathematical study of neural networks with plastic synapses modeled by jump processes. I chose to present a modeling topic instead (see chapter 4).

- *Study of neuromorphic systems* [DGP+18; DVD+21; DMV+20]. In collaboration with S. Barland (INPHYNI) and O. D'Huys (Maastricht University), we studied a physical emulation of a spiking neural network based on a matrix of semiconductor lasers. I participated in the supervision of the doctoral student A. Dolcemascolo supervised by S. Barland. Originally, the project was to implement plastic connections using optical elements but we did not manage to do so. The equations of the system are from laser physics and are thus removed from the subject of this memoir so I decided to not present this work.

- *Development of numerical methods to compute automatically numerical bifurcation diagrams of dynamical systems*, possibly in high dimension and on GPU [Vel20]. These methods are grouped in an open source library BifurcationKit.jl written in the Julia programming language. This library is not based on new algorithms that yield published articles. Hence, I chose not to present this tool although it is very useful to study the long term dynamics of dynamical systems (like the ones of chapter 2).

Chapter 2

Mean-field of networks of generalized integrate-and-fire neurons

We study in this chapter non plastic neural networks of spiking neurons with no spatial extension, e.g. the dendrite is discarded.

Motivations The work presented in this chapter is centered on the study of the long time behavior of a stochastic process $(X_t^{1,N}, \cdots, X_t^{N,N})_{t\geq 0}$ describing a neural network of size N in the limit $N = \infty$. We shall call this limit a *mean-field limit* because the interaction term between the neurons involves an expectation. The limit process $(X_t)_{t\geq 0}$ solves a *nonlinear* stochastic differential equation (SDE) in the sense of McKean meaning that the law of the process is involved in its dynamics. This nonlinear equation is called a McKean-Vlasov SDE.

We shall study the long time behavior of $(X_t)_{t\geq 0}$ using dynamical systems theory, as function of a parameter[1] which is the realm of bifurcation theory [HI11].

The law of $(X_t)_{t\geq 0}$ satisfies a nonlinear Fokker–Planck equation. The equilibria of the nonlinear Fokker–Planck equation are called invariant distributions. Apart from the question of their existence and uniqueness, we are interested in their dynamical stability. If we set the limit process close to an invariant distribution, does it converge to it for large times? Additionally, is it possible to find oscillatory behaviors? These questions can be studied using the spectral properties of the Fokker–Planck equation, by implementing a *Principle of Linearized Stability* [DS86] as in section 2.3 and going beyond as in section 2.4.4.

Note that these questions were already studied numerically in [Bru00] two decades ago ; we would like to make such analysis rigorous albeit for a different model of neuron.

Outline of the chapter We briefly explain the structure of the chapter. We start by presenting the equations of the finite size network and its mean-field limit in section 2.1. We then discuss our choice for the neuron model and our model of interactions before reviewing the literature on

[1] here we consider mainly the connectivity parameter J

mean-fields of spiking neural networks in section 2.2. We then present in section 2.3 the main result of [DV21] concerning the nonlinear stability of the invariant distribution of the mean-field limit in a simple case (basically when there is no drift). Then, in section 2.4, we present some results obtained by Quentin Cormier [Cor21] during his PhD concerning the nonlinear stability of the invariant distributions, improving a lot on [DV21], and concerning the existence of periodic solutions close to a Hopf bifurcation . We chose to present these results because we can compare the tools used in each work and also because the work of Quentin on periodic solutions provides a theoretical basis to the numerical conjectures made in [DV17].

2.1 Description of the model

2.1.1 Description of the finite network

We consider a network of N *excitatory* spiking neurons described by a PDMP (see [Dav93]) $X_t^N = (X_t^{1,N}, \cdots, X_t^{N,N}) \in \mathbb{R}_+^N$. The value of the transmembrane potential at the soma $(X_t^{i,N})_{t\geq 0}$ of the neuron $i \in [\![1, N]\!]$ satisfies a scalar ODE between the jumps (which models the emission of action potentials):

$$\frac{d}{dt} X_t^{i,N} = b(X_t^{i,N})$$

where the vector field $b : \mathbb{R}_+ \to \mathbb{R}$ is a deterministic smooth function. The spiking rate of neuron i at time t is $f(X_t^{i,N})$ and the rate function $f : \mathbb{R}_+ \to \mathbb{R}_+$ is deterministic and smooth. When the neuron i emits a spike at time t_s, its membrane potential is reset $X_{t_s+}^{i,N} = 0$ and the potential of the other neurons is incremented by a fixed, constant in time, value $J_{i\to j}^N \geq 0$ which models the total *synaptic current* caused by the spike of neuron i:

$$\forall j \neq i, \quad X_{t_s+}^{j,N} = X_{t_s-}^{j,N} + J_{i\to j}^N. \tag{2.1.1}$$

We assume that $b(0) \geq 0$ so that the dynamics stays in $\mathbb{R}_+$.

The process can be formally rewritten as a set of SDE driven by Poisson measures. Let $(\mathbf{N}^i(du, dz))_{i=1,\cdots,N}$ be a family of N independent Poisson measures on $\mathbb{R}_+ \times \mathbb{R}_+$ with Lebesgue intensity measure $dudz$. Let $(X_0^{i,N})_{i=1,\cdots,N}$ be a family of N random variables on $\mathbb{R}_+$, independent of the Poisson measures. Then $(X_t^{i,N})_{t\geq 0}$ is a *càdlàg* process solution of the system of SDEs:

$$\begin{aligned} \forall i \in [\![1, N]\!], \quad X_t^{i,N} = X_0^{i,N} + \int_0^t b(X_u^{i,N})du + \underbrace{\sum_{j\neq i} J_{j\to i}^N \int_0^t \int_{\mathbb{R}_+} \mathbb{1}_{\{z\leq f(X_{u-}^{j,N})\}} \mathbf{N}^j(du, dz)}_{\text{synaptic current}} \\ \underbrace{- \int_0^t \int_{\mathbb{R}_+} X_{u-}^{i,N} \mathbb{1}_{\{z\leq f(X_{u-}^{i,N})\}} \mathbf{N}^i(du, dz)}_{\text{reset to 0}}. \end{aligned} \tag{2.1.2}$$

2.1.2 The McKean-Vlasov SDE in the mean-field limit

The main idea of this section is to approximate the time evolution of one neuron, say $(X_t^{1,N})_{t\geq 0}$, interacting with a large number of other neurons, by the solution to a McKean-Vlasov SDE. Hence, we want to approximate the law of the membrane potentials $(X_t^N)_{t\geq 0}$ which belongs to $\mathcal{P}(\mathbb{R}_+^N)$ and satisfy a linear (Fokker-Planck) equation by a distribution belonging to $\mathcal{P}(\mathbb{R}_+)$ and satisfying a nonlinear equation.

We thus look at the mean-field limit $N \to \infty$ of (2.1.2) for which we assume the scaling of the law of large numbers:

$$\forall i, j \in [\![1, N]\!], \quad J_{i\to j}^N := \frac{J}{N} > 0.$$

We suppose that the initial conditions $X_0^{i,N}$ are *i.i.d.* with common law ν. As N goes to infinity, one expects *propagation of chaos*[2] to hold and thus that the law of $(X_t^{p,N}, \cdots, X_t^{k,N})$ for given integers $k \geq p \geq 0$, converges to $\mathcal{L}(X_t) \otimes \cdots \otimes \mathcal{L}(X_t)$ with X_t solution of

$$X_t = X_0 + \int_0^t b(X_u)du + J\int_0^t \mathbb{E}f(X_u)du - \int_0^t \int_{\mathbb{R}_+} X_{u-}\mathbb{1}_{\{z\leq f(X_{u-})\}}\mathbf{N}(du, dz). \tag{MKV}$$

In this equation, $\mathbf{N}$ is a Poisson measure on $\mathbb{R}_+^2$ with Lebesgue intensity measure $dudz$, the initial condition X_0 has law ν and is independent of $\mathbf{N}$. As stated above, this equation is nonlinear because the law of X_t appears in the term $\mathbb{E}f(X_u)$. That the particle system converges to the solution of (MKV) was proven under general assumptions on b, f in [DGL+15; FL16]; the authors also studied the *propagation of chaos*.

2.1.3 The nonlinear Fokker-Planck equation

Let $\nu(t, dx) := \mathcal{L}(X_t)$ be the law of X_t solution of (MKV). It solves the following nonlinear Fokker-Planck equation, in the sense of measures:

$$\begin{aligned} &\partial_t \nu(t, dx) + \partial_x \left[(b(x) + Jr(t))\nu(t, dx)\right] + f(x)\nu(t, dx) = r(t)\delta_0 \\ &\nu(0, dx) = \mathcal{L}(X_0), \quad r(t) := \int_{\mathbb{R}_+} f(x)\nu(t, dx). \end{aligned} \tag{NL-FP}$$

If $\mathcal{L}(X_t)$ has a density for all t, that is $\mathcal{L}(X_t) = g(t, x)dx$, then g solves the following strong form of (NL-FP)

$$\begin{aligned} &\partial_t g(t, x) + \partial_x \left[(b(x) + Jr(t))g(t, x)\right] + f(x)g(t, x) = 0, \\ &g(0, x)dx = \mathcal{L}(X_0), \quad r(t) = \int_{\mathbb{R}_+} f(x)g(t, x)dx, \end{aligned} \tag{NL-FP-strong}$$

with the boundary condition:

$$\forall t > 0, \quad (b(0) + Jr(t))\, g(t, 0) = r(t). \tag{2.1.3}$$

[2] or propagation of independence from $t = 0$

2.2 Selection of earlier works

2.2.1 Remarks on the choice of the network elements

To study the dynamics of networks of spiking neurons, one needs a model of neuron and a model of interactions. Additionally, some of the variability of the spike trains, as seen in biology, can be accounted by a noisy dynamics. How noise is introduced depends on how the action potential is modeled.

One of the earliest model of spiking neuron is that of Lapicque [Lap07] which assumed that the membrane potential satisfies $\tau \dot{V}_t = -V_t + RI$ until the spike time, I accounts for an external input current, τ is a time constant and R is the input resistance. The spike time is set as the time to reach a threshold which is a fixed parameter of the model. Finally, after a spike, the potential is reset to a resting value. Such neuron model is classically called [GKN+14] the *integrate-and-fire* (IF) model. Another way to model spike generation is to assume that spikes are produced intrinsically by the membrane dynamics through the opening and closing of ions channels. Such model [HH52] was proposed by the Nobel price winners Hodgkin and Huxley in 1952. Quadratic and exponential integrate-and-fire models (EIF) are famous examples of the nonlinear IF model. In particular the EIF has good foundations in experiments [BLB+08] and as simplification of the Hodgkin-Huxley model [FHV+03].

In these two models, variability can be simply modeled by adding a diffusion term to the dynamics. Another way to account for variability is to introduce a soft threshold in the *integrate-and-fire* model such that the neuron spikes with a probability which depends on the membrane potential V_t. These are known in the literature as *escape rate* models or *generalized integrate-and-fire* (GIF) models. We refer to [Bri88; Ger95; GKN+14; SDG17] and the references therein for a description of the GIF model. On a side note, the GIF model have been shown to be relevant for modeling real data [MNP+12]. See also [JBH+11] for fitting data to a jump diffusion IF.

Lastly, we need to describe the interactions. As briefly explained in section 1.1 and expended in chapter 4, the neurons are connected by synapses which roughly act as a tab, letting ions flow into the post-synaptic neuron. As a first approximation, one can assume that each pre-synaptic spike from neuron i causes the same electric charge $\propto J_{i\to j}$ to enter the postsynaptic neuron j which somehow justifies our jump condition (2.1.1). One of the first studies of such network is probably [Ger95] and [Ger00]. A more biologically relevant way to model the interaction between neurons is to consider conductance based models (see review on mean-field models of networks of neurons [CCD+20]).

The main reason why we choose to focus on networks of GIF is because it was shown in [DGL+15; FL16] that the mean-field dynamics does not blow up in finite time unlike the case of networks of noisy IF [CCP11; CGG+13; DIR+15].

2.2.2 Related studies based on jump processes

One of the first mathematical studies of networks of GIF [Ger95; Ger00] is [DGL+15] (see also [RT16]) in which the authors studied a close variant of (MKV) ; their mean-field limit writes:

$$X_t = X_0 - \lambda \int_0^t (X_u - \mathbb{E}X_u)\, du + \int_0^t \mathbb{E}f(X_u) du - \int_0^t \int_{\mathbb{R}_+} X_{u-} \mathbb{1}_{\{z \le f(X_{u-})\}} \mathbf{N}(du, dz). \quad (2.2.1)$$

Here, the constant λ is non-negative and the term $-\lambda(X_u - \mathbb{E}X_u)$ stems from modeling electrical synapses in addition to chemical ones[3]. In (MKV), we have discarded electrical synapses and have replaced this term with a more general deterministic drift $b(X_t)$. The authors of [DGL+15] proved existence and uniqueness of a weak solution of (2.2.1) as well as the convergence of the corresponding particle system towards this solution, under the additional assumption that the law of X_0 is compactly supported: there exists $R_0 > 0$ such that $\mathbb{P}(X_0 \in [0, R_0]) = 1$.

In [FL16], the authors were able to remove the compact support assumption of the initial condition. They also obtained results on the long time behavior of the solution of (2.2.1). They proved that (2.2.1) admits exactly two invariant distributions: the first one is δ_0, the second one ν^∞ has a density with an analytical expression. They showed that if $\mathbb{P}(X_0 = 0) < 1$, then δ_0 is not attracting. When $\lambda = 0$, they proved that the non-trivial invariant measure ν^∞ is globally attracting assuming that the law of X_0 has a density. We shall come back to this result in section 2.3 which reviews our work [DV21] where we showed that the convergence rate is locally exponential in time.

In [DV17], we numerically explored the behavior of the solution of (2.2.1) for $\lambda > 0$. We showed that periodic solutions appear for $f(x) = x^p$ with p and λ large enough. We also provided numerical evidences that the transition toward the periodic regime occurs via a Hopf bifurcation of the invariant measure ν^∞. Related considerations were made in the earlier study [Ger00].

The results in [DV21] are not satisfactory in many ways. They require too much regularity for $\mathcal{L}(X_0)$, they assume no drift $b = 0$, etc. This stems from the fact that we did not fully exploit the transport structure of the Fokker-Planck equation associated to (2.2.1). Instead, by relying on a probabilistic counterpart of the method of characteristics, we were able in [CTV20] to express the solution of (MKV) using a scalar quantity solution of a Volterra integral equation. This allowed to study in [CTV20] stability of the invariant distribution ν^∞ for general initial conditions[4]. Furthermore, based on the Lyapunov-Schmidt method, we proved in [CTV21] that (MKV) admits periodic solutions under spectral assumptions reminiscent of the Hopf bifurcation, thereby justifying some of the numerical observations made in [DV17].

This type of model continues to gather significant attention in recent research. Notable studies include investigations into the metastability of finite-sized networks [SDG17; LM22], its spatially structured variations [DOR15], and into its behavior in the case of sparse connectivity [JZ23]. Additionally, some research has been devoted to scaling factors beyond mean-field interactions [Löc22].

Closely related models based on Hawkes processes and some variants have been intensively studied in the neuroscience community [CCD+15; Che17; Aga22]. In particular, some of these

[3] which are accounted by the term $\mathbb{E}f(X_u)$

[4] In an arxiv paper [Cor20] by Q. Cormier, this result was complemented by proving local stability results.

works provide a probabilistic interpretation to the class of time-elapsed models introduced in the PDE setting [PPS09; PPS13; MW18; Gab18]. This time-elapsed model is closely related to [Ger95; Ger00]. Of note, the authors of [MW18] studied the weak form of the time-elapsed model in the space of Radon measures using semigroup theory [EN00], very similarly to the tools used in [DV21] ; see also [Gab18]. The time-elapsed model is closely related to (NL-FP-strong). The main mathematical difference is that the nonlinearity in (NL-FP-strong) is in the transport term making these equations quasilinear [Paz83].

2.3 PDE based approach

We present the results obtained in [DV21] with the postdoc Audric Drogoul. This work proves the local stability of the invariant distribution of the mean-field model in a simple case.

2.3.1 Notations

We denote by $\mathcal{X} := \mathrm{L}^1(\mathbb{R}_+, dl)$ the space of integrable functions from $\mathbb{R}_+$ to $\mathbb{R}$ where l is the Lebesgue measure, $\mathrm{L}^1_+(\mathbb{R}_+)$ its subspace of non-negative functions and $\hat{\mathcal{X}} := \left\{\phi \in \mathcal{X} \mid \int_0^\infty \phi = 0\right\}$ the subspace of functions with zero integral. We also define the Banach space $\mathcal{X}_2^{\mathbf{A}}$ ($\hat{\mathcal{X}}_2^{\mathbf{A}}$ is defined similarly)

$$\mathcal{X}_2^{\mathbf{A}} := \{\phi \in \mathcal{X},\ \phi'' \in \mathcal{X},\ f\phi' \in \mathcal{X},\ f^2\phi \in \mathcal{X},\ \phi(0) = \phi'(0) = 0\}$$

endowed with the norm

$$\|\phi\|_{2,\mathbf{A}} := \|\phi\|_{\mathcal{X}} + \|f^2\phi\|_{\mathcal{X}} + \|f\phi'\|_{\mathcal{X}} + \|\phi''\|_{\mathcal{X}}.$$

2.3.2 Main result

We consider a special case ($b = 0, J = 1$) of (NL-FP-strong):

$$\begin{cases} \partial_t g(t,x) = -a(g(t,\cdot))\partial_x g(t,x) - f(x)g(t,x),\ x,t > 0 \\ g(t,0) = 1, \\ g(0,\cdot) = g_0 \in \mathrm{L}^1_+(\mathbb{R}_+) \end{cases} \tag{2.3.1}$$

where

$$a(g) := \int_0^\infty f(x)g(x)dx. \tag{2.3.2}$$

Equation (2.3.1) has a unique stationary distribution g_∞ in L^1 given by:

$$g_\infty(x) := \exp\left(-\frac{1}{a_\infty}\int_0^x f\right). \tag{2.3.3}$$

We make the following assumptions concerning the rate function f. Typical examples are $f(x) = \exp(x)$ or $f(x) = x^4$.

Assumption 2.1. *f is convex increasing, $f(0) = 0$, $f(x) > 0$ for all $x > 0$, $\lim_\infty f = \infty$ and $f \in C^2(\mathbb{R}_+)$. Further assume that $\sup_{x\geq 1} \frac{f'(x)}{f(x)} + \frac{f''(x)}{f'(x)} < \infty$.*

In [FL16], the authors were able to prove the following result:

Theorem 2.2 ([FL16], proposition 9)**.** *Grant assumptions 2.1. Assume that $f(x) \geq c \cdot x^{\xi}$ for all $x \in [0,1]$ where $c > 0, \xi \geq 1$. For all initial conditions $g_0 \in \mathrm{L}^1_+(\mathbb{R}_+)$ of integral one such that $g(0) = 1$, $g_0 \in C^1_b(\mathbb{R}_+)$, $\int_0^\infty f^2 g_0 < \infty$ and $\int_0^\infty |g_0'| < \infty$, the solution of (2.3.1) converges to g_∞ in L^1:*

$$\|g(t) - g_\infty\|_{\mathrm{L}^1} \underset{t\to\infty}{=} O\left((1+t)^{-1/\xi}\right).$$

We improve some parts of this result in [DV21], namely we improve on the convergence rate but we have a local result.

Assumption 2.3. *f satisfies $f'(0) = 0$.*

Theorem 2.4. *Grant assumptions 2.1 and 2.3. The flow of (2.3.1) converges locally exponentially fast to g_∞ in $\mathcal{X}_2^{\mathbf{A}}$, that is for all $\epsilon > 0$ small enough, there is a neighborhood $\mathcal{V}_\epsilon \subset \{\phi \in \mathrm{L}^1(\mathbb{R}_+),\ \phi'' \in \mathrm{L}^1(\mathbb{R}_+),\ f\phi' \in \mathrm{L}^1(\mathbb{R}_+),\ f^2\phi \in \mathrm{L}^1(\mathbb{R}_+),\ \phi(0) = \phi'(0) = 0,\ \int \phi = 0\}$ and a constant $C_\epsilon \geq 1$ and*

$$\forall g_0 \in g_\infty + \mathcal{V}_\epsilon,\ \forall t \geq 0 \quad \|g(t) - g_\infty\|_{\mathrm{L}^1} \leq \|g(t) - g_\infty\|_{2,\mathbf{A}} \leq C_\epsilon e^{\left(s(\mathbf{A}_|)+\epsilon\right)t} \|g(0) - g_\infty\|_{2,\mathbf{A}}$$

where the spectral bound is known to be negative: $s(\mathbf{A}_|) < 0$.

The approach for proving the above theorem consists in studying (2.3.1) using the theory of semigroups [EN00]. The main argument of the proof is a nonlinear time change coupled with Picard's fixed point theorem.

2.3.3 Interpretation using dynamical system theory

We note that there is a one dimensional family of stationary solutions $(g_\alpha)_{\alpha>0}$ of (2.3.1) with expression

$$g_\alpha(x) := \exp\left(-\frac{1}{\alpha}\int_0^x f\right),$$

and only one of them g_∞, defined above in (2.3.3), is a stationary distribution *i.e.* with integral one. The existence of this family implies that zero is in the spectrum of the linearized equation: the *Principle of Linearized Stability* [DS86] does not apply directly which is a classical result to prove nonlinear stability ; we know however from [FL16] that g_∞ is attracting. There are several strategies to prove the long time convergence to g_α apart from entropy methods [Per07] which we have not looked at.

The first strategy relies on the local attractiveness of a center manifold [HI11] composed of the family $(g_\alpha)_{\alpha>0}$. To prove nonlinear stability, one would need to prove that the center manifold is locally attracting. Unfortunately, it is difficult to achieve such program as it relies on the fact that the linear flow is regularizing, which is not the case of transport equations and thus requires to use regular initial conditions.

The second strategy, which we shall rely on, is based on the observation that the flow of (2.3.1) conserves the mass. Hence, the nonlinear flow is foliated by the linear form $g \to \int_0^\infty g$.

The dynamics on each hyperplane possesses a unique equilibrium which is now hyperbolic. Thus, one can hope to prove nonlinear stability by simpler means in this case.

A third strategy, which is similar to the one used in [GM74], is to study the integral equation (see [FL16]) satisfied by $a(t) := \int_0^\infty f(x)g(t,x)dx$, this equation is akin to a Volterra one. The advantage of this approach lies in a simpler phase space and circumvents the issue of regularization noted above. It also allows to use probability measures for the initial condition. This approach is used in section 2.4.

Using the second strategy, we prove the existence of an exponentially attracting center manifold which is transverse to the hyperplanes associated with the linear form $g \to \int_0^\infty g$. This is noticeable as such a general result is not known for general transport equations. It is for example well known for delay differential equations [HV93; DvGV+95; vGJK+13; VF13] which are a kind of transport equation with a nonlinear boundary condition.

2.3.4 Difficulties and strategy of proof

Our general strategy is similar to that of [DS86; Ioo79]: we apply an iteration scheme to the nonlinear semigroup $\mathbf{S}(t_0)$ of solutions of (2.3.1) at some time fixed t_0 to show that it converges to the fixed point g_∞ with convergence rate that can be estimated. For this approach to work, we need a differentiable semigroup of solutions.

However, $\mathbf{S}$ is not differentiable on $\mathcal{X}_2^{\mathbf{A}}$ because the transport "speed" term $a(g(t,\cdot))$ in (2.3.1) depends on the solution itself $g(t,\cdot)$. To overcome this problem and inspired by [GH90], we perform a change of variable in time to make the transport speed constant by informally dividing (2.3.1) by $a(g(t,\cdot))$. We thus introduce h such that $h(\tau(t),x) := g(t,x)$ with $\tau = \int_0^t a(g(s,\cdot))ds$. This change of variable is possible if $\tau(t)$ is invertible: for example when $t \to a(g(t,\cdot))$ is strictly positive. Hence, we modify (2.3.1) locally (around g_∞) in order to insure that this condition is met. We then show that this new PDE induces a semigroup of solutions which is differentiable and characterizes the asymptotic behavior of the solution of (2.3.1).

2.3.5 Idea of proof

Preliminary step: the linearized equation We study the linear equation around g_∞ by writing $g(t,x) = g_\infty(x) + \phi(t,x)$ and obtain at first order in ϕ:

$$\begin{cases} \partial_t\phi(t,x) &= -a_\infty\partial_x\phi(t,x) - f(x)\phi(t,x) - a(\phi(t,\cdot))\partial_x g_\infty(x), \ x,t>0 \\ \phi(t,0) &= 0. \end{cases} \tag{2.3.4}$$

Using semigroup theory [EN00], we proved that (2.3.4) induces a strongly continuous semigroup $(\mathbf{T}(t))_{t\geq 0}$ of solutions on $\mathcal{X}$. The spectral analysis shows that there is a one dimensional spectral projector $\mathbf{P}_0$ for the zero eigenvalue such that $Ran(\mathrm{Id}-\mathbf{P}_0) = \widehat{\mathcal{X}}$. Writing $(\mathbf{T}_|(t))_{t\geq 0})$ the part of $(\mathbf{T}(t))_{t\geq 0}$ in $\widehat{\mathcal{X}}$, one finds that $(\mathbf{T}_|(t))_{t\geq 0}$ is uniformly exponentially stable, *i.e.* for every positive ϵ small enough, there is a constant $M_\epsilon \geq 1$ such that for all $t \geq 0$

$$\|\mathbf{T}(t) - \mathbf{P}_0\|_{\mathcal{L}(\mathcal{X})} = \left\|\mathbf{T}_|(t)\right\|_{\mathcal{L}(\mathcal{X})} \leq M_\epsilon e^{(s(\mathbf{A}_|)+\epsilon)t} \tag{2.3.5}$$

where $s(\mathbf{A}_|)$ is known to be negative.

Remarks 2.5. *These estimates can be transferred to the norm* $\|\cdot\|_{2,\mathbf{A}}$ *thanks to the Sobolev tower construction for semigroups (see [EN00]).*

Change of variable in time In order to perform a time rescaling, we introduce the cut-off function $\tilde{a}$ which is strictly positive and locally identical to $a(g)$ if this latter is close enough to a_∞:

$$\widetilde{a}(g) := a_\infty + \rho(a(g) - a_\infty).$$

It is based on the approximation of identity ρ shown in figure 2.1.

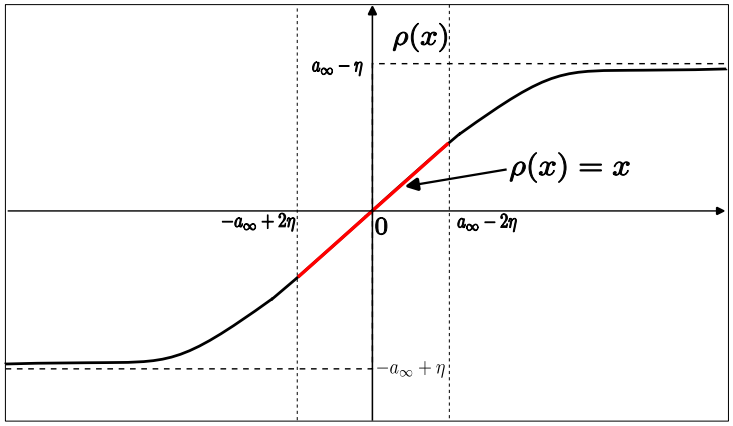

Figure 2.1: Approximation of identity used for the change of time variable, the parameter η satisfies $0 < \eta < a_\infty/2$.

Note that whenever possible, we write $\widetilde{a}(t)$ for $\widetilde{a}(g(t))$ or for $a_\infty + \rho(a(t))$ in case $a \in C^0(\mathbb{R}_+, \mathbb{R})$. We then formally perform the time rescaling:

$$h(\tau(t), x) := \widetilde{g}(t, x) \quad \text{with} \quad \tau(t) := \int_0^t \widetilde{a}(\widetilde{g}(s, \cdot))ds,$$

where $\widetilde{g}$ is the solution of (2.3.1) upon replacing $a(g)$ by $\widetilde{a}(g)$.

Finally, we translate the problem around g_∞ by writing $h = g_\infty + u$, it gives:

$$\begin{cases} \partial_\tau u(\tau, x) = -\partial_x u(\tau, x) - \frac{f(x)u(\tau,x)}{a_\infty + \rho(a(u(\tau)))} + \left(\frac{1}{a_\infty} - \frac{1}{a_\infty + \rho(a(u(\tau)))}\right) f g_\infty, \quad x, \tau > 0 \\ u(\tau, 0) = 0. \end{cases} \tag{2.3.6}$$

To study (2.3.6), we replace $a(u(\tau))$ by some function $a \in C^0(\mathbb{R}_+, \mathbb{R}_+)$ and consider the inhomogeneous problem:

$$\begin{cases} \dot{u}(\tau) = \mathbf{A}(\tau)u(\tau) + g_a(\tau), \ \tau > \sigma \geq 0 \\ u(\sigma) = \phi \in \mathcal{X}_2^{\mathbf{A}}, \end{cases} \tag{NAIH}$$

with

$$g_a(\tau) := \left(\frac{1}{a_\infty} - \frac{1}{a_\infty + \rho(a(\tau))}\right) f g_\infty$$

and $\mathbf{A}(\tau)\phi := -\partial_x\phi - \frac{f\phi}{a_\infty + \rho(a(t))}$. It admits a non-negative $\mathcal{X}_2^{\mathbf{A}}$–valued solution $u(\tau) := \mathbf{V}_a(\tau, \sigma)\phi$ with a closed-form expression. A solution of (2.3.6) is then a solution of (NAIH) such that $a(\tau) = a\left(\mathbf{V}_a(\tau, 0)\phi\right)$ using (2.3.2).

Construction of the re-scaled semigroup We establish the existence and uniqueness of a solution $\mathcal{A}(\phi)$ to the fixed point equation $a(\tau) = \int_0^\infty f\mathbf{V}_a(\tau,0)\phi$ in $C_b^0([0,\infty))$ for $\phi \in \mathcal{X}_2^{\mathbf{A}}$ and conclude on the existence of the nonlinear semigroup $(\mathbf{S}_r(\tau))_{\tau\geq 0}$ of solutions of (2.3.6) given by $\mathbf{S}_r(\tau)\phi := \mathbf{V}_{\mathcal{A}(\phi)}(\tau,0)\phi$. Finally we show that this semigroup is differentiable with differential at $\phi = 0$ given by $\mathbf{T}_|(\tau/a_\infty)$.

Exponential convergence Using a Picard iteration scheme from [Ioo79], we show that the stationary solution 0 of (NAIH) is locally exponentially attracting in $\widehat{\mathcal{X}}_2^{\mathbf{A}}$ meaning that for all $\epsilon > 0$ small enough, there is a neighborhood $\mathcal{V}_\epsilon \subset \widehat{\mathcal{X}}_2^{\mathbf{A}}$ such that

$$\exists C_\epsilon \geq 1 \quad \forall \phi \in \mathcal{V}_\epsilon,\ \forall \tau \geq 0 \quad \|\mathbf{S}_r(\tau)\phi\|_{2,\mathbf{A}} \leq C_\epsilon e^{\left(\frac{s(\mathbf{A}_|)}{a_\infty}+\epsilon\right)\tau}\|\phi\|_{2,\mathbf{A}}.$$

This estimate is based on (2.3.5) and remark 2.5. It is then straightforward to use the inverse time change of variable to obtain the conclusion of theorem 2.4.

2.3.6 Numerical evidences for Hopf bifurcation

The previous analysis provides no information for the case $\lambda \neq 0$ in (2.2.1). We were first convinced with the postdoc Audric Drogoul that local stability would hold in this case and we tried to prove it for some time. However, in [DV17], we managed to numerically find a set of parameters for which the solution of the mean-field (2.2.1) displays self-sustained oscillations (see figure 2.2). We also showed that the stationary distribution can become unstable for some

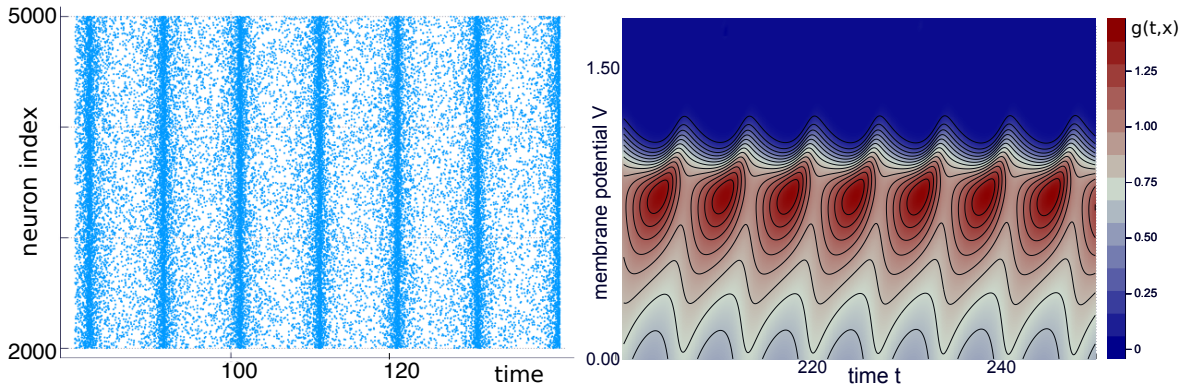

Figure 2.2: Left: Network simulation close to a Hopf bifurcation, network-wide oscillations are observed, $f(x) = x^8, \lambda = 0.3$. Each point represents an action potential emitted by a neuron at a given instant. Right: simulation of the nonlinear Fokker-Planck associated to (2.2.1) close to a Hopf bifurcation. The law $g(t,x)$ is displayed. Parameters: $f(x) = x^8, \lambda = 0.264$.

parameters.

2.4 Approach based on integral equation, PhD of Q. Cormier

The previous approach has many limitations. It does not make it possible to treat convergence in the sense of measures and thus supposes regular initial conditions. It adapts poorly to

more general sub-threshold neural dynamics[5] b which impose non-local and non-linear boundary conditions (see (NL-FP-strong)). Finally, it makes it difficult to apply bifurcation theory [HI11] in order to prove the existence of a Hopf bifurcation and thus to predict self-sustained oscillations, *i.e.* to provide a theoretical basis for the numerical conjectures [DV17], see figure 2.2.

These difficulties have been (partly) overcome by Quentin Cormier during his PhD on the long term behavior of the solutions of (MKV). He studied a nonlinear integral equation of the Volterra type satisfied by the average jump rate $\mathbb{E}(f(X_t))$ where $(X_t)_{t\geq 0}$ is solution to (MKV). This makes it possible to describe the law of the limit process $(X_t)_{t\geq 0}$. He stated a spectral criterion for the stability of invariant distributions [CTV20; Cor20] for measure valued initial laws $\mathcal{L}(X_0)$. Finally, he was able to state a criterion for the existence of a Hopf bifurcation for (MKV) and thus provided tools for the existence of periodic solutions for the mean-field process when the connectivity parameter J is close to a critical value [CTV21].

2.4.1 General strategy

The general strategy for [CTV20; Cor20; CTV21] relies on the following ideas. In short, it allows to reduce the analysis of the long time behavior of the limit process $(X_t)_{t\geq 0}$ to that of the non-autonomous jump rate $\mathbb{E}f(X_t)$. It is convenient to introduce, at this stage, the space of measures:

$$\mathcal{M}(f^2) := \{\nu \in \mathcal{P}(\mathbb{R}_+) : \quad \int_{\mathbb{R}_+} f^2(x)\nu(dx) < \infty\}.$$

Linearized problem

Like in the previous section with (NAIH), we get around the difficulty of studying the nonlinear problem (MKV) by introducing a "linearized" version. Fix $s \geq 0$ and let $\boldsymbol{a} \in \mathrm{L}^1_{loc}([s,\infty),\mathbb{R}_+)$ be a deterministic function, that we call the *external current*[6]. We consider the linear SDE which describes a unique neuron with external current $\boldsymbol{a}$:

$$\forall t \geq s, \quad Y^{\boldsymbol{a},\nu}_{t,s} = Y^{\boldsymbol{a},\nu}_{s,s} + \int_s^t b(Y^{\boldsymbol{a},\nu}_{u,s})du + \int_s^t a_u du - \int_s^t \int_{\mathbb{R}_+} Y^{\boldsymbol{a},\nu}_{u-,s} \mathbb{1}_{\{z\leq f(Y^{\boldsymbol{a},\nu}_{u-,s})\}} \mathbf{N}(du,dz) \quad \text{(LIN)}$$

where $\mathcal{L}(Y^{\boldsymbol{a},\nu}_{s,s}) = \nu \in \mathcal{M}(f^2)$. Under quite general assumptions on b and f, this SDE has a path-wise unique solution ; it also has a unique invariant distribution ν^∞_α when the external current is constant $a_t = \alpha > 0$. We denote the jump rate of this SDE by:

$$\forall t \geq s, \quad r^\nu_{\boldsymbol{a}}(t,s) := \mathbb{E}f(Y^{\boldsymbol{a},\nu}_{t,s}). \tag{2.4.1}$$

Note that if $Y^{\boldsymbol{a},\nu}_{0,0} = X_0$ then $(Y^{\boldsymbol{a},\nu}_{t,0})_{t\geq 0}$ is a solution of (MKV) if it satisfies the closure condition

$$\forall t \geq 0, \quad a_t = Jr^\nu_{\boldsymbol{a}}(t,0).$$

Conversely, any solution to (MKV) is a solution to (LIN) with $a_t = J\mathbb{E}f(X_t)$.

[5] recall that we assumed a null drift $b = 0$ in the previous section

[6] Note that we follow the same notations for a as in section 2.3. Indeed, these notations match when $J = 1$.

Volterra equation satisfied by the jump rate

Looking at (LIN), we consider the density $K^\nu_{\boldsymbol{a}}(t,s)$ of the first jump $\tau_s^{\boldsymbol{a},\nu}$ which has a closed-form expression[7]. We prove in [CTV20] that $r^\nu_{\boldsymbol{a}}$ satisfies the Volterra integral equation

$$\forall t \geq s, \quad r^\nu_{\boldsymbol{a}}(t,s) = K^\nu_{\boldsymbol{a}}(t,s) + \int_s^t K^{\delta_0}_{\boldsymbol{a}}(t,u) r^\nu_{\boldsymbol{a}}(u,s) du. \tag{2.4.2}$$

When $a_t = \alpha$, the above equation is a Volterra equation with a convolution kernel. It holds that $r^\nu_\alpha(t,s) = r^\nu_\alpha(t-s,0)$ and we simply write $r^\nu_\alpha(t) := r^\nu_\alpha(t,0)$.

Transfer of the jump rate asymptotic behavior to the one of $(X_t)_{t\geq 0}$

Using the external current $a_t := J\mathbb{E}f(X_t)$, we can estimate the long time behavior of $(X_t)_{t\geq 0}$ with initial condition $\mathcal{L}(X_0) = \nu \in \mathcal{M}(f^2)$. Assume that there are constants[8] $\lambda, C > 0$ and $\alpha^* \geq 0$ such that

$$\forall t \geq 0, \quad |\mathbb{E}f(X_t) - \nu^\infty_{\alpha^*}(f))| := |\mathbb{E}f(Y^{\boldsymbol{a},\nu}_{t,0}) - \nu^\infty_{\alpha^*}(f))| := |r^\nu_{\boldsymbol{a}}(t,0) - \nu^\infty_{\alpha^*}(f)| \leq Ce^{-\lambda t},$$

where the external current α^* satisfies the closure condition $\alpha^* = J\nu^\infty_{\alpha^*}(f)$. Then, if $\phi : \mathbb{R}_+ \to \mathbb{R}$ is a bounded Lipschitz-continuous function, one finds that

$$\forall\ 0 < \lambda' < \min(\lambda, f(\sigma_0)),\ \exists D > 0 \quad \text{s.t.} \quad \forall t \geq 0, \quad |\mathbb{E}\phi(X_t) - \nu^\infty_{\alpha^*}(\phi)| \leq De^{-\lambda' t} \tag{2.4.3}$$

where $\sigma_0 := \inf\{x \geq 0\ :\ b(x) = 0\}$.

Estimation of the long time behavior of r

The previous paragraph shows that we can restrict the study of the long time behavior of the law of the solution of (MKV) to that of the jump rate. Denote by $\mathcal{B}(\mathbb{R}_+;\mathbb{R})$ the Borel-measurable functions from $\mathbb{R}_+$ to $\mathbb{R}$ and define for any constant $\lambda \geq 0$ the Banach space

$$L^\infty_\lambda := \{\boldsymbol{h} \in \mathcal{B}(\mathbb{R}_+;\mathbb{R}),\ ||\boldsymbol{h}||^\infty_\lambda < \infty\}, \qquad \text{endowed with} \qquad ||\boldsymbol{h}||^\infty_\lambda := \operatorname*{ess\,sup}_{t\geq 0} |h_t| e^{\lambda t}.$$

We first focus on the case of a constant external current, $a_t = \alpha > 0$. Using Laplace transform estimates, one finds in [CTV20] a constant $\lambda^*_\alpha > 0$ such that for all $\lambda \in (0, \lambda^*_\alpha)$ and all initial laws $\nu \in \mathcal{M}(f^2)$:

$$r^\nu_\alpha(\cdot,0) - \nu^\infty_\alpha(f) \in L^\infty_\lambda. \tag{2.4.4}$$

By the previous paragraph, this implies that $Y^{\alpha,\nu}_{t,0}$ converges in law to its invariant distribution ν^∞_α. Then, the result is extended to non constant currents of the form $a_t = \alpha + h_t$ where $\boldsymbol{h}$ belongs to L^∞_λ for some $\lambda < \lambda^*_\alpha$. More specifically, we proved that there exists $\delta > 0$ such that for all $\boldsymbol{h} \in L^\infty_\lambda$ with $||\boldsymbol{h}||^\infty_\lambda < \delta$ and all $\nu \in \mathcal{M}(f^2)$, one has

$$r^\nu_{\alpha+\boldsymbol{h}}(\cdot,0) - \nu^\infty_\alpha(f) \in L^\infty_\lambda.$$

[7] one finds $K^\nu_{\boldsymbol{a}}(t,s) = \int_{\mathbb{R}_+} f(\varphi^{\boldsymbol{a}}_{t,s}(x)) \exp\Big(-\int_s^t f(\varphi^{\boldsymbol{a}}_{u,s}(x))du\Big)\nu(dx)$ where $\varphi^{\boldsymbol{a}}_{t,s}(x_0)$ is the flow of $\dot{x}_t = b(x_t) + a_t$ with initial condition x_0 at time s.

[8] that may depend on b, f, ν, and J

2.4.2 First main result: local stability of invariant distributions

We now present some results of Quentin's thesis [Cor21] concerning the local stability of the invariant distributions based on a spectral condition ; this extends significantly the results of [DV21]. Some conditions are imposed on the drift b and on the rate function f that we shall comment briefly. For $a_t \geq 0$, we call $\varphi_t^{\boldsymbol{a}}(x_0)$ the flow of $\dot{x}_t = b(x_t) + a_t$ with initial condition $x(0) = x_0$.

Assumption 2.6. *The drift $b : \mathbb{R}_+ \to \mathbb{R}$ is $\mathcal{C}^2$, with $b(0) \geq 0$ and*

$$\sup_{x \geq 0} |b'(x)| + |b''(x)| < \infty.$$

This boundedness assumption is used to control the asymptotic behavior of $\phi_t^{\boldsymbol{a}}$ for large t.

Assumption 2.7. *The rate function $f : \mathbb{R}_+ \to \mathbb{R}_+$ is $\mathcal{C}^2$, strictly increasing, with $f(0) = 0$, $\sup_{x \geq 1} \frac{|f''(x)|}{f(x)} < \infty$ and there exists a constant C_f such that*

1. *for all $x, y \geq 0$, $f(xy) \leq C_f(1 + f(x))(1 + f(y))$.*
2. *for all $A > 0$, $\sup_{x \geq 0} Af'(x) - f(x) < \infty$.*
3. *for all $x \geq 0$, $|b(x)| \leq C_f(1 + f(x))$.*

These assumptions are essentially used to provide a unique solution to (MKV). Next, we look at the invariant distributions of (LIN) when $a_t = \alpha > 0$. The trivial distribution δ_0 is invariant for (MKV) if $b(0) = 0$.

Proposition 2.8. *Let f and b such that assumptions 2.6 and 2.7 hold. The non-trivial invariant distributions of (MKV) are $\{\nu_\alpha^\infty \mid \alpha \in (0, \infty), \alpha = J\gamma(\alpha)\}$, where ν_α^∞ is given by*

$$\nu_\alpha^\infty(dx) := \frac{\gamma(\alpha)}{b(x) + \alpha} \exp\left(- \int_0^x \frac{f(y)}{b(y) + \alpha} dy \right) \mathbb{1}_{[0, \sigma_\alpha)}(x) dx$$

with $\gamma(\alpha)$ a normalizing factor. Note that $\gamma(\alpha)$ is the jump rate under ν_α^∞: $\gamma(\alpha) := \nu_\alpha^\infty(f)$. The upper bound σ_α of the support of ν_α^∞ is given by

$$\sigma_\alpha := \lim_{t \to \infty} \varphi_t^\alpha(0) \in \mathbb{R}_+^* \cup \{+\infty\}. \tag{2.4.5}$$

We recover the previous expression (2.3.3) when $b = 0$.

Assumption 2.9. *The constant $\alpha > 0$ satisfies one of the following non-degeneracy conditions:*

$$\sigma_\alpha < \infty \quad \text{and} \quad b'(\sigma_\alpha) < 0 \tag{2.4.6}$$

$$\textbf{or} \qquad \sigma_\alpha = \infty \quad \text{and} \quad \inf_{x \geq 0} b(x) + \alpha > 0. \tag{2.4.7}$$

If $\sigma_\alpha < \infty$, we have a technical restriction on the size of the support of the initial law:

Definition 2.10. *Define*

$$\tilde{\sigma}_\alpha := \inf\{x > \sigma_\alpha \mid b(x) + \alpha = 0\}, \quad \textit{with} \quad \inf \emptyset = +\infty,$$
$$\mathcal{S}_\alpha := \{[0, \beta],\ \sigma_\alpha \leq \beta < \tilde{\sigma}_\alpha\},$$

with the convention that $\mathcal{S}_\alpha := \{\mathbb{R}_+\}$ *when* $\sigma_\alpha = +\infty$.

Given $S \in \mathcal{S}_\alpha$, we denote by $\mathcal{M}_S(f^2)$ the set of probability measures with support included in S and such that $\int_S f^2(x)\mu(dx) < \infty$. We equip $\mathcal{M}_S(f^2)$ with the distance

$$\forall \nu, \mu \in \mathcal{M}(f^2), \quad d(\nu, \mu) := \int_{\mathbb{R}_+} [1 + f^2(x)]|\nu - \mu|(dx). \tag{2.4.8}$$

Finally, for $\alpha > 0$ and ν_α^∞, we define

$$\forall t \geq 0, \quad \Theta_\alpha(t) := \int_0^\infty \left[\frac{d}{dx} r_\alpha^{\delta_x}(t)\right] \nu_\alpha^\infty(dx). \tag{2.4.9}$$

We recall from from (2.4.4) in paragraph 2.4.1 that λ_α^* is related to the largest exponential convergence rate of the jump rate r_α^ν to $\nu_\alpha^\infty(f)$. We have now defined all the quantities to state the main result on the local stability of ν_α^∞.

Theorem 2.11 ([Cor21; Cor20])**.** *Consider an invariant distribution* ν_α^∞ *of* (MKV) *for some* $\alpha > 0$. *Grant assumptions 2.6, 2.7 and 2.9. Define the "abscissa" as:*

$$\lambda'_\alpha := - \sup_{z \in \mathbb{C}, \Re(z) > -\lambda_\alpha^*} \{\Re(z) \mid J\widehat{\Theta}_\alpha(z) = 1\}.$$

It holds that $\lambda'_\alpha \in [-\infty, \lambda_\alpha^*]$. *Assume that*

$$\lambda'_\alpha > 0. \tag{2.4.10}$$

Then for all $\lambda \in (0, \lambda'_\alpha)$, ν_α^∞ *is locally exponentially stable with rate* λ. *That is, for all* $S \in \mathcal{S}_\alpha$ *and all* $\epsilon > 0$, *there exists* $\rho > 0$ *such that*

$$\forall \nu \in \mathcal{M}_S(f^2), \quad d(\nu, \nu_\alpha^\infty) < \rho \implies \sup_{t \geq 0} |J\mathbb{E}f(X_t^\nu) - \alpha| e^{\lambda t} < \epsilon,$$

where (X_t^ν) *is the solution of* (MKV) *with initial law* ν.

We can then apply (2.4.3) to conclude on the convergence in law of $(X_t)_{t \geq 0}$ to ν_α^∞.

In order to apply the previous theorem, we need to compute the zeros of $J\widehat{\Theta}_\alpha(z) - 1$. By differentiating the Volterra equation with respect to x (*e.g.* for the initial law $\nu = \delta_x$), one can obtain an analytical expression for $\widehat{\Theta}_\alpha$ in terms of f, b, α.

Alternatively, one can consider (NL-FP) linearized around ν_α^∞ in the space of measures with zero mass, and show formally that the zeros[9] of $J\widehat{\Theta}_\alpha(z) - 1$ are the eigenvalues associated with the linearized equation. This suggests that the previous theorem should implement a *Principle of Linearized Stability* which is well known in the case of ODEs or "nice" PDEs [Hen81].

[9] more precisely, the ones close to $\{z \in \mathbb{C}\ ;\ \Re(z) = 0\}$

2.4.3 Idea of proof

Thanks to the transfer (2.4.3) of the jump rate asymptotic behavior to the one of $(X_t)_{t\geq 0}$ explained in the section 2.4.1, we can focus on the study of the jump rate. The strategy follows the proof of the implicit function theorem applied to the mapping

$$\Phi(\nu, \boldsymbol{h}) := Jr^{\nu}_{\alpha+\boldsymbol{h}}(\cdot, 0) - (\alpha + \boldsymbol{h}),$$

which maps $\mathcal{M}(f^2) \times L^\infty_\lambda$ to L^∞_λ. Obviously one has $\Phi(\nu^\infty_\alpha, 0) = 0$. We first prove that the function $\boldsymbol{h} \mapsto \Phi(\nu, \boldsymbol{h})$ is Fréchet differentiable on L^∞_λ when $\nu \in \mathcal{M}_S(f^2)$. Its Fréchet derivative at $(\nu^\infty_\alpha, 0)$ is given by

$$\forall c \in L^\infty_\lambda, \quad [D_h\Phi(\nu^\infty_\alpha, 0) \cdot c](t) = -c(t) + J\int_0^t \Theta_\alpha(t-u)c(u)du$$

where Θ_α was introduced in (2.4.9). This linear mapping is invertible when 2.4.10 holds. We then introduce the sequence

$$\boldsymbol{h}_0 := 0, \quad \boldsymbol{h}_{n+1} = \boldsymbol{h}_n - [D_h\Phi(\nu^\infty_\alpha, 0)]^{-1} \cdot \Phi(\nu, \boldsymbol{h}_n)$$

and show that it converges to a solution of $\Phi(\nu, \boldsymbol{h}) = 0$ when ν is close enough to ν^∞_α. This provides the local convergence to ν^∞_α.

Remarks 2.12. *Let us put the two previous approaches of section 2.3 and subsection 2.4.2 in context. There are several ways to prove a Principle of Linearized Stability, and more generally to prove the existence of an (attracting) invariant manifold, for an ODE $\dot{x} = Ax + G(x) \in \mathbb{R}^n$ where A is a matrix and $G(x) = O(x^2)$ near $x = 0$. We denote by $\phi^t(x_0)$ the flow of this ODE.*

1. *A first method is based on the variation of constant formula and on the fact that e^{tA} converges to zero exponentially fast as $t \to \infty$, see [Hen81].*
2. *A second method is to look for solutions of the ODE in the space $\{x \in C(\mathbb{R}_+), e^{\lambda t}x(t)$ is bounded$\}$ for some $\lambda > 0$. This is roughly the strategy of subsection 2.4.2. See also [HI11] for a variant based on the properties of the linear unbounded operator $\frac{d}{dt} - A$.*
3. *Another method [DS86] consists in showing that $x_{n+1} = \phi^1(x_n)$ converges to zero and then extend this convergence to $\phi^t(x_0)$. This is essentially the strategy of section 2.3.*

Each method puts more emphasis on the properties of the nonlinear semigroup $(\phi^t)_{t\geq 0}$ or on the properties of the vector field. In the case of PDE, depending on the regularizing properties of the flow or the ease to build the nonlinear semigroup, some methods are more adapted than the others.

2.4.4 Second main result: around the Hopf bifurcation

In this part, we present the main result of [CTV21] concerning the existence of periodic solutions to (MKV). In essence, this is very close to the Hopf bifurcation theorem. The classical Hopf bifurcation theorem can be found in [Kie03].

Definition 2.13. *A family of probability measures $(\nu(t))_{t\in[0,T]}$ is said to be a T-periodic solution of (MKV) if*

1. $\nu(0) \in \mathcal{M}(f^2)$.
2. *For all $t \in [0,T]$, $\nu(t) = \mathcal{L}(X_t)$ where $(X_t)_{t\in[0,T]}$ is the solution of (MKV) starting from $X_0 \sim \nu(0)$.*
3. *It holds that $\nu(T) = \nu(0)$.*

Consider an invariant measure $\nu^\infty_{\alpha_0}$ of (MKV) for some $\alpha_0 > 0$. We assume that the stability criterion (2.4.10) is not satisfied for α_0:

Assumption 2.14. *There exist $\alpha_0 > 0$ and $\tau_0 > 0$ such that*

$$J\widehat{\Theta}_{\alpha_0}(\tfrac{i}{\tau_0}) = 1 \quad \text{and} \quad \frac{d}{dz}\widehat{\Theta}_{\alpha_0}(\tfrac{i}{\tau_0}) \neq 0.$$

In order ensure that the functional (see paragraph 2.4.5 below) used to find the periodic solutions has a differential with a two-dimensional kernel, we make the following assumption which is very classical in the Hopf bifurcation theorem [Kie03].

Assumption 2.15 (Non-resonance condition)**.** *Assume that for all $n \in \mathbb{Z}\backslash\{-1,1\}$,*

$$J\widehat{\Theta}_{\alpha_0}(\tfrac{in}{\tau_0}) \neq 1.$$

It can be shown that under assumption 2.15, in a neighborhood of $\alpha = \alpha_0$, the invariant measure of (MKV) is (locally) unique and parameterized by α.

We also assume that the eigenvalue $\frac{i}{\tau_0}$ crosses the imaginary axis at non zero speed. This is formalized in the next lemma and hypothesis. At this stage, it is convenient to introduce the function

$$J(\alpha) := \frac{\alpha}{\nu^\infty_\alpha(f)}. \tag{2.4.11}$$

We recall from proposition 2.8 that the nonlinear invariant distributions ν^∞_α are in bijection with the solutions to the equation $J(\alpha) = J$.

Lemma 2.16. *Under assumption 2.14, there exist $\eta_0, \varrho_0 > 0$ and a function $\mathfrak{Z}_0 \in \mathcal{C}^1((\alpha_0 - \eta_0, \alpha_0 + \eta_0); \mathbb{C})$ with $\mathfrak{Z}_0(\alpha_0) = \frac{i}{\tau_0}$ such that for all $z \in \mathbb{C}$ with $|z - \frac{i}{\tau_0}| < \varrho_0$ and for all $\alpha > 0$ with $|\alpha - \alpha_0| < \eta_0$ we have*

$$J(\alpha)\widehat{\Theta}_\alpha(z) = 1 \iff z = \mathfrak{Z}_0(\alpha). \tag{2.4.12}$$

Assumption 2.17. *Assume that $\alpha \mapsto \mathfrak{Z}_0(\alpha)$ crosses the imaginary part with non-vanishing speed, that is*

$$\Re \frac{d}{d\alpha}\mathfrak{Z}_0(\alpha_0) \neq 0.$$

After these assumptions, we are now in position to state the main result of this section concerning the existence of periodic solutions.

Theorem 2.18 ([CTV21])**.** *Consider b, f satisfying assumptions 2.6 and 2.7. Let $\alpha_0, \tau_0 > 0$ be such that 2.9, 2.14 and 2.15 and 2.17 hold. Then, there exists a family of $2\pi\tau_v$-periodic solutions of (MKV), parametrized by $v \in (-v_0, v_0)$, for some $v_0 > 0$. More precisely, there exists a continuous curve $\{(\nu_v(\cdot), \alpha_v, \tau_v),\ v \in (-v_0, v_0)\}$ such that*

1. *For all $v \in (-v_0, v_0)$, $(\nu_v(t))_{t\in\mathbb{R}}$ is a $2\pi\tau_v$-periodic solution of (MKV) with $J = J(\alpha_v)$.*
2. *The curve passes through $(\nu^\infty_{\alpha_0}, \alpha_0, \tau_0)$ at $v = 0$. In particular we have for all $t \in \mathbb{R}$, $\nu_0(t) \equiv \nu^\infty_{\alpha_0}$.*
3. *The "periodic current" $\boldsymbol{a}_v$, defined by*

$$t \mapsto a_v(t) := J(\alpha_v) \int_{\mathbb{R}_+} f(x)\nu_v(t, dx), \tag{2.4.13}$$

   is continuous and $2\pi\tau_v$-periodic. Moreover, its mean over one period is α_v:

$$\frac{1}{2\pi\tau_v} \int_0^{2\pi\tau_v} a_v(u)du = \alpha_v.$$

4. *Furthermore, v is the amplitude of the first harmonic of a_v, that is for all $v \in (-v_0, v_0)$*

$$\frac{1}{2\pi\tau_v} \int_0^{2\pi\tau_v} a_v(u)\cos(u/\tau_v)du = v \quad \text{and} \quad \frac{1}{2\pi\tau_v} \int_0^{2\pi\tau_v} a_v(u)\sin(u/\tau_v)du = 0.$$

Every other periodic solution in a neighborhood of $\nu^\infty_{\alpha_0}$ is obtained from a phase-shift of one such ν_v. More precisely, there exist small enough constants $\epsilon_0, \epsilon_1 > 0$ (only depending on b, f, α_0 and τ_0) such that if $(\nu(t))_{t\in\mathbb{R}}$ is any $2\pi\tau$-periodic solution of (MKV) for some value of $J > 0$ such that

$$|\tau - \tau_0| < \epsilon_0 \quad \text{and} \quad \sup_{t\in[0,2\pi\tau]} \left| J \int_{\mathbb{R}_+} f(x)\nu(t, dx) - \alpha_0 \right| < \epsilon_1,$$

then there exists a shift $\theta \in [0, 2\pi\tau)$ and $v \in (-v_0, v_0)$ such that $J = J(\alpha_v)$ and

$$\forall t \in \mathbb{R}, \quad \nu(t) \equiv \nu_v(t + \theta).$$

This result gives a theoretical ground to the numerical observations made in [DV17] (see also figure 2.2) albeit for a slightly different model (2.2.1). Direct numerical applications of the above theorem to (MKV) can be found in Q. Cormier's thesis [Cor21].

2.4.5 Idea of proof

We give an outline of the proof of theorem 2.18 which is an adaptation of the proof of the Hopf theorem in [Kie03]. It is convenient to introduce some spaces at this stage:

$$C^0_T := \{\boldsymbol{a} \in C^0(\mathbb{R}, \mathbb{R}) \text{ is T-periodic}\}$$
$$C^{0,0}_T := \{\boldsymbol{h} \in C^0_T \text{ such that } \int_0^T h(u)du = 0\}.$$

We first reduce the problem of finding periodic solutions to (MKV) to finding zeros in $C^0_{2\pi\tau}$ of some functional for a period $2\pi\tau$ to be determined.

We thus study an isolated neuron subjected to a periodic external current $\boldsymbol{a} \in C^0_{2\pi\tau}$ such that $\inf a + b(0) > 0$[10]. We obtain an analytical expression for the unique $2\pi\tau$-periodic solution of (LIN). The density $(\tilde{\nu}_{\boldsymbol{a}}(t))_{t\in[0,2\pi\tau]}$ of this solution plays the role of the invariant distribution in the previous section 2.4.2. The jump rate of this solution

$$\rho_{\boldsymbol{a}} := \mathbb{E} f(Y_{t,0}^{\boldsymbol{a},\tilde{\nu}_{\boldsymbol{a}}(0)})$$

belongs to $C^0_{2\pi\tau}$. Consequently, finding a $2\pi\tau$-periodic solution of (MKV) is equivalent to finding $\boldsymbol{a} \in C^0_{2\pi\tau}$ such that

$$\boldsymbol{a} = J\rho_{\boldsymbol{a}}. \tag{2.4.14}$$

Still, the period $2\pi\tau$ is unknown. To address this problem, we re-scale time to only consider 2π-periodic functions. We thus define

$$\forall \boldsymbol{d} \in C^0_{2\pi}, \forall \tau > 0, \quad \rho_{\boldsymbol{d},\tau} := \mathcal{T}_\tau(\rho_{\mathcal{T}_{1/\tau}(\boldsymbol{d})}), \quad \text{with} \quad \forall t \geq 0,\ \mathcal{T}_\tau(\boldsymbol{d})(t) := d(\tau t).$$

Furthermore, if the mean of $\boldsymbol{d}$ over one period is α, that is if $\boldsymbol{d} = \alpha + \boldsymbol{h}$ for some $\boldsymbol{h} \in C^{0,0}_{2\pi}$, we prove that the mean number of spikes over one period only depends on α, namely

$$\frac{1}{2\pi}\int_0^{2\pi} \rho_{\alpha+\boldsymbol{h},\tau}(u)du = \nu^\infty_\alpha(f). \tag{2.4.15}$$

After these preliminaries, we look for periodic solutions using the Lyapunov-Schmidt method. We thus introduce the functional (recall that $J(\alpha) := \frac{\alpha}{\nu^\infty_\alpha(f)}$ from (2.4.11)):

$$(\boldsymbol{h}, \alpha, \tau) \mapsto G(\boldsymbol{h}, \alpha, \tau) := (\alpha + \boldsymbol{h}) - J(\alpha)\rho_{\alpha+\boldsymbol{h},\tau},$$

which maps $C^{0,0}_{2\pi} \times \mathbb{R}^*_+ \times \mathbb{R}^*_+$ to $C^{0,0}_{2\pi}$ using (2.4.15). We obviously have $G(0, \alpha, \tau) = 0$. The roots of G match the periodic solutions of (MKV) by using the current $\boldsymbol{a} := \mathcal{T}_{1/\tau}(\alpha + \boldsymbol{h})$ which solves (2.4.14) with $J = J(\alpha)$.

We then show that G is Frechet differentiable and that $D_h G(0, \alpha_0, \tau_0)$ is a Fredholm operator of index zero, with a kernel of dimension two. We can thus apply the Lyapunov-Schmidt method to obtain an equivalent problem of dimension two, in effect parameterized by the kernel of $D_h G(0, \alpha_0, \tau_0)$. We then find the zeros in $\mathbb{R}^2$ of the reduced problem using the implicit function theorem which gives periodic solutions to (2.4.14).

2.5 Perspectives

Theorem 2.18 gives a theoretical support to the numerical observations made in [DV17]. It is however not completely satisfactory. For example, if we were to vary the parameter J and find a value J_h for which the conditions of the theorem 2.18 are fulfilled, on which side of J_h do the periodic solutions exist? This could be answered by computing the second derivative of the functional G with respect to v as done in [Kie03].

[10] This is satisfied by assumption2.9

Additionally, the theorem 2.18 provides no information on the stability of the periodic solutions. The proof based on the Lyapunov-Schmidt method is not tailored for this question as it merely tackles the question of existence of periodic solutions. One could develop a *Principle of Linearized Stability* like in section 2.4.2, *i.e.* compute the Floquet exponents of the periodic orbit but this seems a lot of work.

A method to answer both questions could be to prove the existence of an invariant and finite dimensional center manifold for (NL-FP) onto which the dynamics is two dimensional thereby allowing the use of bifurcation theory for ODEs. In order to achieve this, one could apply the results of [HI11] but we likely face the same regularization issues that we tried to circumvent in [DV21]. Another idea would be to take inspiration of the tools in [CHT97] which make assumptions on the nonlinear semigroup of solutions of (NL-FP) rather than on the PDE itself [HI11]. This is more in the spirit of overall strategy used in section 2.4.4. See [LP20] for a related approach applied to the mean-field of networks of FitzHugh-Nagumo neurons where the authors prove the existence of periodic orbits using an invariant manifold which stems from the slow-fast dynamics.

The work presented in this chapter on the mean-field limit of stochastic spiking neural networks offers other interesting research perspectives.

- Generalization to the case where the neural dynamics between the jumps is two dimensional or explodes in finite time. This is a class of models widely used in computational neuroscience [Izh06]. I studied this case, numerically, with the postdoc Benjamin Aymard supervised in collaboration with Fabien Campillo (Inria). Many difficulties appear in particular for the existence of invariant probabilities.

- We can consider plastic neural networks by adding a dynamics on the connectivity weight J. This is the subject of Pascal Helson's thesis that I co-supervised with Etienne Tanré (Inria) and in which we restricted ourselves to a much simpler neuron model than the one considered in this chapter. There are therefore many open questions in this case, see [PSW17] for a related study with a diffusive model.

Chapter 3

Networks of neurons interacting through their dendrites

We study in this chapter a mean-field of non plastic networks of spiking neurons each one with a nonlinear dendritic compartment. This is an example for which the mean-field limit is not completely obvious unlike in the previous chapter. This chapter is a summary of the results from [FTV20].

Motivations The starting point of this study is [GVG+18] where it is shown that an isolated neuron with a single dendritic compartment supporting (sodium) dendritic spikes has a smaller firing rate in response to correlated synaptic inputs distributed along the dendrite compared to non correlated ones. This was based on the facts that synaptic inputs generate dendritic spikes and when dendritic spikes collide, they cancel out due to the refractory period (see figure 3.1).

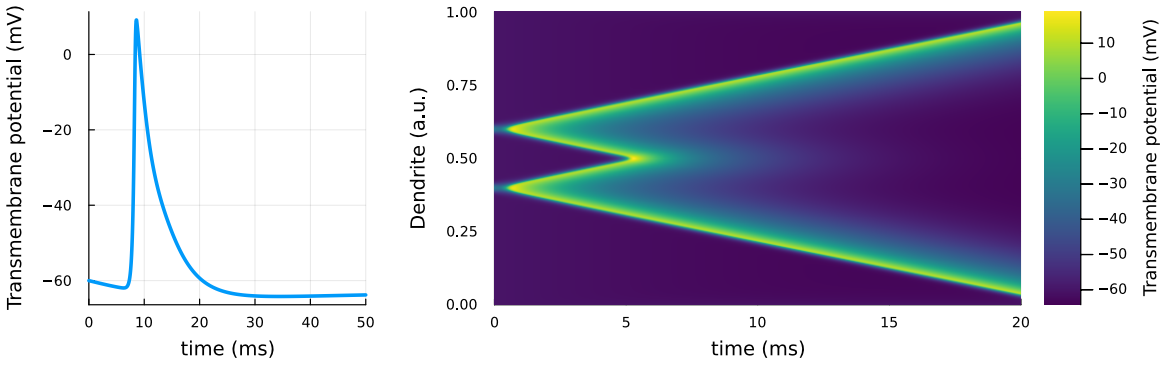

Figure 3.1: Simulation of colliding dendritic spikes using a Hodgkin-Huxley model with diffusive coupling. Left: transmembrane potential at dendritic location $x \approx 0.25$. Right: space-time plot of dendrite transmembrane potential. Two spikes are generated at $t = 0$ which propagate in both directions and annihilate upon collision at $t \approx 5$.

In the previous chapter, we focused on models of neurons without dendrite. Although models of neurons with dendrites have been studied in the literature [RHD01; DRP03], few mathematical studies of such networks are available [IT15]. In the context of synaptic plasticity, the study of such neurons is of great importance because:

1. The synapses are located on the dendrite. The (local) electric potentials produced by the synapse inputs interact to generate an action potential at the level of the soma ; the dendrite is therefore an essential component of the phenomenon of plasticity.
2. The plasticity of synapses is based on the near coincidence of pre-synaptic signals and action potentials back propagating from the soma (bAP). This effect is not taken into account here. See chapter 4 for more details.

In [IT15], the authors investigated a mean-field limit of networks of spiking neurons each one with a dendritic compartment supporting a *diffusive* propagation of electrical potentials. In [FTV20], we considered a network of spiking neurons each one with a dendrite supporting dendritic action potentials [MRH+17] which propagate without alteration and annihilate upon collision ; basically a non-linear version of the diffusive propagation used in [IT15]. The goal of this chapter is to identify the limit process (see (dMKV) below) when the number of neurons tends to infinity, a much more difficult task than in the previous chapter where the limit process was straightforward to identify.

3.1 Description of the network

Remarks 3.1. *In this chapter, we denote by front a dendritic action potential (dAP). We make this choice to follow the terminology of [FTV20].*

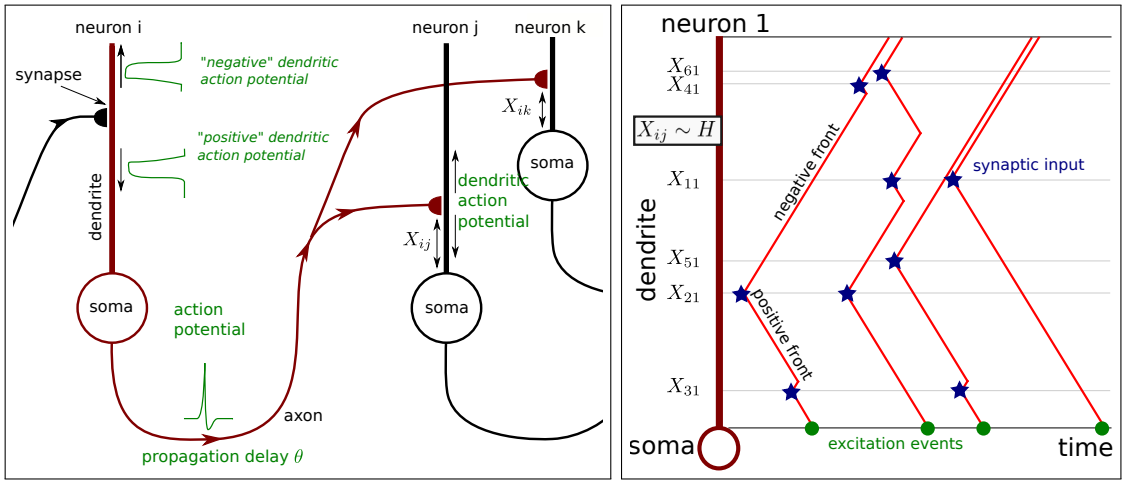

Figure 3.2: Left: layout of the network considered in this chapter. Right: plots of the different quantities involved in the dynamics of fronts in a single dendrite.

We consider a network of n excitatory neurons, each equipped with a linear dendrite of length $L > 0$, and having a soma at one of its two ends. Our setup involves *i.i.d.* Bernoulli random

variables $(\xi_{ij})_{i,j\in\{1,\dots,n\}}$ with parameter $p_n \in (0,1)$, as well as some *i.i.d.* $[0,L]$-valued random variables $(X_{ij})_{i,j\in\{1,\dots,n\}}$ with probability density H on $[0,L]$. If $\xi_{ij}=1$, then the neuron i is connected to the neuron j, and a *synapse* is positioned, on the dendrite of the j-th neuron, at distance X_{ij} from its soma, see figure 3.2 left.

We denote by $V_t^{i,n}$ the transmembrane potential at the soma of the i-th neuron at time $t \geq 0$. We assume that initially, the random variables $(V_0^{i,n})_{i=1,\dots,n}$ are *i.i.d.* with law $f_0 \in \mathcal{P}([v_{min},\infty))$.

3.1.1 Dendritic compartment

When a neuron *spikes* (say, the neuron i, at time τ), its potential is reset to v_{min} (*i.e.* $V_{\tau^+}^{i,n} = v_{min}$) and, for all j such that $\xi_{ij}=1$, two fronts start, after some (propagation) delay θ (*i.e.* at time $\tau+\theta$), on the dendrite of the j-th neuron and at distance X_{ij} of the soma. The fronts, referred to as "positive fronts", move towards the soma, and simultaneously, "negative fronts" move away from the soma.

On the dendrite of each neuron, we thus have fronts moving with constant velocity ρ. Negative fronts disappear upon reaching the end of the dendrite, while the interaction of a positive front with a negative front results in the vanishing of both fronts (see figure 3.1). When a positive front eventually reaches the soma (say, of the i-th neuron at time σ), the membrane potential of neuron i is increased by $w_n > 0$, *i.e.* $V_\sigma^{i,n} = V_{\sigma^-}^{i,n} + w_n$ and the positive front disappears. This occurrence is referred to as an "*excitation event*".

Although it might seem unnatural, we assume that there are no fronts on any dendrite at time 0. This simplifying assumption greatly facilitates the analysis.

3.1.2 Somatic compartment

It remains to describe when the neurons spike. In between jumps (corresponding to *spikes* or *excitation events*), the membrane potentials of all the neurons satisfy the ODE

$$\forall i \in [\![1,n]\!], \quad \frac{d}{dt}V_t^{i,n} = F(V_t^{i,n}),$$

with $F(v_{min}) \geq 0$ so that all membrane potentials remain above v_{min}. Similarly to the previous chapter, the spiking rate of neuron i at time t is $\lambda(V_t^{i,n})$ and the rate function $\lambda : [v_{min},\infty) \mapsto \mathbb{R}_+$ is deterministic. The jump associated to a spike is described in the previous section 3.1.1.

Remarks 3.2. *We call λ the rate function in this chapter. We chose not to follow the notations of the previous chapter where the rate function was written f. Also, the drift here is written F instead of b. Finally, the number of neurons in the network is n whereas it was N in the previous chapter. Indeed, we find it more convenient to follow the notations of [FTV20] in case the reader wants to look at it.*

Remarks 3.3. *We do not discuss the results of [FTV20] concerning another neuron model termed the "hard model" (which is in fact the* integrate-and-fire *model) by lack of space. For this model, we are able to derive an explicit formula for the electric current produced by the excitation events.*

3.2 Heuristic scales and relevant quantities

Each neuron is roughly influenced by $N = np_n$ others and we naturally consider the asymptotic limit $N \to \infty$.

Using a version by Calder, Esedoglu and Hero [CEH14] of some results of Deuschel and Zeitouni [DZ95] concerning the length of the longest increasing subsequence in a cloud of *i.i.d.* points in $[0,1]^2$, we deduce the following result. Consider a single dendrite of length L, as well as a Poisson point process $(T_i, X_i)_{i\geq 1}$ on $[0,\infty) \times [0,L]$, with intensity measure $Ng(t)dtH(x)dx$, H being the repartition density defined in section 3.1. For each $i \geq 1$, one positive and one negative front start from X_i at time T_i traveling with constant velocity $\rho > 0$. Apply the annihilation rules described above in subsection 3.1.1 and call $L_N(t)$ the number of *excitation events* occurring during $[0,t]$. Under a few assumptions on H and g, in probability,

$$\lim_{N\to\infty} \frac{L_N(t)}{\sqrt{N}} = \Gamma_t(g),$$

where $\Gamma_t(g)$ is deterministic and more or less explicit, see definition 3.8.

We are interested in a regime in which each neuron spikes around once per unit of time. This implies that on each dendrite, there are around $2N$ fronts starting per unit of time. Even if we are clearly not in a strict Poissonian case, it seems reasonable to think that there will be around $\sqrt{N}$ excitation events per unit of time (for each neuron). Consequently, each neuron will see its membrane potential increased by $w_n\sqrt{N}$ per unit of time and we naturally consider the asymptotic

$$w_n\sqrt{N} \to w \in (0,\infty).$$

Smaller values of w_n would make negligible the influence of the *excitation events*, while higher values of w_n would lead to explosion (infinite frequency of spikes).

One could be surprised by this normalization $N^{-1/2}$ (and not N^{-1} for example) which is the right scaling for the electric current from the dendrite to the soma to be non trivial as the number of synapses goes to infinity.

3.3 Formulation of the nonlinear problem

The influence of a given neuron (say, the one labeled 2) on another one (say, the one labeled 1) being small (because the neuron 2 only produces a proportion $1/(np_n) \ll 1$ of the fronts influencing the neuron 1), we expect that some asymptotic independence should hold true. Such a phenomenon is usually called *propagation of chaos*, see previous chapter section 2.1.2.

Our aim is to prove, **assuming** propagation of chaos, as well as some conditions on the parameters of the models, that there is a unique possible reasonable limit process in the regime $N = np_n \to \infty$ and $w_n\sqrt{N} \to w \in (0,\infty)$.

We thus formulate the following *nonlinear* problem. Fix an initial distribution $f_0 \in \mathcal{P}([v_{min},\infty))$ for V_0. Can one find a deterministic non-decreasing continuous function $(\kappa_t)_{t\geq 0}$ starting from 0

such that, when considering the process

$$V_t = V_0 + \int_0^t F(V_s)ds + \kappa_t + \underbrace{\sum_{s\in[0,t]} (v_{min} - V_{s-})\mathbb{1}_{\Delta J_s \neq 0}}_{resets\ to\ v_{min}\ after\ spikes},$$

with spike counting process J_t jumping at rate $\lambda(V_t)$ [1], and denoting by $(T_k)_{k\geq 1}$ its jumping times:

- introduce an *i.i.d.* family $(X_i)_{i=1,\dots,N}$ with density H and an *i.i.d.* family $((T_k^i)_{k\geq 1})_{i=1,\dots,N}$ of copies of $(T_k)_{k\geq 1}$,
- create, on a single linear dendrite with length L, one positive front and one negative front from X_i (for all $i = 1, \dots, N$) at each instant $T_k^i + \theta$ (for all $k \geq 1$), moving with velocity ρ, and subjected to the annihilation procedure described in subsection 3.1.1 and,

when denoting by K_t^N the resulting number of *excitation events* occurring during $[0, t]$, does one have

$$\forall t \geq 0, \quad \lim_{N\to\infty} wN^{-1/2}K_t^N = \kappa_t \quad ?$$

Under a few conditions on f_0, F, λ and H, we prove the existence of a unique solution $(\kappa_t)_{t\geq 0}$ to the above problem. Furthermore, the process $(V_t)_{t\geq 0}$ solves a nonlinear Poisson-driven stochastic differential equation and $\kappa_t = \Gamma_t((\mathbb{E}[\lambda(V_s)])_{s\geq 0})$ where Γ_t is defined in section 3.2. Our conditions are quite general when the delay θ is positive, and rather restrictive, at least from a mathematical point of view, when $\theta = 0$.

3.4 Notations and main results

We expose our notation, assumptions and main results in details.

Assumption 3.4. *The length $L > 0$, the speed $\rho > 0$ and the minimum membrane potential v_{min} are fixed.*

3.4.1 Partial order and associated longest chains

We first study the number of (positive) fronts hitting the soma of a dendrite, named *excitation events*. It appears that it can be easily expressed using a partial order.

Definition 3.5 (Partial order)**.** *We introduce the partial order $\preceq$ on $[0, \infty) \times [0, L]$ defined by*

$$(s, x) \preceq (s', x') \text{ if } |x - x'| \leq \rho \cdot (s' - s).$$

We say that $(s, x) \prec (s', x')$ if $(s, x) \preceq (s', x')$ and $(s, x) \neq (s', x')$.

[1] all this can be properly written using Poisson measures

For a Radon point measure[2] $\nu = \sum_{i\in I} \delta_{M_i}$, the set $\mathcal{S}_\nu = \{M_i : i \in I\}$ consisting of distinct points of $[0,\infty) \times [0,L]$, we define $A(\nu) \in \mathbb{N} \cup \{\infty\}$ as the length of the longest increasing subsequence of $\mathcal{S}_\nu$. In other words,

$$A(\nu) := \sup\{k \geq 0 : \text{there exist } i_1, \dots, i_k \in I \text{ such that } M_{i_1} \prec \cdots \prec M_{i_k}\}.$$

For $t \geq 0$, we introduce

$$D_t := \{(s,x) \in [0,\infty) \times [0,L] : (s,x) \preceq (t,0)\} \tag{3.4.1}$$

and set $A_t(\nu) := A(\nu|_{D_t})$.

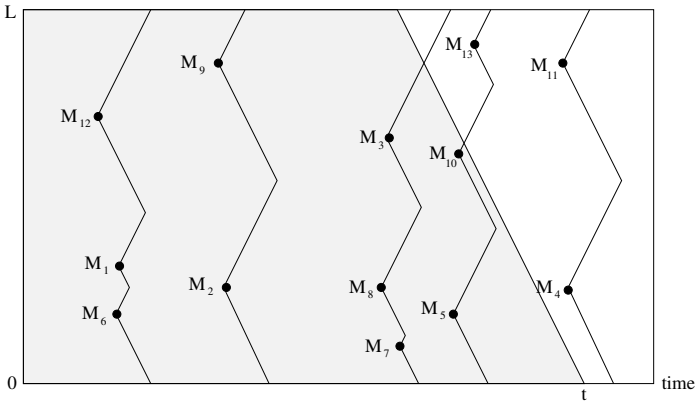

Figure 3.3: Space-time diagrams of front propagation. y-axis is dendrite, x-axis is time. All oblique segments have slopes $\pm\rho$. The points $(M_i)_{i=1}^{13}$ are the support of the Radon point measure ν. The domain in gray is D_t. For example $M_1 \prec M_2 \prec M_8 \prec M_5 \prec M_4$ so that $A(\nu) = 4$.

The following fact, crucial to our study, is closely linked with Hammersley's lines, see *e.g.* Cator and Groeneboom [CG05].

Proposition 3.6. *Consider a Radon point measure $\nu = \sum_{i\in I} \delta_{M_i}$, the set $\mathcal{S}_\nu := \{M_i = (t_i, x_i) : i \in I\}$ consisting of distinct points of $[0,\infty) \times [0,L]$. Consider a dendrite, represented by the segment $[0,L]$, with its soma located at 0. For each $i \in I$, make start two fronts from x_i at time t_i, one* positive front *going toward the soma and one* negative front *going away from the soma. Assume that all the fronts move with constant velocity ρ. When two fronts meet, they disappear. When a front reaches one of the extremities of the dendrite, it disappears.*
We assume that

$$\text{for all } i,j \in I \text{ with } i \neq j,\ |x_j - x_i| \neq \rho \cdot |t_j - t_i|, \tag{3.4.2}$$

which implies that no front starts precisely from some (space/time) position where there is already a front. The number of fronts hitting the soma is given by $A(\nu)$ and the number of fronts hitting the soma before time t is given by $A_t(\nu)$.

The following observation is obvious by definition (although not completely obvious from the point of view of fronts).

[2] We recall that a nonnegative measure ν on $[0,\infty) \times [0,L]$ is *Radon* if $\nu(B) < \infty$ for all compact subset B of $[0,\infty) \times [0,L]$.

Remarks 3.7. *Consider two Radon point measures ν and ν' on $[0,\infty)\times[0,L]$ such that $\nu \leq \nu'$ (i.e. $\mathcal{S}_\nu \subset \mathcal{S}_{\nu'}$). Then $A(\nu) \leq A(\nu')$ and, for all $t \geq 0$, $A_t(\nu) \leq A_t(\nu')$.*

3.4.2 The functional Γ

The role of Γ was explained roughly in section 3.2. See Deuschel and Zeitouni [DZ95] for quite similar considerations.

Definition 3.8. *Fix a continuous function $H : [0,L] \mapsto \mathbb{R}_+$. For $g : [0,\infty) \mapsto \mathbb{R}_+$ measurable and $t \geq 0$, we set*

$$\Gamma_t(g) := \sup_{\beta\in\mathcal{B}_t} \mathcal{I}_t(g,\beta) \quad \text{where} \quad \mathcal{I}_t(g,\beta) := \sqrt{\frac{2}{\rho}} \int_0^t \sqrt{H(\beta(s))g(s)[\rho^2 - (\beta'(s))^2]}ds,$$

$\mathcal{B}_t$ being the set of C^1-functions $\beta : [0,t] \mapsto [0,L]$ such that $\beta(t) = 0$ and $\sup_{[0,t]} |\beta'(s)| < \rho$.

It is important, in the above definition, to require H to be continuous. Modifying the value of H at one single point can change the value of $\Gamma_t(g)$. The following observations are immediate.

Remarks 3.9.

(i) Consider $\beta \in \mathcal{B}_t$. The condition $\sup_{[0,t]} |\beta'(s)| < \rho$ implies that the map $s \mapsto (s,\beta(s))$ is increasing for the order $\prec$. The conditions that β is $[0,L]$-valued and that $\beta(t) = 0$ imply that for all $s \in [0,t]$, $(s,\beta(s)) \in D_t$.

(ii) If $H(0) = \max_{[0,L]} H$, then $\Gamma_t(g) = \sqrt{2\rho H(0)} \int_0^t \sqrt{g(s)}ds$ for all $t \geq 0$.

Concerning (ii), it suffices to note that $\beta \equiv 0$ maximizes $\mathcal{I}_t(g,\beta)$.

3.4.3 The spiking model

We describe the hypothesis underlying the spiking dynamics of $V_t^{i,n}$. We impose some of the following conditions.

Assumption 3.10.

(i) There are $p \geq 1$ and $C > 0$ such that the initial distribution $f_0 \in \mathcal{P}([v_{min},\infty))$ satisfies $\int_{v_{min}}^\infty (v - v_{min})^p f_0(dv) < \infty$.

(ii) The continuous rate function $\lambda : [v_{min},\infty) \mapsto \mathbb{R}_+$ satisfies $\lambda(v) \leq C(1 + (v - v_{min}))^p$ for all $v \geq v_{min}$, $C > 0$ being a constant. Also, λ vanishes on a neighborhood of v_{min}, i.e.

$$\alpha := \inf\{v \geq v_{min} : \lambda(v) > 0\} \in (v_{min},\infty). \tag{3.4.3}$$

(iii) The drift $F : [v_{min},\infty) \mapsto \mathbb{R}$ is locally Lipschitz continuous, satisfies $F(v_{min}) \geq 0$ and $F(v) \leq C(1 + (v - v_{min}))$ for all $v \geq v_{min}$.

(iv) The repartition density H of the connections is continuous on $[0,L]$.

Remarks 3.11.

- *The assumption $F(v_{min}) \geq 0$ ensures that the solution of (3.4.4) stays in $[v_{min}, \infty)$.*
- *Assumption 3.10 (ii) induces a refractory period: a neuron spiking at time t cannot spike again during $(t, t+\delta]$ for some deterministic $\delta > 0$.*

Additionally, we may require stronger assumptions when the propagation delay is zero: $\theta = 0$.

Assumption 3.12. *With α defined in (3.4.3),*

- *The initial distribution f_0 is compactly supported, $f_0((\alpha, \infty)) > 0$,*
- *$F(\alpha) \geq 0$,*
- *λ is locally Lipschitz continuous on $[v_{min}, \infty)$ and positive and non-decreasing on (α, ∞).*

In the next proposition, we describe the dynamics of an isolated neuron subjected to a non-negative electric current r_t.

Proposition 3.13. *Grant assumption 3.10. Consider $r : [0, \infty) \mapsto \mathbb{R}_+$ continuous, non-decreasing and such that $r_0 = 0$. Let V_0 be f_0-distributed and let $\mathbf{N}(dt, du)$ be a Poisson measure on $[0, \infty) \times [0, \infty)$ with intensity $dtdu$, independent of V_0. Let $\mathcal{F}_t = \sigma(\{V_0, \mathbf{N}(A) : A \in \mathcal{B}([0,t] \times [0, \infty))\})$ be the filtration associated to $V_0, \mathbf{N}$. There is a pathwise unique càdlàg $(\mathcal{F}_t)_{t\geq 0}$-adapted process $(V_t^r)_{t\geq 0}$ solving*

$$V_t^r = V_0 + \int_0^t F(V_s^r)ds + r_t + \int_0^t \int_0^\infty (v_{min} - V_{s-}^r)\mathbb{1}_{\{u \leq \lambda(V_{s-}^r)\}}\mathbf{N}(ds, du). \tag{3.4.4}$$

It takes values in $[v_{min}, \infty)$ and satisfies $\mathbb{E}[\sup_{[0,T]}(V_t^r - v_{min})^p] < \infty$ for all $T > 0$. We set

$$J_t^r := \sum_{s \leq t} \mathbb{1}_{\{\Delta V_t^r \neq 0\}} = \int_0^t \int_0^\infty \mathbb{1}_{\{u \leq \lambda(V_{s-}^r)\}}\mathbf{N}(ds, du).$$

The process $(V_t^r)_{t\geq 0}$ represents the time evolution of the membrane potential at the soma of one neuron, *assuming* that the excitation events resulting from the interaction with all other neurons during $[0, t]$ produces an increase of potential equal to r_t, and J_t^r stands for its number of spikes during $[0, t]$. Indeed, between its spike instants, the membrane potential V_t^r evolves as $V' = F(V) + r_t'$. The Poisson integral is precisely designed so that V^r is reset to v_{min} (since $V_{s-}^r + (v_{min} - V_{s-}^r) = v_{min}$) at rate $\lambda(V_{s-}^r)$.

3.4.4 Main results

The next proposition is the main step for identifying the mean-field limit (dMKV). We recall from the previous proposition that J_t^r stands for the number of jumps of the process $(V_t^r)_{t\geq 0}$ during $[0, t]$.

Proposition 3.14. *Grant assumption 3.10 and fix a delay $\theta \geq 0$. Fix a non-decreasing continuous function $r : [0, \infty) \mapsto \mathbb{R}_+$ with $r_0 = 0$. Consider an i.i.d. family $((J_t^{r,i})_{t\geq 0})_{i\geq 1}$ of copies of $(J_t^r)_{t\geq 0}$. For each $i \geq 1$, denote by $(T_k^i)_{k\geq 1}$ the jump instants of $(J_t^{r,i})_{t\geq 0}$, written in chronological order (i.e. $T_k^i < T_{k+1}^i$). Consider an i.i.d. family $(X_i)_{i\geq 1}$ of random variables with density H, independent of the family $((J_t^{r,i})_{t\geq 0})_{i\geq 1}$. For $N \geq 1$, let $\nu_N^r = \sum_{i=1}^N \sum_{k\geq 1} \delta_{(T_k^i+\theta, X_i)}$. Then for any $t \geq 0$,*

$$\lim_{N\to\infty} N^{-1/2} A_t(\nu_N^r) = \Gamma_t(h_r^\theta) \text{ a.s.},$$

where

$$h_r(t) := \mathbb{E}[\lambda(V_t^r)] \text{ and } h_r^\theta(t) := h_r(t-\theta)\mathbb{1}_{\{t\geq\theta\}}.$$

Let us explain this result. If we have N independent neurons whose electric potentials evolve as $(V_t^r)_{t\geq 0}$. If all the spikes from these neurons create fronts (after a delay θ) on the dendrite of another neuron, say labeled 0, and these fronts evolve and annihilate as described in proposition 3.6, then the number of fronts hitting the soma of the 0-labeled neuron between 0 and t equals $A_t(\nu_N^r)$. If each of these *excitation events* induces an increase of the soma membrane potential of neuron 0 by

$$w_N = wN^{-1/2}$$

(with $w > 0$), then, at the limit, the membrane potential will be increased by $w\Gamma_t(h_r^\theta)$ during $[0, t]$.

Remarks 3.15. *Note that the measure ν_N^r in proposition 3.14 contains events with non negative times $T_k^i + \theta$ meaning that the dendrite of the 0-labeled neuron is initially empty.*

We are now in position to state the main result of this chapter in which we identify the mean-field limit of the finite network of neurons, essentially identifying the dynamics of the 0-labeled neuron.

Theorem 3.16. *Grant assumption 3.10 and fix $w > 0$ and $\theta \geq 0$.*

(i) A non-decreasing continuous $\kappa : [0, \infty) \mapsto \mathbb{R}_+$ such that $\kappa_0 = 0$ solves $w\Gamma_t(h_\kappa^\theta) = \kappa_t$ for all $t \geq 0$ if and only if $\kappa = w\Gamma((\mathbb{E}[\lambda(V_{s-\theta})]\mathbb{1}_{\{s\geq\theta\}})_{s\geq 0})$, for some $[v_{min}, \infty)$-valued càdlàg $(\mathcal{F}_t)_{t\geq 0}$-adapted solution $(V_t)_{t\geq 0}$ to the nonlinear SDE (here V_0, $\mathbf{N}$ and $(\mathcal{F}_t)_{t\geq 0}$ are as in proposition 3.13):

$$V_t = V_0 + \int_0^t F(V_s)ds + w\Gamma_t((\mathbb{E}[\lambda(V_{s-\theta})]\mathbb{1}_{\{s\geq\theta\}})_{s\geq 0}) + \int_0^t \int_0^\infty (v_{min} - V_{s-})\mathbb{1}_{\{u\leq\lambda(V_{s-})\}}\mathbf{N}(ds, du) \quad \text{(dMKV)}$$

satisfying $\mathbb{E}[\sup_{[0,T]}(V_t - v_{min})^p] < \infty$ for all $T > 0$.

(ii) Assume either that $\theta > 0$ or grant assumption 3.12. Then there exists a unique $[v_{min}, \infty)$-valued càdlàg $(\mathcal{F}_t)_{t\geq 0}$-adapted solution $(V_t)_{t\geq 0}$ to (dMKV) such that for all $T > 0$, $\mathbb{E}[\sup_{[0,T]}(V_t - v_{min})^p] < \infty$.

Remarks 3.17. *Observe that if the density H reaches its maximum at 0, then (dMKV) has a simpler form, since*

$$w\Gamma_t((\lambda(V_{s-\theta})]\mathbb{1}_{\{s\geq\theta\}})_{s\geq 0}) = \int_0^{(t-\theta)\vee 0} \sqrt{\gamma\mathbb{E}[\lambda(V_s)]}ds$$

with $\gamma = 2\rho H(0)w^2$, see remark 3.9.

Consider the n-particle system described in section 3.1 and denote by $(V_t^{1,n})_{t\geq 0}$ the time-evolution of the membrane potential of the first neuron and by $(J_t^{1,n})_{t\geq 0}$ the process counting its spikes. Theorem 3.16 tells us that, *if propagation of chaos holds true* and under our assumptions, $(V_t^{1,n})_{t\geq 0}$ should tend in law (in the regime $N = np_n \to \infty$ and $w_n = wN^{-1/2}$) to the unique solution $(V_t)_{t\geq 0}$ of (dMKV). See section 3.3 for additional explanations.

Assumption 3.10 seems rather realistic. It is crucial for our proof of proposition 3.14 that λ vanishes in a neighborhood of v_{min}, since it allows us to use the results of Calder, Esedoglu and Hero [CEH14]. The growth condition on F is one-sided and sufficiently general to our opinion, however, it is only here to prevent explosion and it should be possible to replace it by a weaker condition like $F(v) \leq (v-v_{min})\lambda(v)+C(1+(v-v_{min}))$, at the price of more complicated proofs. Hence we believe that when $\theta > 0$, our assumptions are rather reasonable.

On the contrary, when $\theta = 0$, our conditions are restrictive, at least from a mathematical point of view. This comes from two problems when studying the nonlinear SDE (dMKV). First, the term $\Gamma_t((\mathbb{E}[\lambda(V_s)])_{s\geq 0})$ involves something like $\int_0^t \sqrt{\mathbb{E}[\lambda(V_s)]}ds$, and the square root is rather unpleasant. To solve this problem, we use that $f_0((\alpha,\infty)) > 0$ and $F(\alpha) \geq 0$ imply that $s \mapsto \mathbb{E}[\lambda(V_s)]$ is *a priori* bounded from below on each compact time interval. Since α is thought to be rather close to v_{min}, we believe these two conditions are not too restrictive in practice. Second, the coefficients of (dMKV) are only locally Lipschitz continuous, which is always a problem for nonlinear SDEs. Here we roughly solve the problem by assuming that f_0 is compactly supported, which propagates with time. However, one may use the ideas of [FL16] to remove this compact support assumption, here again, at the price of a much more complicated proof.

3.5 On the stationary solutions of the limit model

As in the previous chapter, we would like to gain some information on the long term behavior of the mean-field limit. A first step is thus to study the stationary distributions of (dMKV).

We show, with the help of numerical computations, that, depending on the parameters, there may be 1 or 3 stationary solutions for the limit model (and sometimes 2 in some critical cases). In this section, we assume that $F(v) = I - v$ for some $I > 0$. We also assume for simplicity that $\theta = 0$ (no delay), that $v_{min} = 0$ and that $H(0) = \max_{[0,1]} H$, so that the nonlinear SDE (dMKV) reads

$$V_t = V_0 + \int_0^t \left(I - V_s + \sqrt{\gamma\mathbb{E}[\lambda(V_t)]}\right)ds - \int_0^t\int_0^\infty V_{s-}\mathbb{1}_{\{u\leq\lambda(V_{s-})\}}\mathbf{N}(ds,du), \tag{3.5.1}$$

with $\gamma := 2\rho H(0)w^2 > 0$. Finally, although such an explicit form is only necessary at the end of the current section, we assume that $\lambda(v) = (v-\alpha)_+^p$ for some $\alpha > 0$ and some $p \in \mathbb{N}^*$.

Assumptions 3.10 and 3.12 are satisfied (for a large class of initial conditions) if $I \geq \alpha$, but we may also study stationary solutions when $I \in (0, \alpha)$.

Definition 3.18. *We say that $g \in \mathcal{P}([0,\infty))$ is an invariant distribution for (3.5.1) if, setting $m = \int_0^\infty \lambda(v) g(dv)$ and $a = I + \sqrt{\gamma m}$, the solution $(V_t^a)_{t\geq 0}$ to*

$$V_t^a = V_0 + \int_0^t (a - V_s^a) ds - \int_0^t \int_0^\infty V_{s-}^a \mathbb{1}_{\{u \leq \lambda(V_{s-}^a)\}} \mathbf{N}(ds, du) \tag{3.5.2}$$

starting from some g-distributed V_0 is such that $\mathcal{L}(V_t^a) = g$ for all $t \geq 0$.

For $a > 0$, we define the constant

$$K_a := \int_0^a \frac{1}{v-a} \exp\Big(- \int_0^v \frac{\lambda(x)}{a-x} dx \Big) dv.$$

We clearly have $K_a = \infty$ if $a \in (0, \alpha]$, because $\lambda = 0$ on $[0, \alpha]$, and $K_a \in (0, \infty)$ for all $a > \alpha$ (because λ is continuous and $\lambda(a) > 0$). As in [FL16, Proposition 21], we have the following result.

Proposition 3.19. *Fix $a > 0$. The linear SDE (3.5.2) has a pathwise unique solution (for any initial condition $V_0 \geq 0$), and has a unique invariant probability measure $g_a \in \mathcal{P}([0,\infty))$, given by*

$$g_a = \delta_a \text{ if } a \in (0, \alpha] \text{ and } g_a(dv) = \frac{1}{K_a(v-a)} \exp\Big(- \int_0^v \frac{\lambda(x)}{a-x} dx \Big) \mathbb{1}_{\{v \in [0,a)\}} dv \text{ if } a > \alpha.$$

Furthermore, we have $\int_0^\infty \lambda(v) g_a(dv) = K_a^{-1}$ with the convention that $1/\infty = 0$ when $a \in (0, \alpha]$.

The conditions are slightly different from those of [FL16, Proposition 21] (mainly because $\alpha = 0$ there), but the extension is straightforward. We can now study existence of invariant distributions of (3.5.1).

Lemma 3.20. *We have the following properties:*

(i) $g \in \mathcal{P}([0,\infty))$ is an invariant distribution for (3.5.1) if and only if there is $a > 0$ such that $g = g_a$ and $\varphi_\gamma(a) = I$, where $\varphi_\gamma(a) := a - \sqrt{\gamma / K_a}$.

(ii) For any fixed $\gamma > 0$, the function φ_γ is continuous on $[0,\infty)$, one has $\varphi_\gamma(0) = 0$ and $\lim_{a\to\infty} \varphi_\gamma(a) = \infty$, so that for any $I > 0$, (3.5.1) has at least one invariant distribution g, which is non-trivial if $I > \alpha$ (because $g = g_a$ for some $a \geq \varphi_\gamma(a) = I > \alpha$).

Concerning the uniqueness/non-uniqueness of this invariant distribution, the theoretical computations seem quite involved and we did not succeed in obtaining a proof. We thus decided to compute numerically $a \mapsto \varphi_\gamma(a)$ in a few situations.

Let us comment on figure 3.4. Recall that for $\gamma > 0$ and $I > 0$, each stationary solution to (3.5.1) corresponds to one solution a of $\varphi_\gamma(a) = Ix$.

• If $\lambda(v) = v^2$, for any $\gamma > 0$, the equation $\varphi_\gamma(a) = I$ (with $I > 0$ fixed) seems to have exactly one solution, for all $I > 0$.

• If $\lambda(v) = (v-1)_+^2$, $\lambda(v) = v^4$ or $\lambda(v) = (v-1)_+^4$, it seems that there are $0 < \gamma_1 < \gamma_2$ (*e.g.*, $\gamma_1 \simeq 1.5$ and $\gamma_2 \simeq 12$ when $\lambda(v) = (v-1)_+^4$) such that

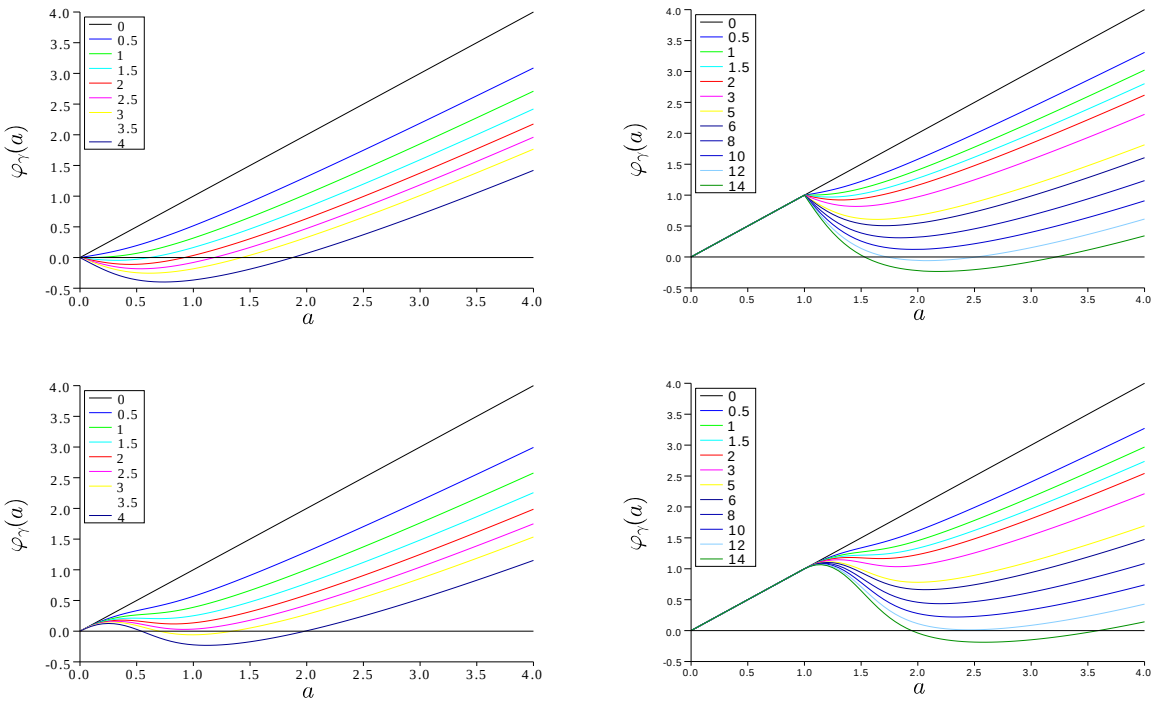

Figure 3.4: Plots of $a \mapsto \varphi_\gamma(a)$ for different values of γ, when $\lambda(v) = v^2$ (up left), $\lambda(v) = (v-1)_+^2$ (up right), $\lambda(v) = v^4$ (down left), $\lambda(v) = (v-1)_+^4$ (down right),

(a) if $\gamma \in (0, \gamma_1)$, then for all $I > 0$, $\varphi_\gamma(a) = I$ has exactly one solution,

(b) if $\gamma \in (\gamma_1, \gamma_2)$, then there are $0 < J_\gamma < I_\gamma$ such that, if $I \in (0, J_\gamma)$, $\varphi_\gamma(a) = I$ has exactly one solution, if $I \in (J_\gamma, I_\gamma)$, $\varphi_\gamma(a) = I$ has exactly three solutions and if $I > I_\gamma$, $\varphi_\gamma(a) = I$ has exactly one solution,

(c) if $\gamma \in (\gamma_2, \infty)$, then there is $I_\gamma > 0$ such that for all $I \in (0, I_\gamma)$, $\varphi_\gamma(a) = I$ has exactly three solutions and if $I > I_\gamma$, $\varphi_\gamma(a) = I$ has exactly one solution (which is nontrivial).

3.6 Ideas of proofs and related hypothesis

Let us consider the case where the dendrite of (say) neuron 1 receives synaptic inputs composed of *i.i.d.* copies $(T_k^i)_{k\geq 1}$, for each $i \geq 1$, of the spiking times of neuron 1 and distributed along the dendrite of neuron 1 using the probability density H (see section 3.1). These synaptic inputs have space-time locations (X_{i1}, T_k^i) ; see figure 3.5. In particular, they belong to horizontal lines so that these synaptic inputs cannot be a realization of a Poisson process. This prevents us from using directly the results of [CEH14] concerning the asymptotic behavior of the length of the longest increasing sub-sequence of synaptic inputs.

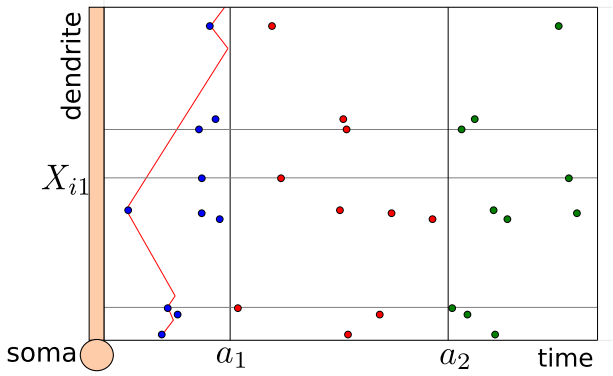

Figure 3.5: Schematics of the deterministic time-dendrite partition. The first negative/positive fronts are shown in red. A few horizontal lines are shown to display the synaptic inputs locations (dots) from a single neuron.

We thus try to get closer to the setting of [CEH14], so that the synaptic inputs are "close" to a Poisson process. The main idea of assumptions 3.10, 3.12 is to ensure that we can partition time with *deterministic* subsets $[a_k, a_{k+1})$ such that at most one point (X_{i1}, T_k^i) lies in $[a_k, a_{k+1}) \times [0, L]$ for each i (see figure 3.5).

If the drift is $F(v) = 1$, we can easily obtain such partition by preventing the jumps for some time α thanks to condition 3.10 (ii). The proof of theorem 3.16 then proceeds by showing that such partition exists for general drifts F.

We thus have a situation closer to the main hypothesis of [CEH14] but we still have to generalize these results to our setting, namely by showing proposition 3.14 which is based on the next lemma 3.21. The proof of lemma 3.21 is arguably the most technical one of [FTV20], and we shall only comment it very briefly.

Lemma 3.21. *Let H be a continuous probability density on $[0, L]$. Fix $0 \le b_0 < b_1 < \dots$ and consider, for each $k \ge 0$, a probability density g_k on $[b_k, \infty)$, continuous on $[b_k, b_{k+1}]$. Consider an i.i.d. family $(X_i)_{i\ge1}$ of $[0, L]$-valued random variables with density H and, for each $k \ge 0$, an i.i.d. family $(T_k^i)_{i\ge1}$ of $[b_k, \infty)$-valued random variables with density g_k. We assume that for each $k \ge 0$, the family $(X_i)_{i\ge1}$ is independent of the family $(T_k^i)_{i\ge1}$ (but the families $(X_i, T_k^i)_{i\ge1}$ and $(X_i, T_\ell^i)_{i\ge1}$, with $k \ne \ell$, are allowed to be correlated in any possible way). For each $N \ge 1$, we set*

$$\nu_N := \sum_{i=1}^{N} \sum_{k\ge0} \mathbb{1}_{\{T_k^i \le b_{k+1}\}} \delta_{(T_k^i, X_i)}.$$

Then

$$\lim_{N\to\infty} \frac{A_t(\nu_N)}{\sqrt{N}} = \Gamma_t(g) \quad a.s.$$

for each $t \ge 0$, where $g(s) := \sum_{k\ge0} g_k(s) \mathbb{1}_{\{s\in[b_k, b_{k+1}]\}}$.

Let us comment on the proof. Using a change of variable, we first adapt theorem 1.2 of [CEH14] valid for the partial order $\trianglelefteq$ on $\mathbb{R}^2$ defined by

$$(y_1, y_2) \trianglelefteq (y_1', y_2') \text{ if } y_1 \le y_1' \text{ and } y_2 \le y_2'.$$

The result of this adaptation is as follows.

Fix $0 \leq a < b$ and a continuous density h on $[a,b]$. Consider an *i.i.d.* family $(Z_i)_{i\geq 1}$ of $[a,b]\times[0,L]$-valued random variables with density $h(s)H(x)$. Then, for $N \geq 1$, define $\pi_N := \sum_1^N \delta_{Z_i}$. For any bounded open domain $B \subset [0,\infty)\times[0,L]$ with Lipschitz boundary, the a.s. limit $\lim_{N\to\infty} \frac{A(\pi_N|_B)}{\sqrt{N}}$ can be identified explicitly.

We then apply this result to prove lemma 3.21 by estimating $\liminf_N A_t(\nu_N)/\sqrt{N}$ and $\limsup_N A_t(\nu_N)/\sqrt{N}$ separately, this is arguably the most delicate part .

3.6.1 Idea of proof of proposition 3.6

Recall that this proposition relates the number of *excitation events* to the length of the longest sub-sequence. We provide a partial proof of this proposition because it is quite simple and intuitive. Writing it formally is long though.

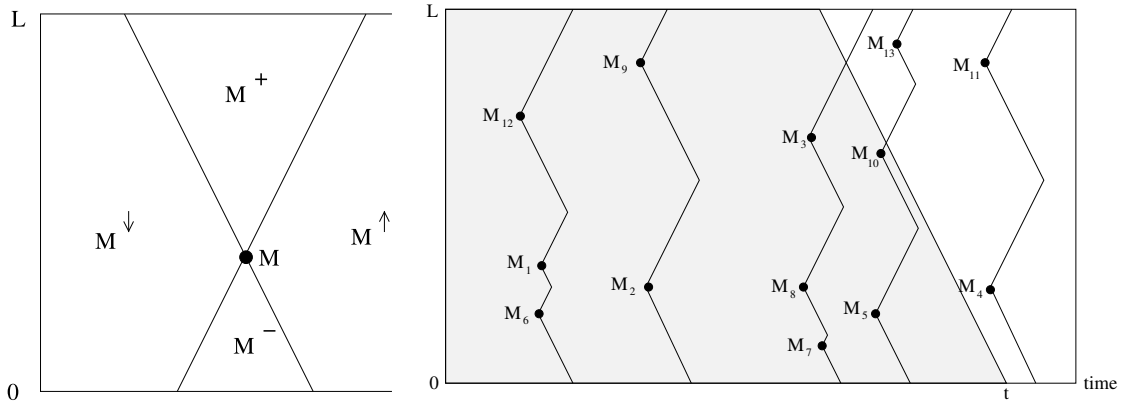

Figure 3.6: Space-time diagrams of front propagation. y-axis is dendrite, x-axis is time. All oblique segments have slopes $\pm\rho$. Left: plot of the four sets $M^{\downarrow}$, $M^{\uparrow}$, M^{+} and M^{-}. Right: The domain in gray is D_t. Here we have $G_1 = \{M_1, M_6, M_{12}\}$, $G_2 = \{M_2, M_9\}$, $G_3 = \{M_3, M_7, M_8\}$, $G_4 = \{M_5, M_{10}, M_{13}\}$ and $G_5 = \{M_4, M_{11}\}$. We also have $P_1 = M_6$, $P_2 = M_1$ and $P_3 = M_{12}$.

We first introduce some notations. For $M = (r, y) \in [0,\infty)\times[0,L]$, we denote by $M_s = r$ its time coordinate and by $M_x = y$ its space coordinate. We recall that $M \preceq N$ if $|M_x - N_x| \leq \rho(N_s - M_s)$, which means that N belongs to the cone with apex M delimited by the half-lines $\{(r, M_x + \rho(r - M_s)) : r \geq M_s\}$ and $\{(r, M_x - \rho(r - M_s)) : r \geq M_s\}$. We also recall that $M \prec N$ if $M \preceq N$ and $M \neq N$. We say that $M \perp N$ if M and N are not comparable, *i.e.* if neither $M \preceq N$ nor $N \preceq M$. Observe that $M \perp N$ if and only if $|M_x - N_x| > \rho|M_s - N_s|$, whence in particular $M_x \neq N_x$ and $|M_s - N_s| \leq L/\rho$.

For $M \in [0,\infty)\times[0,L]$, we introduce the four sets, see figure 3.6 left,

$$M^{\downarrow} := \{Q \in [0,\infty)\times[0,L] : Q \prec M\}, \quad M^{+} := \{Q \in [0,\infty)\times[0,L] : Q \perp M, Q_x > M_x\},$$
$$M^{\uparrow} := \{Q \in [0,\infty)\times[0,L] : M \prec Q\}, \quad M^{-} := \{Q \in [0,\infty)\times[0,L] : Q \perp M, Q_x < M_x\}.$$

Let $\nu = \sum_{i\in I} \delta_{M_i}$ be Radon, the set $\mathcal{S}_\nu := \{M_i = (t_i, x_i) : i \in I\}$ consisting of distinct points of $[0,\infty)\times[0,L]$. We assume[3] that $\nu \neq 0$ and (3.4.2). We recall that $A(\nu) \in \mathbb{N}\cup\{\infty\}$ and

[3] because otherwise the result is obvious

$A_t(\nu) \in \mathbb{N}$ were introduced in definition 3.5. We call $B(\nu) \in \mathbb{N} \cup \{\infty\}$ the total number of fronts hitting the soma and $B_t(\nu) \in \mathbb{N}$ the number of fronts hitting the soma before time t.

If two fronts start from M (*i.e.* start from $M_x \in [0, L]$ at time $M_s \geq 0$), the positive one is, if not previously annihilated, at position $M_x - \rho(r - M_s)$ at time $r \in [M_s, M_s + M_x/\rho)$ and hits the soma at time $M_s + M_x/\rho$; the negative one is, if not previously annihilated, at position $M_x + \rho(r - M_s)$ at time $r \in [M_s, M_s + (L - M_x)/\rho)$ and disappears at time $M_s + (L - M_x)/\rho$. We have the two following rules: for two distinct points $M, N \in \mathcal{S}_\nu$,

(a) if $M \prec N$, *i.e.* $M \in N^\downarrow$ or, equivalently, $N \in M^\uparrow$, the fronts starting from M cannot meet those starting from N. Indeed, $M \prec N$ and (3.4.2) imply that $|M_x - N_x| < \rho(N_s - M_s)$ and a little study shows that for all $r \geq N_s$, $\{M_x - \rho(r - M_s), M_x + \rho(r - M_s)\} \cap \{N_x - \rho(r - N_s), N_x + \rho(r - N_s)\} = \emptyset$;

(b) if $M \perp N$ and $M_x < N_x$ (*i.e.* if $M \in N^-$ or, equivalently, $N \in M^+$) the positive front starting from N meets the negative front starting from M *if none of these two fronts have been previously annihilated*. More precisely, they meet at $[N_x + M_x + \rho(N_s - M_s)]/2 \in [0, L]$ at time $(N_x - M_x + \rho(N_s + M_s))/(2\rho)$, which is greater than $M_s \vee N_s$.

Step 1. We prove that $A(\nu) = B(\nu)$.

Step 1.1. We introduce G_1, the set of all minimal (for $\prec$) elements of $\mathcal{S}_\nu$. See figure 3.6 right. This set is non empty because $\nu \neq 0$. It is also bounded (and thus finite since $\#(G_1) = \nu(G_1)$ and since ν is Radon): fix $M \in G_1$ and observe that $G_1 \subset \{M\} \cup M^+ \cup M^- \subset [0, M_s + L/\rho] \times [0, L]$. We thus may write $G_1 = \{P^1, \dots, P^k\}$, ordered in such a way that $P^1_x < P^2_x < \cdots < P^k_x$.

We now show that all the fronts starting in G_1 annihilate, except the positive one starting from P^1 (it reaches the soma at time $P^1_s + P^1_x/\rho$) and the negative one starting from P^k (it reaches the other extremity of the dendrite). See figure 3.6 right.

- We first verify by contradiction that the positive front starting from P^1 hits the soma. If this is not the case, then, due to the above rules (a)-(b), it has been annihilated by some front starting from some $Q \in \mathcal{S}_\nu \cap P^{1-}$. This is not possible, because $\mathcal{S}_\nu \cap P^{1-} = \emptyset$.

  Indeed, assume that $\mathcal{S}_\nu \cap P^{1-} \neq \emptyset$ and consider a minimal (for $\prec$) element Q of $\mathcal{S}_\nu \cap P^{1-}$. Then Q is minimal in $\mathcal{S}_\nu$ because else, we could find $M \in \mathcal{S}_\nu \cap Q^\downarrow$, whence $M \in \mathcal{S}_\nu \cap Q^\downarrow \cap (P^{1-})^c$ (since Q is minimal in $\mathcal{S}_\nu \cap P^{1-}$) whence $M \prec P^1$ (because $M \prec Q$, $Q \in P^{1-}$ and $M \notin P^{1-}$ implies that $M \prec P^1$), which is not possible because P^1 is minimal. So Q is minimal in $\mathcal{S}_\nu$, *i.e.* $Q \in G_1$, and we furthermore have $Q_x < P^1_x$. This contradicts the definition of P^1.

- Similarly, one verifies that the negative front starting from P^k hits the other extremity ($x = L$) of the dendrite.

- We finally fix $i \in \{1, \dots, k-1\}$ and show by contradiction that the negative front starting from P^i does meet the positive front starting from P^{i+1}. We omit the details as they are very similar to the ones of the two previous cases.

Step 1.2. If $\mathcal{S}_\nu \setminus G_1 = \emptyset$, we go directly to the *concluding step*. Otherwise, we introduce the (finite) set G_2 of all the minimal elements of $\mathcal{S} \setminus G_1$. The fronts starting from a point in G_2 cannot be annihilated by those starting from a point in G_1 (because as seen in *Step 1.1*, all the

fronts in G_1 do annihilate together, except one that does hit the soma and one that does hit the other extremity: the fronts starting in G_1 do not interact with those starting in $\mathcal{S}_\nu \setminus G_1$). And one can show, exactly as in *Step 1.1*, that all the fronts starting in G_2 annihilate, except one positive front that hits the soma and one negative front that hits the other extremity.

Step 1.3. If $\mathcal{S}_\nu \setminus (G_1 \cup G_2) = \emptyset$, we go directly to the *concluding step*. Otherwise, we introduce the (finite) set G_3 of all the minimal elements of $\mathcal{S} \setminus (G_1 \cup G_2)$. As previously, the fronts starting from a point in G_3 cannot be annihilated by those starting from a point in $G_1 \cup G_2$. And one can show, exactly as in Step 1.1, that all the fronts starting in G_3 annihilate, except one positive front that hits the soma and one negative front that hits the other extremity.

Step 1.4. If $\mathcal{S}_\nu \setminus (G_1 \cup G_2 \cup G_3) = \emptyset$, etc.

Concluding step. If the procedure stops after a finite number of steps, then there exists $n \in \mathbb{N}_*$ such that $\mathcal{S}_\nu = \cup_{k=1}^n G_k$, where G_1 is the set of all minimal elements of $\mathcal{S}_\nu$ and, for all $k = 2, \dots, n$, G_k is the set of all minimal elements of $\mathcal{S}_\nu \setminus (\cup_{i=1}^{k-1} G_i)$. We have seen that for each $k = 1, \dots, n$, exactly one front starting from a point in G_k hits the soma, so that $B(\nu) = n$. And we also have $A(\nu) = n$. Indeed, choose $Q_n \in G_n$, there is necessarily $Q_{n-1} \in G_{n-1}$ such that $Q_{n-1} \prec Q_n$, ..., and there is necessarily $Q_1 \in G_1$ such that $Q_1 \prec Q_2$. We end with an increasing sequence $Q_1 \prec \cdots \prec Q_n$ of points of $\mathcal{S}_\nu$, whence $A(\nu) \geq n$. We also have $A(\nu) \leq n$ because otherwise, we could find a sequence $R_1 \prec \cdots \prec R_{n+1}$ of points of $\mathcal{S}_\nu$, and $\mathcal{S}_\nu \setminus (\cup_{k=1}^n G_k)$ would contain at least R_{n+1} and thus would not be empty.

If the procedure never stops, we have $A(\nu) = B(\nu) = \infty$ in which case $A(\nu) = B(\nu)$, as desired.

Step 2. We now fix $t \geq 0$. By *Step 1* applied to $\nu|_{D_t}$, we know that $B(\nu|_{D_t}) = A(\nu|_{D_t})$, which equals $A_t(\nu)$ by definition. To conclude the proof, it thus only remains to check that $B_t(\nu) = B(\nu|_{D_t})$. We omit the details as they do not bring anything new.

3.6.2 Idea of proof of proposition 3.14

The strategy of the proof is to apply lemma 3.21. We prove the first part of proposition 3.14 concerning the existence of a partition that we described in section 3.6 and highlight the main arguments of the rest of the proof which rely on the application of lemma 3.21.

We recall that a non-decreasing continuous function $r : [0, \infty) \mapsto \mathbb{R}_+$ with $r_0 = 0$ is fixed, as well as the initial distribution f_0 on $[v_{min}, \infty)$ of V_0, that $(V_t^r)_{t \geq 0}$ is the unique solution to (3.4.4) and that $J_t^r := \sum_{s \leq t} \mathbb{1}_{\{\Delta V_{s-}^r \neq 0\}}$ is the number of jumps of $(V_t^r)_{t \geq 0}$ during $[0, t]$.

Lemma. *There is a deterministic and increasing sequence $(a_k)_{k \geq 0}$ such that $a_0 = 0$, $\lim_k a_k = \infty$ and a.s., for all $k \geq 0$, $J_{a_{k+1}}^r - J_{a_k}^r \in \{0, 1\}$. This sequence only depends on α, v_{min}, r, F.*

Proof. For $t_0 \geq 0$ and $v_0 \geq v_{min}$ we define $(z_{t_0, v_0}(t))_{t \geq t_0}$ as the unique solution to

$$z_{t_0,v_0}(t) = v_0 + \int_{t_0}^t F(z_{t_0,v_0}(s))ds + r_t - r_{t_0}.$$

It is valued in $[v_{min}, \infty)$ because $F(v_{min}) \geq 0$ and r is non-decreasing. For all $t_0 < t_1 \leq t$, we have

$$z_{t_1,v_{min}}(t) \leq z_{t_0,v_{min}}(t). \tag{3.6.1}$$

This follows from the comparison theorem, because $z_{t_1,v_{min}}(t_1) = v_{min} \le z_{t_0,v_{min}}(t_1)$ and since $(z_{t_1,v_{min}}(t))_{t\ge t_1}$ and $(z_{t_0,v_{min}}(t))_{t\ge t_1}$ solve the same Volterra equation (with different initial conditions). Also, since $F(v) \le C(1 + (v - v_{min}))$, we have for all $t \ge t_0$ and all $v_0 \ge v_{min}$:

$$z_{t_0,v_0}(t) - v_{min} \le [v_0 - v_{min} + r_t - r_{t_0} + C(t - t_0)] \exp(C(t - t_0)). \tag{3.6.2}$$

By assumption 3.10, we have $\lambda(v) = 0$ for $v \in [v_{min}, \alpha]$, with $\alpha > v_{min}$. We introduce the increasing sequence $(a_k)_{k\ge0}$ defined recursively by $a_0 = 0$ and, for $k \ge 0$,

$$a_{k+1} := \inf\{t \ge a_k : z_{a_k,v_{min}}(t) \ge \alpha\} \wedge (a_k + 1),$$

with the convention that $\inf \emptyset = \infty$.

Fix $k \ge 0$, denote by $\tau_1 < \tau_2$ the first and second instants of jump of V^r after a_k. If $\tau_1 > a_{k+1}$, then $J^r_{a_{k+1}} - J^r_{a_k} = 0$. Otherwise, we have $V^r_{\tau_1} = v_{min}$ and, during $[\tau_1, \tau_2)$, we have $V^r_t = z_{\tau_1,v_{min}}(t)$, whence $V^r_t \le z_{a_k,v_{min}}(t)$ by (3.6.1) and since $\tau_1 \ge a_k$, and thus $V^r_t \le \alpha$ during $[\tau_1, \tau_2 \wedge a_{k+1})$. Thus the rate of jump satisfies $\lambda(V^r_t) = 0$ during $[\tau_1, \tau_2 \wedge a_{k+1})$, so that $\tau_2 > a_{k+1}$ and $J^r_{a_{k+1}} - J^r_{a_k} = 1$.

It remains to verify that $\lim_k a_k = \infty$. We fix $\eta \in (0, 1)$ such that $v_{min} + C\eta e^{C\eta} \le (v_{min} + \alpha)/2$ and we set $\varepsilon = (\alpha - v_{min})e^{-C\eta}/2$. We claim that for all $k \ge 0$, we have either $a_{k+1} - a_k \ge \eta$ or $r_{a_{k+1}} - r_{a_k} \ge \varepsilon$. Indeed, if $a_{k+1} - a_k < \eta \le 1$, then $a_{k+1} = \inf\{t \ge a_k : z_{a_k,v_{min}}(t) \ge \alpha\}$, whence $\alpha = z_{a_k,v_{min}}(a_{k+1}) \le v_{min} + (r_{a_{k+1}} - r_{a_k} + C(a_{k+1} - a_k))e^{C(a_{k+1}-a_k)}$ by (3.6.2). Hence $\alpha \le v_{min} + (r_{a_{k+1}} - r_{a_k})e^{C\eta} + C\eta e^{C\eta} \le (v_{min} + \alpha)/2 + (r_{a_{k+1}} - r_{a_k})e^{C\eta}$, whence $r_{a_{k+1}} - r_{a_k} \ge \varepsilon$.

One easily concludes that $\lim_k a_k = \infty$: if $a_\infty = \lim_k a_k < \infty$, then there is k_0 such that $a_{k+1} - a_k < \eta$ (and thus $r_{a_{k+1}} - r_{a_k} \ge \varepsilon$) for all $k \ge k_0$, whence $r_{a_\infty} = \sum_{k\ge0}(r_{a_{k+1}} - r_{a_k}) = \infty$. This is not possible since r is $\mathbb{R}_+$-valued. □

We now highlight the key remaining elements of the proof of proposition 3.14.

Step 1. For $k \ge 0$, let $S_k := \inf\{t \ge a_k : \Delta V^r_t \ne 0\} = \inf\{t \ge a_k : \Delta J^r_t = 1\}$ be the first jump time after a_k. The law of S_k has a continuous density g_k on $[a_k, \infty)$.

Step 2. Setting $h_r(t) := \sum_{k\ge0} g_k(t)\mathbb{1}_{\{t\in[a_k,a_{k+1})\}}$, it holds that $h_r(t) = \mathbb{E}[\lambda(V^r_t)]$ for almost every $t \ge 0$.

Step 3. Observe that for the successive jump times $T_1 < T_2 < \dots$ of $(V^r_t)_{t\ge0}$, we have

$$\nu^r_N := \sum_{i=1}^N \sum_{k\ge1} \delta_{(T^i_k+\theta,X_i)} = \sum_{i=1}^N \sum_{k\ge0} \mathbb{1}_{\{S^i_k+\theta<b_{k+1}\}}\delta_{(S^i_k+\theta,X_i)},$$

where $b_k := a_k + \theta$. Indeed, S_k is the first jump time after a_k and there is at most one jump during $[a_k, a_{k+1})$. We thus can directly apply lemma 3.21 to conclude that indeed, for any $t \ge 0$, $\lim_{N\to\infty} N^{-1/2}A_t(\nu^r_N) = \Gamma_t(h^\theta_r)$ a.s., where $h^\theta_r(t) := \sum_{k\ge0} g_k(t - \theta)\mathbb{1}_{\{t\in[a_k+\theta,a_{k+1}+\theta)\}}$ (observe that the density of $S^i_k + \theta$ is $g_k(t - \theta)\mathbb{1}_{\{t\ge\theta\}} = g_k(t - \theta)\mathbb{1}_{\{t\ge a_k+\theta\}}$), whence indeed $h^\theta_r(t) = \mathbb{E}[\lambda(V^r_{t-\theta})]\mathbb{1}_{\{t\ge\theta\}}$ by *Step 2*.

3.7 Bibliographical comments on the longest increasing sequences

The problem of computing the length L_N of the longest increasing sequence in a random permutation of $\{1, \dots, N\}$ was introduced by Ulam [Ula61]. Hammersley [Ham72] understood that a clever way to attack the problem is to note that L_N is also the length of the longest increasing sequence, for the usual partial order in $\mathbb{R}^2$, of a cloud composed of N *i.i.d.* points uniformly distributed in the square $[0,1]^2$. He also proved the existence of a constant c such that $L_N \sim c\sqrt{N}$ as $N \to \infty$. Versik and Kerov [VK77] and Logan and Shepp [LS77] showed that $c = 2$. Simpler proofs and/or stronger results were then found by Bollobás and Winkler [BW88], Aldous and Diaconis [AD95], Cator and Groeneboom [CG05], etc. Let us also mention the recent work of Basdevant, Gerin, Gouéré and Singh [BGG$^+$18].

As already mentioned in subsection 3.2, we use the results of Calder, Esedoglu and Hero [CEH14], that generalize those of Deuschel and Zeitouni [DZ95] and that concern the limit behavior of the longest ordered increasing sequence of a cloud composed of N *i.i.d.* points with general smooth distribution g in the square $[0,1]^2$ (or in a compact domain). These results strongly rely on the fact that since g is smooth, it is almost constant on small squares. Hence, on any small square, we can more or less apply the results of [VK77; LS77]. Of course, this is technically involved, but the main difficulty in all this work was to understand the constant 2 (note that the value of the corresponding constant is still unknown in higher dimension).

Of course, a little work is needed: we cannot apply directly the results of [CEH14], because we are not in presence of an *i.i.d.* cloud. However, as we have seen, the situation is rather favorable.

3.8 Perspectives

Compared to the previous chapter, we have only "identified" the limit process. However, we have yet to analyze its dynamics as in chapter 2. In the case where the density H reaches its maximum at 0, the model is very close to the setting of the previous chapter, see remark 3.17. In the general case, it should yield interesting developments thanks to the coupling between the dynamics and optimization problem associated to Γ. This study could be an interesting prospect to understand the impact of the nonlinear properties of the dendrite on the dynamics of the network.

The limiting equation (dMKV) is based on the (unproven) assumption of asymptotic independence of the neurons when the network size N is large (propagation of chaos). An important question remains open: does propagation of chaos holds true? This seems very difficult to prove rigorously, in particular because the results of [DZ95; CEH14] would have to be generalized to the case of non-independent random point clouds.

More biological details could be taken into account. For example, once could consider branches on the dendrite or the interaction with bAP.

We have investigated the mean-field limits of non-plastic neural networks in the last two chapters. In relation with the research program presented in section 1.3, a next step would be to study spiking networks with plastic synapses and large number of neurons, as was done

during the thesis of P. Helson [Hel21]. This seems a formidable task though, much more intricate than the already difficult case where the neurons do not have a dendritic compartment as in the previous chapter.

In the next chapter, we present a new model of excitatory synapse in which we study the induction of synaptic plasticity.

Chapter 4

Modelling the excitatory synapse

For this last chapter, I wish to present some of Yuri Rodrigues' work [RTM+23] obtained during his PhD [Rod21] which I co-supervised with H. Marie (IPMC). The goal of this thesis was to model the induction of synaptic plasticity in excitatory synapses.

This work was selected by the "Société des Neurosciences" to be in the "Highlights 2023".

Abstract The study of synaptic plasticity is an important step towards understanding brain learning. Existing plasticity models are either 1) *top-down* and interpretable [CQC+01; CG10; GB12], but not flexible enough to accommodate experimental data, or 2) *bottom-up* and biologically realistic [BI99; CPX+16; BST+19; ZSC+21; CAA+22], but complex to interpret and difficult to fit to the data. To avoid the shortcomings of these approaches, we present a novel plasticity model based on a geometric approach that relates the dynamics of two synaptic enzymes to plasticity outcomes. We use this association in a model of induction of hippocampal synaptic plasticity that includes the dynamics of membrane potential, calcium, two enzymes CaMKII and calcineurin (CaN), as well as a precise description of the sources of intrinsic noise. With a single set of parameters, we demonstrate in [RTM+23] the robustness of the model by reproducing nine *ex-vivo* experiments covering different plasticity protocols depending on the precise moment of emission of action potentials, the dependence on the frequency of the stimuli, the age of the animals and the experimental conditions (temperature, etc.).

The aim of this chapter is to present the model which describes the first elements of the molecular cascade involved in synaptic plasticity but which neglects the pathways downstream of the enzymes[1] CaMKII / Calcinerin (CaN).

We will not cover all the results of [RTM+23]. The research question is to identify principles that allow, from the stochastic dynamics of the couple (CaN, CaMKII), to predict synaptic plasticity. The main difficulties of this undertaking are the noisy dynamics and the need to take into account the multiple external parameters (temperature, age of the animals, concentration

[1] these enzymes are crucial for long-term plasticity, cf. [GFF+98; OWW05]

of magnesium, etc) for the adequacy with the experimental data. Our approach provides a direct biophysical link with the first components of the molecular cascade, which simplifies the prediction of biological phenomena. It bypasses the difficulty of describing the rest of the molecular cascade which is not well understood quantitatively.

4.1 Introduction

To understand how brains learn, we need to identify the rules governing how synapses change their strength in neural circuits. The dominant principle at the basis of current models of synaptic plasticity is the Hebb postulate [Heb49] which states that neurons with correlated electrical activity strengthen their synaptic connections, while neurons active at different times weaken their connections. A "bidirectional learning rules" based on the precise spiking times of connected neurons, currently known as spike timing-dependent plasticity (STDP), was anticipated by many researchers. Experimental evidences for this rule would be found by [MS95; BP98].

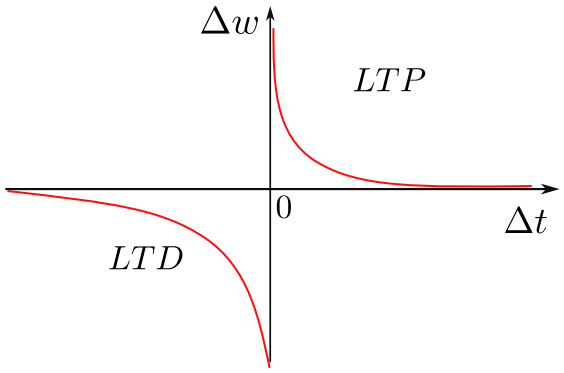

Canonical STDP window (see also [GKV+96]). Δt is the difference between the arrival times of the bAP and AP. Δw is the synaptic weight change. LTP (resp. LTD) corresponds to $\Delta w > 0$ (resp. $\Delta w < 0$).

Definition 4.1 (Canonical STDP (from [TOS+16]))**.** *Canonical spike-timing-dependent plasticity (STDP) occurs when a presynaptic spike is paired with a postsynaptic action potential (bAP) and has two defining characteristics: (1) the magnitude of synaptic plasticity is inversely related to the millisecond delay between the pre- and the postsynaptic spikes and (2) the direction of plasticity is determined by the temporal order of the spikes, with pre- before-post leading to long-term potentiation (LTP) and post-before-pre leading to long-term depression (LTD).*

STDP models [BA96; GKV+96; EPE+99] were formulated based on the experimental observations that precise timing of pre- and post-synaptic spiking determines whether synapses are strengthened or weakened [DGG+96; TM97; BP98; MGS11]. However, experiments also found that plasticity induction depends on the rate and number of stimuli delivered to the synapse [DB92; STN01], and the level of dendritic spine depolarization [ABS90; MJ97; SH06; GSS02; HS09]. The lack of satisfactory plasticity models based solely on neural spiking times prompted researchers to consider simple models based on synapse biochemistry [CQC+01; CQB+05].

In 1989, John Lisman proposed a role for postsynaptic calcium signaling in synaptic plasticity [Lis89] with moderate levels of calcium transients causing long-term depression (LTD) and high calcium transients causing long-term potentiation (LTP) ; this has been called the *calcium hypothesis* since then in the literature. This hypothesis has been the basis of several previous

models [SBC02; KB02] which assumed that the amplitude of postsynaptic calcium controls long-term alterations in synaptic strength.

However experimental data suggests that calcium dynamics are also important [YTZ99; MKS01; WGN+05; NS06; TOS+16]. As a result, subsequent phenomenological models of plasticity incorporated slow variables that integrate the fast synaptic input signals, loosely modeling calcium and its downstream effectors [AGH+03; RGB+05; RTG+10; CG10; KM11; GB12; HUK+13; STB14; DB16]. Additionally, more detailed models tried to explicitly describe the molecular pathways integrating the calcium dynamics and its stochastic nature [CGC+07; SK05; MZL+05; ZH10; YSB+04]. However, even these models do not account for data showing that plasticity is highly sensitive to physiological conditions such as the developmental age of the animal [DB93; MFP03; CH12; CQK+20], extracellular calcium and magnesium concentrations [MM92; IAB+20] and temperature [VKC+04; WW06; KS06]. This limits the predictive power of this class of plasticity models.

An alternative approach taken by several groups [BI99; JDD+17; BST+19; CAA+22; ZSC+21] was to model the complex molecular cascade leading to synaptic weight changes. The main benefit is the direct correspondence between the model's components and biological elements, but at the price of numerous poorly constrained parameters. Additionally, the increased number of nonlinear equations and stochasticity makes fitting to plasticity experiment data difficult [MIE+20].

Subtle differences between experimental STDP protocols can produce completely different synaptic plasticity outcomes, indicative of finely tuned synaptic behavior. To tackle this problem, we devised a new plasticity rule based on a bottom-up, data-driven approach by building a biologically-grounded model of plasticity induction at a single rat hippocampal CA3–CA1 synapse. We focused on this synapse type because of the abundant published experimental data that can be used to quantitatively constrain the model parameters. Compared to previous models in the literature, we aimed for an intermediate level of detail: enough biophysical components to capture the key dynamical processes underlying plasticity induction, but not the detailed molecular cascade underlying plasticity expression; much of which is poorly quantified for the various experimental conditions we cover in our study [RTM+23].

Our model is centered on dendritic spine electrical dynamics, calcium signaling and immediate downstream molecules, which we then map to synaptic strength change via a geometric readout mechanism. The model assumes that a compartment-based description of calcium-triggered processes is sufficient to reproduce known properties of LTP and LTD induction. Also, neither spatially-resolved elements [BKK+15; GTM16] nor calcium-independent processes are required to predict the observed synaptic change. Crucially, the model also captured intrinsic noise based on the stochastic switching of synaptic receptors and ion channels [YMC+99; RST11]. We report that, with a single set of parameters, the model could account for published data from spike-timing and frequency-dependent plasticity experiments, and variations in physiological parameters influencing plasticity outcomes. We also tested how the model responded to *in vivo*-like spike timing jitter and spike failures (see also [CPM+18]).

4.2 Description of one particular experimental protocol

We reproduce several experiments in [RTM+23] but by lack of space, we chose to focus on [TOS+16]. In this *ex vivo* experimental study on adult rat hippocampus with blocked GABAr, the authors excite a CA1 neuron with pre / post-synaptic spikes and record the evolution of the synaptic strength. The stimulation protocols are represented in figure 4.1 a and the results are plotted in red in figure 4.1 b. What is remarkable is that some of these results are at odds with the canonical STDP (recall definition 4.1); one would for example expect that the 1Pre1Post10 causal protocol would reliably induce LTP whereas data shows a big variance in the response.

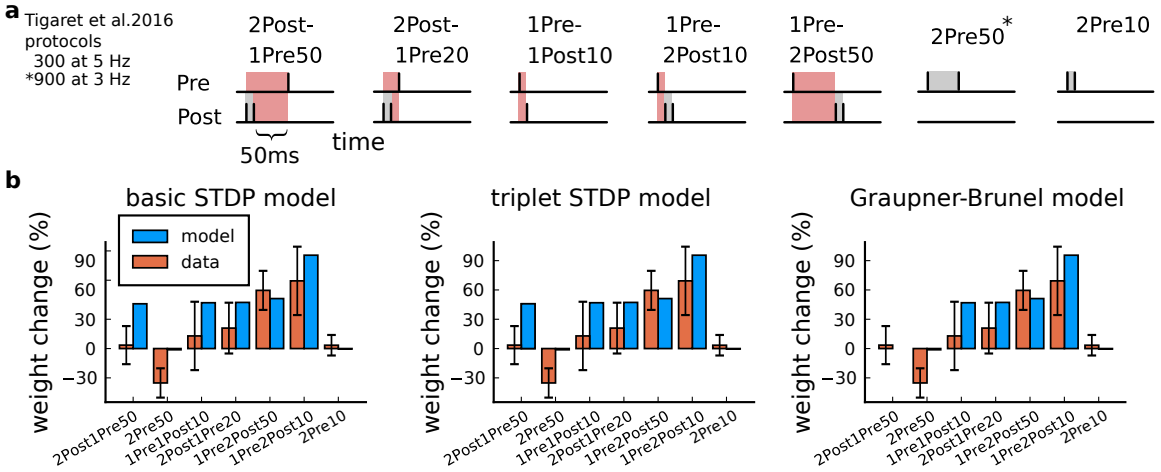

Figure 4.1: **Experimental protocols and standard models failure a**) Schematics of [TOS+16] protocols, adapted from Figure 2 b in [TOS+16]. Each vertical black segment represents a spike applied to the pre/post synaptic neuron. The last number, for example 10 in 1Pre1Post10, is the time interval between Pre and Post. Each pattern is repeated 300 times at 5Hz (or 900 times at 3Hz for 2Pre50). **b)** Standard models for predicting plasticity fail to account for [TOS+16] data. Mean weight change for the Tigaret's data (red), error bars denote ±1 s.d. Plasticity protocols indicated by labels on x-axis. Blue bars show mean plasticity predicted for the same protocols by classic STDP model [SMA+00], triplet STDP model [PG06], or Graupner-Brunel calcium-based STDP [GB12] model.

The second part of figure 4.1 highlights the difficulties faced by standard plasticity models to account for [TOS+16] data such as those regarding the 1Pre1Post10 protocol. More models are reviewed in [TOS+16].

4.3 Brief description of the model without the readout

The main question is to predict whether the synapse strengthens or weakens given the times of arrival of the APs[2] at the pre/post synaptic side depending on the experimental conditions. At the synapse level, the pre-synaptic side only "sees" AP whereas we assume that the post-synaptic side is stimulated by bAPs. The near coincidence of APs / bAPs is what drives synaptic plasticity.

[2]these are both AP and bAP

These APs cause changes in the membrane potential of the post-synaptic side by the ions influxes through open receptors. Calcium, one of those ions, then interacts through Calmodulin with two enzymes CaMKII and CaN which are crucial for synaptic plasticity (see figure 4.2). We limit ourselves in [RTM+23] to modeling *only* the induction of synaptic plasticity and not the structural changes following this induction (such as the insertion of new receptors for example).

The model also describes the pre-synaptic components and more precisely the pool of vesicles containing the Glutamate (Glu) neurotransmitter. It is important to do so to account for the lack of synaptic transmission when the pre-synaptic side is strongly stimulated which depletes the vesicles.

Given the smallness of the dendritic spine supporting the synapse, the number of receptors is small $O(10)$ allowing an individual description by time continuous Markov chains: the noise is therefore an intrinsic component of the model.

The membrane potential of the spine V_{sp} and of the dendrite V_{dend}, the calcium concentration Ca in the post-synaptic side, the Calmodulin (CaM) activity and the activity of the two enzymes[3] $CaMKII$, CaN are described by *continuous variables*, see red variables in figure 4.2.

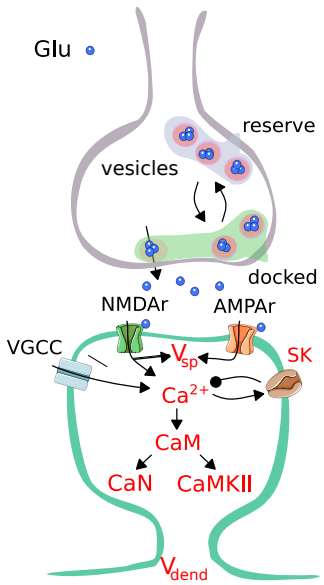

Figure 4.2: Schematic of the synapse model. Variables in black are modeled with Markov chains, those in red with continuous variables.

Formally, the synapse model is thus a PDMP. Indeed, all receptors/channels (except SK channels) are described with a continuous time Markov chain whose transition rates may depend on some *continuous variable*.

Let us describe more precisely two components of the model to give an idea of the formalism. The Markov chain modeling the dynamics of the L-type VGCCs[4] has transition rates depending on the spine membrane potential V_{sp}:

$$O_{L1} \underset{\alpha^L(V_{sp})}{\overset{\beta_1^L(V_{sp})}{\rightleftharpoons}} C_0 \underset{\beta_2^L(V_{sp})}{\overset{\alpha^L(V_{sp})}{\rightleftharpoons}} O_{L2}$$

for some $\alpha^L, \beta_1^L, \beta_2^L$ rate functions. It has two open states, O_{L1} and O_{L2} and one closed C_0. The spine *continuous variable* membrane potential V_{sp} satisfies the ODE in between the jumps[5]

$$C_{sp} \cdot \frac{dV_{sp}}{dt} = g_{neck} \cdot (V_{dend} - V_{sp}) + g_L^{sp} \cdot (E_{rev} - V_{sp}) + I_T + I_L + I_R + I_{NMDA} + I_{AMPA} + I_{SK}$$

[3] A detailed model of these two enzymes seems difficult, for example CaMKII has an astronomical number of internal states.

[4] voltage-gated calcium channel

[5] which are the Markov chains transitions

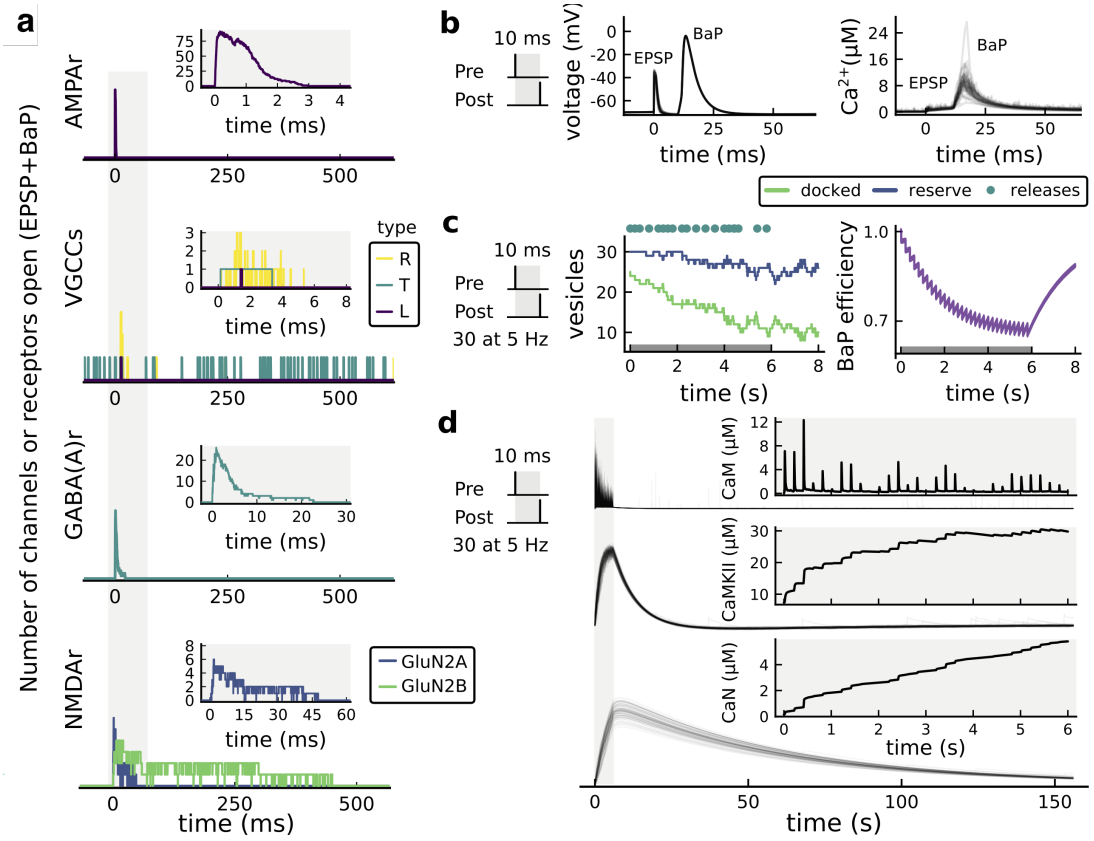

Figure 4.3: **The synapse model, its timescales and mechanisms**. **a**) Stochastic dynamics of the different ligand-gated and voltage-gated ion channels in the model in response to a single stimulus 1Pre. Plots show the total number of open channels as a function of time. The insets show a zoomed time axis highlighting the difference in timescale of the activity among the channels. **b**) Dendritic spine membrane potential (left) and calcium concentration (right) as function of time for a single causal (1Pre1Post10) stimulus (EPSP: single excitatory postsynaptic potential 1Pre; BaP: single back-propagating action potential 1Post). **c**) Left: depletion of vesicle pools (reserve and docked) induced by 30 pairing repetitions delivered at 5 Hz. Right: bAP efficiency as function of time. bAP efficiency phenomenologically captures the distance-dependent attenuation of bAP. **d**) Concentration of active enzyme for CaM, CaN and CaMKII, as function of time triggered by 30 repetitions of 1Pre1Post10 pairing stimulations delivered at 5 Hz. The vertical grey bar is the duration of the stimuli, 6 s. The multiple traces in panels **c** (right) and **e** reflect the run-to-run variability due to the inherent stochasticity in the model.

where g_{neck}, g_L^{sp} are conductances and C_{sp} is the spine membrane capacitance. The last terms are ionic currents, for example $I_L \propto (n_{O_{L1}} + n_{O_{L2}})$ is the ionic current through the L-type VGCC and $n_{O_{L1}}$ is the number of VGCC in the state O_{L1}.

The simulation of these equations is based on the algorithm [Vel15] implemented in the Julia package PiecewiseDeterministicMarkovProcesses.jl. The synapse model is available at the link SynapseElife. An example of the dynamics of the main components of the model is shown in figure 4.3.

Basic mechanism for activating CaMKII / CaN

After this brief description of the model components, we give the reader an intuition for activating the two proteins CaMKII and CaN. From the figure 4.2, it appears that the activation of the proteins is only function of the Calcium concentration. Calcium mostly enters the post synaptic side through NMDA receptors when they are open. They open when glutamate has been released upon an AP reaching the synapse and when the postsynaptic transmembrane potential is high enough, for example when a bAP reaches the synapse. Thus, the near coincidence of arrivals of APs and bAPs is what mainly triggers the activation CaMKII and CaN.

We now describe how this activation leads to synaptic weight change using a phenomenological model. We thus search for a criterion on the activity CaMKII / CaN which produces LTP or LTD.

4.3.1 Description of the readout and of one experimental result

After describing the key elements of the model up to the enzymes CaMKII/CaN, we still need to provide the mechanism, called "readout", which controls whether the synapse strengthens, weakens or keeps its current strength. To do this, we need to understand how the two enzymes behave in response to different stimuli.

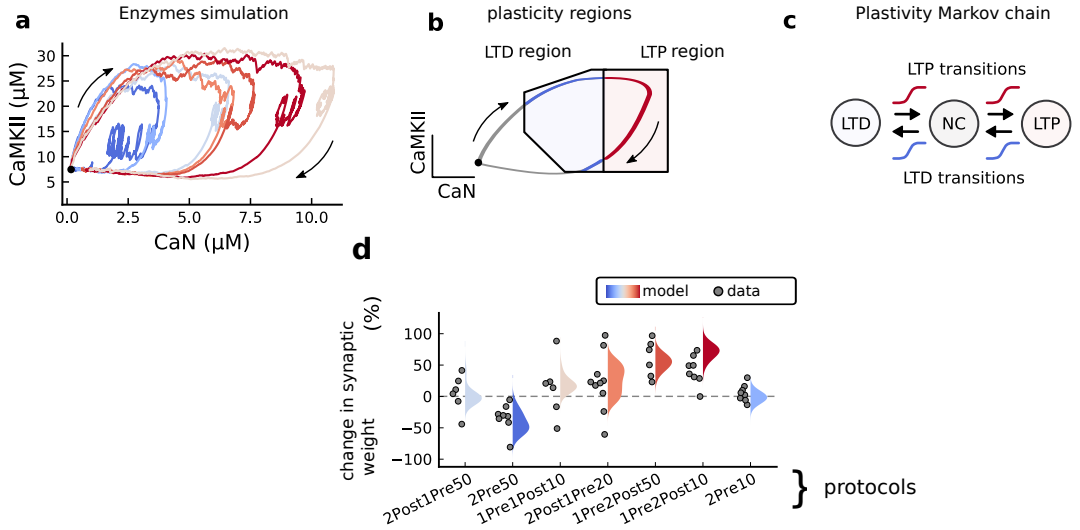

Figure 4.4: **a)** Dynamics in the (CaN,CaMKII) plane for the protocols listed on the abscissa of d). The arrow indicates the time evolution. **b)** Regions of plasticity used to describe the transition rates of the plasticity Markov chain shown in c). **c)** Markov chain of plasticity with LTD (depression), NC (no change) and LTP (potentiation) states. **d)** Reproduction of the results from [TOS+16].

It is remarkable that for the different protocols, the activity of the enzymes follows a rather characteristic curve in the $CaN - CaMKII$ plane, see figure 4.4 a where each color codes for a protocol of [TOS+16] as shown in figure 4.1 a. The experimental data indicates that the red (resp. blue) curves of figure 4.4 a are associated with potentiation (LTP) (resp. depression (LTD)) and this suggests to define two polygonal *plasticity regions*, one for LTP and one for LTP (cf. figure 4.4 b). The underlying theoretical idea is that the plasticity region in which

the trajectory spends the most time gives the final state of the synapse (LTP/LTD/No change). Formally, this final state is modeled by a continuous time Markov chain (see figure 4.4 c) whose transition rates are functions of the indicators of the plasticity regions of figure 4.4 b. *Plasticity regions* and the *plasticity Markov chain* rates are fitted to data from [TOS+16], cf. figure 4.4 d. The model manages to capture some of the variance of the data although we did not try to explicitly fit the data distribution.

It is remarkable that the same set of parameters makes it possible to reproduce nine different experiments, showing the robustness of the model and its ability to integrate the different experimental modalities (external magnesium, animal age, temperature, etc.)

4.4 Perspectives

Besides providing a biophysical model of rat CA3-CA1 synapse, the main contribution from this work is the new mechanism[6] relating enzyme dynamics to plasticity outcome. The central finding is that the activity of CaN/CaMKII, although stochastic, can be separated in the plane according to the experimental protocol (*cf.* figure 4.4 a). This separability, as well as the flexibility of the model via the adjustment of plasticity regions, allowed us to reproduce data from different experiments using a single fixed set of model parameters. In passing, the main prediction of the model is that the activity in the CaN/CaMKII plane is structured and allows to predict the plasticity outcome.

We have identified some limitations of the model (see [RTM+23]) and possible research perspectives (see also the recent review [ODo23]) and we shall only discuss a few. First, we modeled only one synapse whereas synapses (which form clusters on the dendrite) share resources and this impacts plasticity. Second, even though the model reproduces the initial phase of plasticity in the first 30 to 60 minutes after induction, we did not take into account the slower processes dependent on protein synthesis, maintenance processes, etc. at later time scales. Third, we did not analyze in detail the effect of extrinsic parameters, such as the "size" of the synapse which is related to the number of receptors.

Thus, the development of this model opens the way to interesting perspectives in neurobiology but also in machine learning. It should become a valuable tool for neurophysiologists to predict the outcome of *in silico* synapse plasticity, thereby optimizing experiment time and reducing animal usage. It could also be adapted and simplified for use in bio-inspired machine learning.

Another interesting research avenue would be to simplify the model into a phenomenological one like [GB12] and keeping the readout mechanism. One could then embed it into the simplified networks studied in the previous chapters. This last perspective remains highly non trivial though.

[6] which is still speculative

Chapter 5

Conclusion

The intersection of dynamical systems theory, probability theory, and mathematical neuroscience is indeed a fertile ground where fundamental questions in one field are enriched by concepts and results from the others.

The goal of the exposed research project was to study the dynamics of networks of stochastic spiking neurons with plastic connections. We tackled this question under the mean field assumption. My long-term goal was to obtain a closed-form formulation of the dynamics of the connection weights, independent of a description of the neuron dynamics. This seems feasible thanks to the separation of time scales, as synaptic plasticity is slow compared to spiking dynamics. Despite some promising results presented in the thesis of P. Helson [Hel21], our progress was mainly in the study of *non plastic* neural networks, leaving several open questions.

Several perspectives were discussed in chapters 2, 3 concerning the study of *non plastic* networks of spiking neurons. The most immediate is to generalize to 2D neuron dynamics and link the network dynamics to that of the underlying neurons. For instance, if the network consists of bursting neurons, what is the dynamics of the mean field? This question is particularly interesting in light of recent models of the whole brain described by graphs whose connections are derived from functional magnetic resonance imaging (fMRI), where each node represents a cortical area [WKK+19]. In these studies [DPM+13; WKK+19], the node dynamics is a phenomenological mean field model expressed as SDEs as opposed to the McKean-Vlasov formulation used in this memoir. It would be invaluable, at least for computational neuroscience, to compare the two formulations and identify their differences. See also the recent work on a conductance-based model of spiking neurons [AGD24]. Additionally, exploring different connectivity modalities, such as sparse networks as opposed to those used in this memoir, is a very interesting perspective from both mathematical and computational viewpoints.

The spatial organization of the (visual) cortex in mammals suggests examining space-dependent neural networks and studying their dynamics (localized solutions, wave propagation, etc.) in the context of spatially distributed spiking networks. This is theme of research I chose not to present in this memoir (see section 1.5.) The field has been actively researched in the context of neural fields (see work by G. Faye [Fay19]). For the models discussed in this memoir, this

seems to be an important research avenue (see recent thesis [Aga23]).

A final general perspective concerns the study of network models that do not rely on the mean field assumption. This area is currently under-explored in the mathematical neuroscience community.

Lastly, despite having a "standard model" for the propagation of trans-membrane electric potentials and spiking, the field of computational neuroscience still lacks a "standard model" of synapse and more precisely of synaptic plasticity which strikes a reasonable balance between the biophysics and the abstraction associated to the unknowns.

Chapter 6

List of publications

During Phd

[VF13] Romain Veltz and Olivier Faugeras. A Center Manifold Result for Delayed Neural Fields Equations. *SIAM Journal on Mathematical Analysis*, 45(3):1527–1562, January 2013. DOI: 10.1137/110856162 (cited on page 16).

After Phd

[RTV+13] James Rankin, Émilien Tlapale, Romain Veltz, Olivier Faugeras, and Pierre Kornprobst. Bifurcation analysis applied to a model of motion integration with a multistable stimulus. *Journal of Computational Neuroscience*, 34(1):103–124, February 2013. DOI: 10.1007/s10827-012-0409-5.

[Vel13] Romain Veltz. Interplay Between Synaptic Delays and Propagation Delays in Neural Field Equations. *SIAM Journal on Applied Dynamical Systems*, 12(3):1566–1612, January 2013. DOI: 10.1137/120889253 (cited on page 6).

[VCF15] Romain Veltz, Pascal Chossat, and Olivier Faugeras. On the Effects on Cortical Spontaneous Activity of the Symmetries of the Network of Pinwheels in Visual Area V1. *The Journal of Mathematical Neuroscience (JMN)*, 5(1):1–28, May 2015. DOI: 10.1186/s13408-015-0023-8 (cited on page 6).

[VF15] Romain Veltz and Olivier Faugeras. ERRATUM: A Center Manifold Result for Delayed Neural Fields Equations. *SIAM Journal on Mathematical Analysis*, 47(2):1665–1670, January 2015. DOI: 10.1137/140962279.

[VS15] Romain Veltz and Terrence J. Sejnowski. Periodic Forcing of Inhibition-Stabilized Networks: Nonlinear Resonances and Phase-Amplitude Coupling. *Neural Computation*, 27(12):2477–2509, December 2015. DOI: 10.1162/NECO_a_00786.

[DV17] Audric Drogoul and Romain Veltz. Hopf bifurcation in a nonlocal nonlinear transport equation stemming from stochastic neural dynamics. *Chaos: An Interdisciplinary Journal of Nonlinear Science*, 27(2), February 2017. DOI: 10.1063/1.4976510 (cited on pages 10, 13, 18, 19, 25, 26).

[DGP+18] A. Dolcemascolo, B. Garbin, B. Peyce, R. Veltz, and S. Barland. Resonator neuron and triggering multipulse excitability in laser with injected signal. *Physical Review E*, 98(6), December 2018. DOI: 10.1103/PhysRevE.98.062211 (cited on page 7).

[GVG+18] Tomasz Górski, Romain Veltz, Mathieu Galtier, Hélissande Fragnaud, Jennifer S. Goldman, Bartosz Teleńczuk, and Alain Destexhe. Dendritic sodium spikes endow neurons with inverse firing rate response to correlated synaptic activity. *Journal of Computational Neuroscience*, 45(3):223–234, December 2018. DOI: 10.1007/s10827-018-0707-7 (cited on pages 5, 29).

[SFV19] Anna Song, Olivier Faugeras, and Romain Veltz. A neural field model for color perception unifying assimilation and contrast. *PLOS Computational Biology*, 15(6):e1007050, June 2019. DOI: 10.1371/journal.pcbi.1007050 (cited on page 6).

[ADV+20] Daniele Avitabile, Mathieu Desroches, Romain Veltz, and Martin Wechselberger. Local Theory for Spatio-Temporal Canards and Delayed Bifurcations. *SIAM Journal on Mathematical Analysis*, 52(6):5703–5747, January 2020. DOI: 10.1137/19M1306610 (cited on page 7).

[CTV20] Quentin Cormier, Etienne Tanré, and Romain Veltz. Long time behavior of a mean-field model of interacting neurons. *Stochastic Processes and their Applications*, 130(5):2553–2595, May 2020. DOI: 10.1016/j.spa.2019.07.010 (cited on pages 13, 19, 20).

[DMV+20] A. Dolcemascolo, A. Miazek, R. Veltz, F. Marino, and S. Barland. Effective low-dimensional dynamics of a mean-field coupled network of slow-fast spiking lasers. *Physical Review E*, 101(5), May 2020. DOI: 10.1103/PhysRevE.101.052208 (cited on page 7).

[FTV20] Nicolas Fournier, Etienne Tanré, and Romain Veltz. On a toy network of neurons interacting through their dendrites. *Annales de l'Institut Henri Poincaré, Probabilités et Statistiques*, 56(2):1041–1071, May 2020. DOI: 10.1214/19-AIHP993 (cited on pages 6, 29–31, 41).

[Vel20] Romain Veltz. BifurcationKit.jl, July 2020. URL: https://hal.archives-ouvertes.fr/hal-02902346 (cited on page 7).

[CTV21] Quentin Cormier, Etienne Tanré, and Romain Veltz. Hopf bifurcation in a Mean-Field model of spiking neurons. *Electronic Journal of Probability*, 26:1–40, January 2021. DOI: 10.1214/21-EJP688 (cited on pages 13, 19, 23, 25).

[DVD+21] Otti D'Huys, Romain Veltz, Axel Dolcemascolo, Francesco Marino, and Stéphane Barland. Canard resonance: on noise-induced ordering of trajectories in heterogeneous networks of slow-fast systems. *Journal of Physics: Photonics*, 3(2), April 2021. DOI: 10.1088/2515-7647/abcbe3 (cited on page 7).

[DV21] Audric Drogoul and Romain Veltz. Exponential stability of the stationary distribution of a mean field of spiking neural network. *Journal of Differential Equations*, 270:809–842, January 2021. DOI: 10.1016/j.jde.2020.08.001 (cited on pages 10, 13–15, 21, 27).

[FSV22] Olivier D. Faugeras, Anna Song, and Romain Veltz. Spatial and color hallucinations in a mathematical model of primary visual cortex. *Comptes Rendus. Mathématique*, 360(G1):59–87, 2022. DOI: 10.5802/crmath.289 (cited on page 6).

[CDI+23] Magda Chafaï, Ariane Delrocq, Perrine Inquimbert, Ludivine Pidoux, Kevin Delanoe, Maurizio Toft, Frederic Brau, Eric Lingueglia, Romain Veltz, and Emmanuel Deval. Dual contribution of ASIC1a channels in the spinal processing of pain information by deep projection neurons revealed by computational modeling. *PLOS Computational Biology*, 19(4), April 2023. DOI: 10.1371/journal.pcbi.1010993 (cited on page 7).

[RTM+23] Yuri Elias Rodrigues, Cezar M Tigaret, Hélène Marie, Cian O'Donnell, and Romain Veltz. A stochastic model of hippocampal synaptic plasticity with geometrical readout of enzyme dynamics. *eLife*, 12, August 2023. DOI: 10.7554/eLife.80152 (cited on pages 49, 51–53, 56).

Pre-publications

[Vel15] Romain Veltz. A new twist for the simulation of hybrid systems using the true jump method. *arXiv:1504.06873*, 2015. DOI: 10.48550/arXiv.1504.06873 (cited on page 54).

[ACV19] Benjamin Aymard, Fabien Campillo, and Romain Veltz. Mean-field limit of interacting 2D nonlinear stochastic spiking neurons, June 2019. DOI: 10.48550/arXiv.1906.10232.

Other publications

[Lap07] Louis Lapicque. Recherches quantitatives sur l'excitation électrique des nerfs traitée comme une polarisation. *J. Physiol. Pathol. Gen.*, 9:567–578, 1907 (cited on page 12).

[Heb49] Donald Olding Hebb. The organization of behavior: a neuropsychological theory, 1949 (cited on page 50).

[HH52] A. L. Hodgkin and A. F. Huxley. A quantitative description of membrane current and its application to conduction and excitation in nerve. *The Journal of Physiology*, 117(4):500–544, August 1952. DOI: 10.1113/jphysiol.1952.sp004764 (cited on page 12).

[Ula61] Ulam. Monte Carlo calculations in problems of mathematical physics. *Modern mathematics for the engineer: Second series*, 1961 (cited on page 46).

[Ham72] J. M. Hammersley. A few seedlings of research. *Proceedings of the Sixth Berkeley Symposium on Mathematical Statistics and Probability, Volume 1: Theory of Statistics*:345–394, 1972. University of California Press, Berkeley, CA, (cited on page 46).

[WC72] Hugh R. Wilson and Jack D. Cowan. Excitatory and Inhibitory Interactions in Localized Populations of Model Neurons. *Biophysical Journal*, 12(1):1–24, January 1972. DOI: 10.1016/S0006-3495(72)86068-5 (cited on page 6).

[GM74] Morton E. Gurtin and Richard C. MacCamy. Non-linear age-dependent population dynamics. *Archive for Rational Mechanics and Analysis*, 54(3):281–300, 1974. DOI: 10.1007/bf00250793 (cited on page 16).

[LS77] B. F Logan and L. A Shepp. A variational problem for random Young tableaux. *Advances in Mathematics*, 26(2):206–222, November 1977. DOI: 10.1016/0001-8708(77)90030-5 (cited on page 46).

[VK77] Anatolii Moiseevich Veršik and Sergei V Kerov. Asymptotic behavior of the Plancherel measure of the symmetric group and the limit form of Young tableaux. In *Dokl. Akad. Nauk SSSR*, volume 233, pages 1024–1027, 1977. Issue: 6 (cited on page 46).

[Fen79] Neil Fenichel. Geometric singular perturbation theory for ordinary differential equations. *Journal of Differential Equations*, 31(1):53–98, January 1979. DOI: 10.1016/0022-0396(79)90152-9 (cited on page 7).

[Ioo79] G. Iooss. *Bifurcation of maps and applications*, volume 36 of *North-Holland Math. Stud.* Elsevier, Amsterdam, 1979. DOI: 10.1016/s0304-0208(08)x7076-8 (cited on pages 16, 18).

[Hen81] Daniel Henry. *Geometric Theory of Semilinear Parabolic Equations*. Springer Berlin Heidelberg, 1981. ISBN: 978-3-540-38528-8. DOI: 10.1007/bfb0089647. ISSN: 1617-9692 Publication Title: Lecture Notes in Mathematics (cited on pages 22, 23).

[Paz83] A. Pazy. *Semigroups of linear operators and applications to partial differential equations*, volume 44 of *Appl. Math. Sci.* Springer, Cham, 1983. DOI: 10.1007/978-1-4612-5561-1. ISSN: 0066-5452 (cited on page 14).

[DS86] W. Desch and W. Schappacher. Linearized stability for nonlinear semigroups. In *Differential Equations in Banach Spaces*. Volume 1223, pages 61–73. Springer Berlin Heidelberg, Berlin, Heidelberg, 1986. ISBN: 978-3-540-47350-3. DOI: 10.1007/BFb0099183. (Visited on 02/24/2024). Series Title: Lecture Notes in Mathematics (cited on pages 9, 15, 16, 23).

[BW88] Béla Bollobás and Peter Winkler. The longest chain among random points in Euclidean space. *Proceedings of the American Mathematical Society*, 103(2):347–353, 1988. DOI: 10.1090/S0002-9939-1988-0943043-6 (cited on page 46).

[Bri88] D. R. Brillinger. Maximum likelihood analysis of spike trains of interacting nerve cells. *Biological Cybernetics*, 59(3):189–200, August 1988. DOI: 10.1007/BF00318010 (cited on page 12).

[Lis89] John Lisman. A mechanism for the Hebb and the anti-Hebb processes underlying learning and memory. *Proceedings of the National Academy of Sciences*, 86(23):9574–9578, 1989. DOI: 10.1073/pnas.86.23.9574 (cited on page 50).

[ABS90] Alain Artola, S Bröcher, and Wolf Singer. Different voltage-dependent thresholds for inducing long-term depression and long-term potentiation in slices of rat visual cortex. *Nature*, 347(6288):69–72, 1990. DOI: 10.1038/347069a0 (cited on page 50).

[GH90] A. Grabosch and H. J. a. M. Heijmans. Cauchy problems with state-dependent time evolution. *Japan Journal of Applied Mathematics*, 7(3):433–457, 1990. DOI: 10.1007/BF03167853 (cited on page 16).

[DB92] SM Dudek and MF Bear. Homosynaptic long-term depression in area CA1 of hippocampus and effects of N-methyl-D-aspartate receptor blockade. *Proceedings of the National Academy of Sciences*, 89(10):4363, 1992. DOI: 10.1073/pnas.89.10.4363 (cited on page 50).

[MM92] Rosel M Mulkey and Robert C Malenka. Mechanisms underlying induction of homosynaptic long-term depression in area CA1 of the hippocampus. *Neuron*, 9(5):967–975, 1992. DOI: 10.1016/0896-6273(92)90248-c (cited on page 51).

[Dav93] Mark H. A. Davis. *Markov models and optimization*. Monographs on statistics and applied probability. Chapman & Hall, London ; New York, 1st ed edition, 1993. ISBN: 0-412-31410-X. DOI: 10.1201/9780203748039 (cited on pages 5, 10).

[DB93] Serena M Dudek and Mark F Bear. Bidirectional long-term modification of synaptic effectiveness in the adult and immature hippocampus. *Journal of Neuroscience*, 13(7):2910–2918, 1993. DOI: 10.1523/jneurosci.13-07-02910.1993 (cited on page 51).

[HV93] Jack K. Hale and Sjoerd M. Verduyn Lunel. *Introduction to functional differential equations*, volume 99 of *Appl. Math. Sci.* New York, NY: Springer-Verlag, 1993. ISBN: 0-387-94076-6. DOI: 10.1007/978-1-4612-4342-7 (cited on page 16).

[AD95] D. Aldous and P. Diaconis. Hammersley's interacting particle process and longest increasing subsequences. *Probability Theory and Related Fields*, 103(2):199–213, 1995. DOI: 10.1007/BF01204214 (cited on page 46).

[DZ95] Jean-Dominique Deuschel and Ofer Zeitouni. Limiting Curves for I.I.D. Records. *The Annals of Probability*, 23(2):852–878, April 1995. DOI: 10.1214/aop/1176988293 (cited on pages 32, 35, 46).

[DvGV+95] Odo Diekmann, Stephan A. van Gils, Sjoerd M. Verduyn Lunel, and Hans-Otto Walther. *Delay equations. Functional-, complex-, and nonlinear analysis*, volume 110 of *Appl. Math. Sci.* New York, NY: Springer-Verlag, 1995. ISBN: 0-387-94416-8. DOI: 10.1007/978-1-4612-4206-2 (cited on page 16).

[Ger95] Wulfram Gerstner. Time structure of the activity in neural network models. *Physical Review E*, 51(1):738–758, January 1995. DOI: 10.1103/PhysRevE.51.738 (cited on pages 12–14).

[MS95] H Markram and B Sakmann. Action potentials propagating back into dendrites trigger changes in efficacy of single-axon synapses between layer V pyramidal neurons. In *Soc. Neurosci. Abstr*, volume 21, page 2007, 1995. Issue: 3 (cited on page 50).

[BA96] Kenneth I Blum and Larry F Abbott. A model of spatial map formation in the hippocampus of the rat. *Neural computation*, 8(1):85–93, 1996. DOI: 10.7551/mitpress/4924.003.0010 (cited on page 50).

[DGG+96] Dominique Debanne, Nathalie C Guerineau, BH Gähwiler, and Scott M Thompson. Paired-pulse facilitation and depression at unitary synapses in rat hippocampus: quantal fluctuation affects subsequent release. *The Journal of physiology*, 491(1):163–176, 1996. DOI: 10.1016/0928-4257(94)90044-2 (cited on page 50).

[GKV+96] Wulfram Gerstner, Richard Kempter, J Leo Van Hemmen, and Hermann Wagner. A neuronal learning rule for sub-millisecond temporal coding. *Nature*, 383(6595):76–78, 1996. DOI: 10.1038/383076a0 (cited on page 50).

[CHT97] Xu-Yan Chen, Jack K. Hale, and Bin Tan. Invariant Foliations for C1 Semigroups in Banach Spaces. *Journal of Differential Equations*, 139(2):283–318, September 1997. DOI: 10.1006/jdeq.1997.3255 (cited on page 27).

[MJ97] Jeffrey C Magee and Daniel Johnston. A synaptically controlled, associative signal for Hebbian plasticity in hippocampal neurons. *Science*, 275(5297):209–213, 1997. DOI: 10.1126/science.275.5297.209 (cited on page 50).

[TM97] Misha V Tsodyks and Henry Markram. The neural code between neocortical pyramidal neurons depends on neurotransmitter release probability. *Proceedings of the national academy of sciences*, 94(2):719–723, 1997. DOI: 10.1073/pnas.94.2.719 (cited on page 50).

[BP98] Guo-qiang Bi and Mu-ming Poo. Synaptic modifications in cultured hippocampal neurons: dependence on spike timing, synaptic strength, and postsynaptic cell type. *Journal of neuroscience*, 18(24):10464–10472, 1998. DOI: 10.1523/jneurosci.18-24-10464.1998 (cited on page 50).

[GFF+98] Karl Peter Giese, Nikolai B Fedorov, Robert K Filipkowski, and Alcino J Silva. Autophosphorylation at Thr286 of the calcium-calmodulin kinase II in LTP and learning. *Science*, 279(5352):870–873, 1998. DOI: 10.1126/science.279.5352.870 (cited on page 49).

[BI99] Upinder S. Bhalla and Ravi Iyengar. Emergent Properties of Networks of Biological Signaling Pathways. *Science*, 283(5400):381–387, January 1999. DOI: 10.1126/science.283.5400.381 (cited on pages 49, 51).

[EPE+99] Christian W Eurich, Klaus Pawelzik, Udo Ernst, Jack D Cowan, and John G Milton. Dynamics of self-organized delay adaptation. *Physical Review Letters*, 82(7):1594, 1999. DOI: 10.1103/physrevlett.82.1594 (cited on page 50).

[YTZ99] Shao-Nian Yang, Yun-Gui Tang, and Robert S Zucker. Selective induction of LTP and LTD by postsynaptic $[Ca^{2+}]_i$ elevation. *Journal of neurophysiology*, 81(2):781–787, 1999. DOI: 10.1152/jn.1999.81.2.781 (cited on page 51).

[YMC+99] Rafael Yuste, Ania Majewska, Sydney S Cash, and Winfried Denk. Mechanisms of calcium influx into hippocampal spines: heterogeneity among spines, coincidence detection by NMDA receptors, and optical quantal analysis. *Journal of Neuroscience*, 19(6):1976–1987, 1999. DOI: 10.1523/jneurosci.19-06-01976.1999 (cited on page 51).

[Bru00] Nicolas Brunel. Dynamics of sparsely connected networks of excitatory and inhibitory spiking neurons. *Journal of computational neuroscience*, 8(3):183–208, 2000. DOI: 10.1023/A:1008925309027 (cited on page 9).

[EN00] Klaus-Jochen Engel and Rainer Nagel. *One-parameter semigroups for linear evolution equations*, volume 194 of *Grad. Texts Math.* Berlin: Springer, 2000. ISBN: 0-387-98463-1. DOI: 10.1007/b97696. ISSN: 0072-5285 (cited on pages 6, 14–17).

[Ger00] Wulfram Gerstner. Population Dynamics of Spiking Neurons: Fast Transients, Asynchronous States, and Locking. *Neural Computation*, 12(1):43–89, January 2000. DOI: 10.1162/089976600300015899 (cited on pages 12–14).

[SMA+00] S. Song, K. D. Miller, L. F. Abbott, et al. Competitive Hebbian learning through spike-timing-dependent synaptic plasticity. *Nature neuroscience*, 3:919–926, 2000. DOI: 10.1038/78829 (cited on page 52).

[CQC+01] Gastone C. Castellani, Elizabeth M. Quinlan, Leon N Cooper, and Harel Z. Shouval. A biophysical model of bidirectional synaptic plasticity: Dependence on AMPA and NMDA receptors. *Proceedings of the National Academy of Sciences*, 98(22):12772–12777, October 2001. DOI: 10.1073/pnas.201404598 (cited on pages 49, 50).

[MKS01] Tomoyuki Mizuno, Ichiro Kanazawa, and Masaki Sakurai. Differential induction of LTP and LTD is not determined solely by instantaneous calcium concentration: an essential involvement of a temporal factor. *European Journal of Neuroscience*, 14(4):701–708, 2001. DOI: 10.1046/j.0953-816x.2001.01679.x (cited on page 51).

[RHD01] Michael Rudolph, Nicolas Hô, and Alain Destexhe. Synaptic background activity affects the dynamics of dendritic integration in model neocortical pyramidal neurons. *Neurocomputing*. Computational Neuroscience: Trends in Research 2001, 38-40:327–333, June 2001. DOI: 10.1016/S0925-2312(01)00356-3 (cited on page 30).

[STN01] Per Jesper Sjöström, Gina G Turrigiano, and Sacha B Nelson. Rate, timing, and cooperativity jointly determine cortical synaptic plasticity. *Neuron*, 32(6):1149–1164, 2001. DOI: 10.1016/s0896-6273(01)00542-6 (cited on page 50).

[GSS02] Nace L Golding, Nathan P Staff, and Nelson Spruston. Dendritic spikes as a mechanism for cooperative long-term potentiation. *Nature*, 418(6895):326–331, 2002. DOI: 10.1038/nature00854 (cited on page 50).

[KB02] Uma R Karmarkar and Dean V Buonomano. A model of spike-timing dependent plasticity: one or two coincidence detectors? *Journal of neurophysiology*, 88(1):507–513, 2002. DOI: 10.1152/jn.2002.88.1.507 (cited on page 51).

[SBC02] Harel Z Shouval, Mark F Bear, and Leon N Cooper. A unified model of NMDA receptor-dependent bidirectional synaptic plasticity. *Proceedings of the National Academy of Sciences*, 99(16):10831–10836, 2002. DOI: 10.1073/pnas.152343099 (cited on page 51).

[AGH+03] Henry DI Abarbanel, Leif Gibb, Ramón Huerta, and Mikhail I Rabinovich. Biophysical model of synaptic plasticity dynamics. *Biological cybernetics*, 89(3):214–226, 2003. DOI: 10.1007/s00422-003-0422-x (cited on page 51).

[DRP03] Alain Destexhe, Michael Rudolph, and Denis Paré. The high-conductance state of neocortical neurons in vivo. *Nature Reviews Neuroscience*, 4(9):739–751, September 2003. DOI: 10.1038/nrn1198 (cited on page 30).

[FHV+03] Nicolas Fourcaud-Trocmé, David Hansel, Carl Van Vreeswijk, and Nicolas Brunel. How spike generation mechanisms determine the neuronal response to fluctuating inputs. *The Journal of neuroscience*, 23(37):11628–11640, 2003. DOI: 10.1523/JNEUROSCI.23-37-11628.2003 (cited on page 12).

[Kie03] Hansjörg Kielhöfer. *Bifurcation theory: an introduction with applications to PDEs*, number 156 in Applied mathematical sciences. Springer, New York, 2003. ISBN: 978-0-387-40401-1. DOI: 10.1007/978-1-4614-0502-3 (cited on pages 23–26).

[MFP03] Rhiannon M Meredith, Anna M Floyer-Lea, and Ole Paulsen. Maturation of long-term potentiation induction rules in rodent hippocampus: role of GABAergic inhibition. *Journal of Neuroscience*, 23(35):11142–11146, 2003. DOI: 10.1523/jneurosci.23-35-11142.2003 (cited on page 51).

[Koc04] Christof Koch. *Biophysics of computation: information processing in single neurons*. Computational neuroscience. Oxford Univ. Press, New York, 2004. ISBN: 978-0-19-518199-9. DOI: 10.1093/oso/9780195104912.001.0001 (cited on pages 4, 5).

[VKC+04] Maxim Volgushev, Igor Kudryashov, Marina Chistiakova, Mikhail Mukovski, Johannes Niesmann, and Ulf T Eysel. Probability of transmitter release at neocortical synapses at different temperatures. *Journal of neurophysiology*, 92(1):212–220, 2004. DOI: 10.1152/jn.01166.2003 (cited on page 51).

[YSB+04] Luk Chong Yeung, Harel Z Shouval, Brian S Blais, and Leon N Cooper. Synaptic homeostasis and input selectivity follow from a calcium-dependent plasticity model. *Proceedings of the National Academy of Sciences*, 101(41):14943–14948, 2004. DOI: 10.1073/pnas.0405555101 (cited on page 51).

[CQB+05] Gastone C Castellani, Elizabeth M Quinlan, Ferdinando Bersani, Leon N Cooper, and Harel Z Shouval. A model of bidirectional synaptic plasticity: from signaling network to channel conductance. *Learning & Memory*, 12(4):423–432, 2005. DOI: 10.1101/lm.80705 (cited on page 50).

[CG05] Eric Cator and Piet Groeneboom. Hammersley's process with sources and sinks. *The Annals of Probability*, 33(3):879–903, May 2005. DOI: 10.1214/009117905000000053 (cited on pages 34, 46).

[MZL+05] Paul Miller, Anatol M Zhabotinsky, John E Lisman, and Xiao-Jing Wang. The stability of a stochastic CaMKII switch: dependence on the number of enzyme molecules and protein turnover. *PLoS biology*, 3(4), 2005. DOI: 10.1371/journal.pbio.0030107 (cited on page 51).

[OWW05] Daniel H. O'Connor, Gayle M. Wittenberg, and Samuel S.-H. Wang. Dissection of Bidirectional Synaptic Plasticity Into Saturable Unidirectional Processes. *Journal of Neurophysiology*, 94(2):1565–1573, August 2005. DOI: 10.1152/jn.00047.2005 (cited on page 49).

[RGB+05] Jonathan E. Rubin, Richard C. Gerkin, Guo-Qiang Bi, and Carson C. Chow. Calcium Time Course as a Signal for Spike-Timing–Dependent Plasticity. *Journal of Neurophysiology*, 93(5):2600–2613, May 2005. DOI: 10.1152/jn.00803.2004 (cited on page 51).

[SK05] Harel Z Shouval and Georgios Kalantzis. Stochastic properties of synaptic transmission affect the shape of spike time–dependent plasticity curves. *Journal of neurophysiology*, 93(2):1069–1073, 2005. DOI: 10.1152/jn.00504.2004 (cited on page 51).

[WGN+05] Huai-Xing Wang, Richard C. Gerkin, David W. Nauen, and Guo-Qiang Bi. Coactivation and timing-dependent integration of synaptic potentiation and depression. *Nature Neuroscience*, 8(2):187–193, 2005. DOI: 10.1038/nn1387 (cited on page 51).

[Izh06] Eugene M. Izhikevich. *Dynamical Systems in Neuroscience: The Geometry of Excitability and Bursting*. The MIT Press, July 2006. ISBN: 978-0-262-27607-8. DOI: 10.7551/mitpress/2526.001.0001 (cited on page 27).

[KS06] Vitaly A Klyachko and Charles F Stevens. Temperature-dependent shift of balance among the components of short-term plasticity in hippocampal synapses. *Journal of Neuroscience*, 26(26):6945–6957, 2006. DOI: 10.1523/jneurosci.1382-06.2006 (cited on page 51).

[NS06] Thomas Nevian and Bert Sakmann. Spine Ca^{2+} signaling in spike-timing-dependent plasticity. *Journal of Neuroscience*, 26(43):11001–11013, 2006. DOI: 10.1523/jneurosci.1749-06.2006 (cited on page 51).

[PG06] Jean-Pascal Pfister and Wulfram Gerstner. Triplets of spikes in a model of spike timing-dependent plasticity. *Journal of Neuroscience*, 26(38):9673–9682, 2006. DOI: 10.1523/jneurosci.1425-06.2006 (cited on page 52).

[SH06] Per Jesper Sjöström and Michael Häusser. A cooperative switch determines the sign of synaptic plasticity in distal dendrites of neocortical pyramidal neurons. *Neuron*, 51(2):227–238, 2006. DOI: 10.1016/j.neuron.2006.06.017 (cited on page 50).

[WW06] Gayle M Wittenberg and Samuel S-H Wang. Malleability of spike-timing-dependent plasticity at the CA3–CA1 synapse. *Journal of Neuroscience*, 26(24):6610–6617, 2006. DOI: 10.1523/jneurosci.5388-05.2006 (cited on page 51).

[CGC+07] Yidao Cai, Jeffrey P Gavornik, Leon N Cooper, Luk C Yeung, and Harel Z Shouval. Effect of stochastic synaptic and dendritic dynamics on synaptic plasticity in visual cortex and hippocampus. *Journal of neurophysiology*, 97(1):375–386, 2007. DOI: 10.1152/jn.00895.2006 (cited on page 51).

[Per07] Benoît Perthame. *Transport equations in biology*. Front. Math. Basel: Birkhäuser, 2007. ISBN: 3-7643-7841-7. DOI: 10.1007/978-3-7643-7842-4. ISSN: 1660-8046 (cited on page 15).

[BLB+08] Laurent Badel, Sandrine Lefort, Thomas K. Berger, Carl C. H. Petersen, Wulfram Gerstner, and Magnus J. E. Richardson. Extracting non-linear integrate-and-fire models from experimental data using dynamic I–V curves. *Biological Cybernetics*, 99(4):361–370, November 2008. DOI: 10.1007/s00422-008-0259-4 (cited on page 12).

[HS09] Jason Hardie and Nelson Spruston. Synaptic depolarization is more effective than back-propagating action potentials during induction of associative long-term potentiation in hippocampal pyramidal neurons. *Journal of Neuroscience*, 29(10):3233–3241, 2009. DOI: 10.1523/jneurosci.6000-08.2009 (cited on page 50).

[PPS09] Khashayar Pakdaman, Benoît Perthame, and Delphine Salort. Dynamics of a structured neuron population. *Nonlinearity*, 23(1):55, December 2009. DOI: 10.1088/0951-7715/23/1/003 (cited on page 14).

[CG10] Claudia Clopath and Wulfram Gerstner. Voltage and spike timing interact in STDP–a unified model. *Frontiers in synaptic neuroscience*, 2:25, 2010. DOI: 10.3389/fnsyn.2010.00025 (cited on pages 49, 51).

[RTG+10] Owen Rackham, Krasimira Tsaneva-Atanasova, Ayalvadi Ganesh, and Jack Mellor. A Ca^{2+}-based computational model for NMDA receptor-dependent synaptic plasticity at individual post-synaptic spines in the hippocampus. *Frontiers in synaptic neuroscience*, 2:31, 2010. DOI: 10.3389/fnsyn.2010.00031 (cited on page 51).

[ZH10] Shangyou Zeng and William R Holmes. The effect of noise on CaMKII activation in a dendritic spine during LTP induction. *Journal of neurophysiology*, 103(4):1798–1808, 2010. DOI: 10.1152/jn.91235.2008 (cited on page 51).

[CCP11] María J Cáceres, José A Carrillo, and Benoît Perthame. Analysis of Nonlinear Noisy Integrate & Fire Neuron Models: blow-up and steady states. *The Journal of Mathematical Neuroscience*, 1(1):7, 2011. DOI: 10.1186/2190-8567-1-7 (cited on page 12).

[HI11] Mariana Haragus and Gérard Iooss. *Local Bifurcations, Center Manifolds, and Normal Forms in Infinite-Dimensional Dynamical Systems*. Springer London, London, 2011. ISBN: 978-0-85729-111-0 978-0-85729-112-7. DOI: 10.1007/978-0-85729-112-7 (cited on pages 6, 9, 15, 19, 23, 27).

[JBH+11] Patrick Jahn, Rune W. Berg, Jørn Hounsgaard, and Susanne Ditlevsen. Motoneuron membrane potentials follow a time inhomogeneous jump diffusion process. *Journal of Computational Neuroscience*, 31(3):563–579, November 2011. DOI: 10.1007/s10827-011-0326-z (cited on page 12).

[KM11] Arvind Kumar and Mayank R. Mehta. Frequency-Dependent Changes in NMDAR-Dependent Synaptic Plasticity. *Frontiers in Computational Neuroscience*, 5, 2011. DOI: 10.3389/fncom.2011.00038 (cited on page 51).

[MGS11] Henry Markram, Wulfram Gerstner, and Per Jesper Sjöström. A history of spike-timing-dependent plasticity. *Frontiers in synaptic neuroscience*, 3:4, 2011. DOI: 10.3389/fnsyn.2011.00004 (cited on page 50).

[RST11] Claire Ribrault, Ken Sekimoto, and Antoine Triller. From the stochasticity of molecular processes to the variability of synaptic transmission. *Nature Reviews Neuroscience*, 12(7):375, 2011. DOI: 10.1038/nrn3025 (cited on page 51).

[CH12] Guan Cao and Kristen M Harris. Developmental regulation of the late phase of long-term potentiation (L-LTP) and metaplasticity in hippocampal area CA1 of the rat. *Journal of neurophysiology*, 107(3):902–912, 2012. DOI: 10.1152/jn.00780.2011 (cited on page 51).

[GB12] Michael Graupner and Nicolas Brunel. Calcium-based plasticity model explains sensitivity of synaptic changes to spike pattern, rate, and dendritic location. *Proceedings of the National Academy of Sciences*, 109(10):3991–3996, 2012. DOI: 10.1073/pnas.1109359109 (cited on pages 49, 51, 52, 56).

[MNP+12] Skander Mensi, Richard Naud, Christian Pozzorini, Michael Avermann, Carl C. H. Petersen, and Wulfram Gerstner. Parameter extraction and classification of three cortical neuron types reveals two distinct adaptation mechanisms. *Journal of Neurophysiology*, 107(6):1756–1775, March 2012. DOI: 10.1152/jn.00408.2011. Publisher: American Physiological Society (cited on page 12).

[CGG+13] José A. Carrillo, María d M. González, Maria P. Gualdani, and Maria E. Schonbek. Classical Solutions for a Nonlinear Fokker-Planck Equation Arising in Computational Neuroscience. *Communications in Partial Differential Equations*, 38(3):385–409, March 2013. DOI: 10.1080/03605302.2012.747536 (cited on page 12).

[DPM+13] Gustavo Deco, Adrián Ponce-Alvarez, Dante Mantini, Gian Luca Romani, Patric Hagmann, and Maurizio Corbetta. Resting-State Functional Connectivity Emerges from Structurally and Dynamically Shaped Slow Linear Fluctuations. *Journal of Neuroscience*, 33(27):11239–11252, July 2013. DOI: 10.1523/JNEUROSCI.1091-13.2013. Publisher: Society for Neuroscience Section: Articles (cited on page 57).

[HUK+13] Minoru Honda, Hidetoshi Urakubo, Takuya Koumura, and Shinya Kuroda. A common framework of signal processing in the induction of cerebellar LTD and cortical STDP. *Neural Networks*, 43:114–124, July 2013. DOI: 10.1016/j.neunet.2013.01.018 (cited on page 51).

[Kan13] Eric R. Kandel. *Principles of neural science*. McGraw-Hill, New York, 5th ed edition, 2013. ISBN: 978-0-07-139011-8 (cited on pages 3, 4).

[PPS13] Khashayar Pakdaman, Benoît Perthame, and Delphine Salort. Relaxation and Self-Sustained Oscillations in the Time Elapsed Neuron Network Model. *SIAM Journal on Applied Mathematics*, 73(3):1260–1279, January 2013. DOI: 10.1137/110847962 (cited on page 14).

[vGJK+13] S. A. van Gils, S. G. Janssens, Yu. A. Kuznetsov, and S. Visser. On local bifurcations in neural field models with transmission delays. *Journal of Mathematical Biology*, 66(4-5):837–887, 2013. DOI: 10.1007/s00285-012-0598-6 (cited on page 16).

[CEH14] Jeff Calder, Selim Esedoḡlu, and Alfred O. Hero. A Hamilton–Jacobi Equation for the Continuum Limit of Nondominated Sorting. *SIAM Journal on Mathematical Analysis*, 46(1):603–638, January 2014. DOI: 10.1137/13092842X (cited on pages 32, 38, 40, 41, 46).

[GKN+14] Wulfram Gerstner, Werner M. Kistler, Richard Naud, and Liam Paninski. *Neuronal dynamics: from single neurons to networks and models of cognition*. Cambridge University Press, 2014. ISBN: 978-1-107-44761-5. DOI: 10.1017/CBO9781107447615 (cited on pages 4, 5, 12).

[STB14] Dominic Standage, Thomas Trappenberg, and Gunnar Blohm. Calcium-dependent calcium decay explains STDP in a dynamic model of hippocampal synapses. *PloS one*, 9(1), 2014. DOI: 10.1371/journal.pone.0086248 (cited on page 51).

[BKK+15] Thomas M. Bartol, Daniel X. Keller, Justin P. Kinney, Chandrajit L. Bajaj, Kristen M. Harris, Terrence J. Sejnowski, and Mary B. Kennedy. Computational reconstitution of spine calcium transients from individual proteins. *Frontiers in Synaptic Neuroscience*, 7, October 2015. DOI: 10.3389/fnsyn.2015.00017 (cited on page 51).

[CCD+15] Julien Chevallier, María José Cáceres, Marie Doumic, and Patricia Reynaud-Bouret. Microscopic approach of a time elapsed neural model. *Mathematical Models and Methods in Applied Sciences*, 25(14):2669–2719, December 2015. DOI: 10.1142/S021820251550058X (cited on page 13).

[DGL+15] Anna De Masi, Antonio Galves, Eva Löcherbach, and Errico Presutti. Hydrodynamic limit for interacting neurons. *Journal of Statistical Physics*, 158(4):866–902, 2015. DOI: 10.1007/s10955-014-1145-1 (cited on pages 5, 6, 11–13).

[DIR+15] François Delarue, James Inglis, Sylvain Rubenthaler, and Etienne Tanré. Global solvability of a networked integrate-and-fire model of McKean-Vlasov type. *The Annals of Applied Probability*, 25(4):2096–2133, 2015. DOI: 10.1214/14-AAP1044 (cited on pages 5, 12).

[DOR15] Aline Duarte, Guilherme Ost, and Andrés A. Rodríguez. Hydrodynamic Limit for Spatially Structured Interacting Neurons. *Journal of Statistical Physics*, 161(5):1163–1202, December 2015. DOI: 10.1007/s10955-015-1366-y (cited on page 13).

[IT15] J. Inglis and D. Talay. Mean-Field Limit of a Stochastic Particle System Smoothly Interacting Through Threshold Hitting-Times and Applications to Neural Networks with Dendritic Component. *SIAM Journal on Mathematical Analysis*, 47(5):3884–3916, January 2015. DOI: 10.1137/140989042 (cited on pages 5, 30).

[CPX+16] Yihui Cui, Ilya Prokin, Hao Xu, Bruno Delord, Stephane Genet, Laurent Venance, and Hugues Berry. Endocannabinoid dynamics gate spike-timing dependent depression and potentiation. *Elife*, 5, 2016. DOI: 10.7554/elife.13185 (cited on page 49).

[DB16] Maurizio De Pittà and Nicolas Brunel. Modulation of synaptic plasticity by glutamatergic gliotransmission: A modeling study. *Neural plasticity*, 2016. DOI: 10.1155/2016/7607924. Publisher: Hindawi Publishing Corporation (cited on page 51).

[FL16] Nicolas Fournier and Eva Löcherbach. On a toy model of interacting neurons. *Annales de l'Institut Henri Poincaré, Probabilités et Statistiques*, 52(4):1844–1876, November 2016. DOI: 10.1214/15-AIHP701 (cited on pages 5, 11–13, 15, 16, 38, 39).

[GTM16] Thom Griffith, Krasimira Tsaneva-Atanasova, and Jack R. Mellor. Control of Ca^{2+} Influx and Calmodulin Activation by SK-Channels in Dendritic Spines. *PLOS Computational Biology*, 12(5), May 2016. DOI: 10.1371/journal.pcbi.1004949 (cited on page 51).

[RT16] Philippe Robert and Jonathan Touboul. On the Dynamics of Random Neuronal Networks. *Journal of Statistical Physics*, 165(3):545–584, November 2016. DOI: 10.1007/s10955-016-1622-9 (cited on page 13).

[TOS+16] Cezar M Tigaret, Valeria Olivo, Josef HLP Sadowski, Michael C Ashby, and Jack R Mellor. Coordinated activation of distinct Ca^{2+} sources and metabotropic glutamate receptors encodes Hebbian synaptic plasticity. *Nature communications*, 7, 2016. DOI: 10.1038/ncomms10289 (cited on pages 50–52, 55, 56).

[Che17] Julien Chevallier. Mean-field limit of generalized Hawkes processes. *Stochastic Processes and their Applications*, 127(12):3870–3912, December 2017. DOI: 10.1016/j.spa.2017.02.012 (cited on page 13).

[JDD+17] Joanna Jedrzejewska-Szmek, Sriraman Damodaran, Daniel B. Dorman, and Kim T. Blackwell. Calcium dynamics predict direction of synaptic plasticity in striatal spiny projection neurons. *European Journal of Neuroscience*, 45(8):1044–1056, April 2017. DOI: 10.1111/ejn.13287 (cited on page 51).

[MRH+17] Jason J. Moore, Pascal M. Ravassard, David Ho, Lavanya Acharya, Ashley L. Kees, Cliff Vuong, and Mayank R. Mehta. Dynamics of cortical dendritic membrane potential and spikes in freely behaving rats. *Science*, 355(6331), March 2017. DOI: 10.1126/science.aaj1497 (cited on pages 4, 5, 30).

[PSW17] Benoît Perthame, Delphine Salort, and Gilles Wainrib. Distributed synaptic weights in a LIF neural network and learning rules. *Physica D: Nonlinear Phenomena*, 353-354:20–30, September 2017. DOI: 10.1016/j.physd.2017.05.005 (cited on page 27).

[SDG17] Tilo Schwalger, Moritz Deger, and Wulfram Gerstner. Towards a theory of cortical columns: From spiking neurons to interacting neural populations of finite size. *PLOS Computational Biology*, 13(4), 2017. DOI: 10.1371/journal.pcbi.1005507 (cited on pages 12, 13).

[BGG+18] A.-L. Basdevant, L. Gerin, J.-B. Gouéré, and A. Singh. From Hammersley's lines to Hammersley's trees. *Probability Theory and Related Fields*, 171(1):1–51, June 2018. DOI: 10.1007/s00440-017-0772-2 (cited on page 46).

[CPM+18] Yihui Cui, Ilya Prokin, Alexandre Mendes, Hugues Berry, and Laurent Venance. Robustness of STDP to spike timing jitter. *Scientific reports*, 8(1):1–15, 2018 (cited on page 51).

[Gab18] Pierre Gabriel. Measure solutions to the conservative renewal equation. *ESAIM: Proceedings and Surveys*, 62:68–78, 2018. DOI: 10.1051/proc/201862186206 (cited on page 14).

[MW18] S. Mischler and Q. Weng. Relaxation in Time Elapsed Neuron Network Models in the Weak Connectivity Regime. *Acta Applicandae Mathematicae*, 157(1):45–74, October 2018. DOI: 10.1007/s10440-018-0163-4 (cited on page 14).

[BST+19] Kim T Blackwell, Armando G Salinas, Parul Tewatia, Brad English, Jeanette Hellgren Kotaleski, and David M Lovinger. Molecular mechanisms underlying striatal synaptic plasticity: relevance to chronic alcohol consumption and seeking. *European Journal of Neuroscience*, 49(6):768–783, 2019. DOI: 10.1111/ejn.13919 (cited on pages 49, 51).

[Fay19] Grégory Faye. *Some propagation phenomena in local and nonlocal reaction-diffusion equations - A dynamical systems approach*. Thesis, Université de Toulouse 3 Paul Sabatier, April 2019. URL: https://hal.archives-ouvertes.fr/tel-02087834 (visited on 11/30/2022) (cited on page 57).

[WKK+19] Peng Wang, Ru Kong, Xiaolu Kong, Raphaël Liégeois, Csaba Orban, Gustavo Deco, Martijn P. van den Heuvel, and B.T. Thomas Yeo. Inversion of a large-scale circuit model reveals a cortical hierarchy in the dynamic resting human brain. *Science Advances*, 5(1):eaat7854, January 2019. DOI: 10.1126/sciadv.aat7854. Publisher: American Association for the Advancement of Science (cited on page 57).

[CCD+20] M. Carlu, O. Chehab, L. Dalla Porta, D. Depannemaecker, C. Héricé, M. Jedynak, E. Köksal Ersöz, P. Muratore, S. Souihel, C. Capone, Y. Zerlaut, A. Destexhe, and M. di Volo. A mean-field approach to the dynamics of networks of complex neurons, from nonlinear Integrate-and-Fire to Hodgkin–Huxley models. *Journal of Neurophysiology*, 123(3):1042–1051, March 2020. DOI: 10.1152/jn.00399.2019 (cited on page 12).

[CQK+20] Mélissa Cizeron, Zhen Qiu, Babis Koniaris, Ragini Gokhale, Noboru H Komiyama, Erik Fransén, and Seth GN Grant. A brain-wide atlas of synapses across the mouse lifespan. *Science*, 2020. DOI: 10.1126/science.aba3163 (cited on page 51).

[Cor20] Quentin Cormier. A mean-field model of Integrate-and-Fire neurons: non-linear stability of the stationary solutions. *arXiv:2002.08649*, March 2020. DOI: 10.48550/arXiv.2002.08649 (cited on pages 13, 19, 22).

[IAB+20] Yanis Inglebert, Johnatan Aljadeff, Nicolas Brunel, and Dominique Debanne. Synaptic plasticity rules with physiological calcium levels. *Proceedings of the National Academy of Sciences*, 2020. DOI: 10.1073/pnas.2013663117 (cited on page 51).

[LP20] Eric Luçon and Christophe Poquet. Emergence of Oscillatory Behaviors for Excitable Systems with Noise and Mean-Field Interaction: A Slow-Fast Dynamics Approach. *Communications in Mathematical Physics*, 373(3):907–969, February 2020. DOI: 10.1007/s00220-019-03641-y (cited on page 27).

[MIE+20] Tuomo Mäki-Marttunen, Nicolangelo Iannella, Andrew G Edwards, Gaute T Einevoll, and Kim T Blackwell. A unified computational model for cortical post-synaptic plasticity. *Elife*, 9, 2020. DOI: 10.7554/eLife.55714 (cited on page 51).

[Cor21] Quentin Cormier. *Long time behavior of a mean-field model of interacting spiking neurons*. PhD thesis, Université Côte d'Azur, January 2021. URL: https://inria.hal.science/tel-03123384 (cited on pages 10, 21, 22, 25).

[Hel21] Pascal Helson. *Plasticity in networks of spiking neurons in interaction*. PhD thesis, Université Côte d'Azur, March 2021. URL: https://hal.science/tel-03200979 (cited on pages 5, 7, 47, 57).

[RV21] Philippe Robert and Gaëtan Vignoud. Stochastic Models of Neural Synaptic Plasticity: A Scaling Approach. *SIAM Journal on Applied Mathematics*, 81(6):2362–2386, January 2021. DOI: 10.1137/20M1382891 (cited on page 5).

[Rod21] Yuri Elias Rodrigues. *Unifying experimental heterogeneity in a geometrical synaptic plasticity model*. PhD thesis, Université Côte d'Azur, June 2021. URL: https://tel.archives-ouvertes.fr/tel-03369169 (cited on pages 6, 49).

[ZSC+21] Yili Zhang, Paul D. Smolen, Leonard J. Cleary, and John H. Byrne. Quantitative description of the interactions among kinase cascades underlying long-term plasticity of Aplysia sensory neurons. *Scientific Reports*, 11(1), July 2021. DOI: 10.1038/s41598-021-94393-0 (cited on pages 49, 51).

[Aga22] Zoé Agathe-Nerine. Multivariate Hawkes processes on inhomogeneous random graphs. *Stochastic Processes and their Applications*, 152:86–148, October 2022. DOI: 10.1016/j.spa.2022.06.019 (cited on page 13).

[CAA+22] Giuseppe Chindemi, Marwan Abdellah, Oren Amsalem, Ruth Benavides-Piccione, Vincent Delattre, Michael Doron, András Ecker, Aurélien T. Jaquier, James King, Pramod Kumbhar, Caitlin Monney, Rodrigo Perin, Christian Rössert, Anil M. Tuncel, Werner Van Geit, Javier DeFelipe, Michael Graupner, Idan Segev, Henry Markram, and Eilif B. Muller. A calcium-based plasticity model for predicting long-term potentiation and depression in the neocortex. *Nature Communications*, 13(1):3038, June 2022. DOI: 10.1038/s41467-022-30214-w (cited on pages 49, 51).

[LWD+22] Matthew E. Larkum, Jiameng Wu, Sarah A. Duverdin, and Albert Gidon. The Guide to Dendritic Spikes of the Mammalian Cortex *In Vitro* and *In Vivo*. *Neuroscience*. Dendritic contributions to biological and artificial computations, 489:15–33, May 2022. DOI: 10.1016/j.neuroscience.2022.02.009 (cited on page 4).

[Löc22] Eva Löcherbach. Fluctuations for mean field limits of interacting systems of spiking neurons. *arXiv:2201.09255*, January 2022. DOI: 10.48550/arXiv.2201.09255 (cited on page 13).

[LM22] Eva Löcherbach and Pierre Monmarché. Metastability for systems of interacting neurons. *Annales de l'Institut Henri Poincaré, Probabilités et Statistiques*, 58(1):343–378, February 2022. DOI: 10.1214/21-AIHP1164 (cited on page 13).

[Aga23] Zoé Agathe-Nerine. *Hawkes processes on random graphs in neuroscience : large population limit and long time stability*. PhD thesis, Université Paris Cité, November 2023. URL: https://theses.fr/2023UNIP7028 (visited on 07/13/2024) (cited on page 58).

[JZ23] Pierre-Emmanuel Jabin and Datong Zhou. The mean-field Limit of sparse networks of integrate and fire neurons. *arXiv:2309.04046*, September 2023. DOI: 10.48550/arXiv.2309.04046 (cited on page 13).

[ODo23] Cian O'Donnell. Nonlinear slow-timescale mechanisms in synaptic plasticity. *Current Opinion in Neurobiology*, 82, October 2023. DOI: 10.1016/j.conb.2023.102778 (cited on page 56).

[PWI+23] Pojeong Park, David Wong-Campos, Daniel G. Itkis, Yitong Qi, Hunter Davis, Jonathan B. Grimm, Sarah E. Plutkis, Luke Lavis, and Adam E. Cohen. Dendritic voltage imaging reveals biophysical basis of associative plasticity rules, June 2023. DOI: 10.1101/2023.06.02.543490 (cited on page 4).

[AGD24] David Aquilué-Llorens, Jennifer S. Goldman, and Alain Destexhe. High-Density Exploration of Activity States in a Multi-Area Brain Model. *Neuroinformatics*, 22(1):75–87, January 2024. DOI: 10.1007/s12021-023-09647-1 (cited on page 57).